THE CONTROL OF ARM MOVEMENTS TOWARDS VISUAL TARGETS IN 3-D SPACE

een wetenschappelijke proeve op het gebied van de
Natuurwetenschappen, Wiskunde en Informatica

Proefschrift

ter verkrijging van de graad van doctor
aan de Katholieke Universiteit Nijmegen,
op gezag van de Rector Magnificus, Prof. dr. C.W.P.M. Blom
volgens besluit van het College van Decanen
in het openbaar te verdedigen op vrijdag 25 juni 2004
des morgens om 10.30 uur precies

door

Maria Anna Admiraal

geboren op 11 juni 1974 te Tegelen

Promotor:	Prof. dr. C.C.A.M. Gielen
Manuscript Commissie:	Prof. dr. C.J. Erkelens (Universiteit Utrecht) Prof. dr. H. Bekkering Dr. J. Smeets (Erasmus Universiteit Rotterdam)

Admiraal, M.A.

ISBN: 90-9018168-7

Printed by PrintPartners Ipskamp, Enschede

CONTENTS

CHAPTER 1

GENERAL INTRODUCTION

In everyday life we interact with the objects that we see in our environment. Without much thinking we can adequately grasp an object, even if we have seen it in the past and are looking elsewhere at the time of reaching. The reaching movement to different objects at the same location relative to the subject can be very different depending on the object that is reached for (a hot cup of coffee, a good glass of wine, or a tennis ball). Nevertheless, we can do so even if the object of interest is out of view at the time of reaching. Somehow, we have stored the location of the object that we have to reach for, and we are able to generate an adequate movement with high enough accuracy.

It is generally accepted that, when an object is observed, the Central Nervous System (CNS) forms and stores an *internal representation* of the 3-D location of the object based on the 2-D images on the retinas of the two eyes. With this internal representation, the CNS is able to generate the appropriate activation of muscles in the arm to move the hand to the right position. Often, such a reaching movement towards a distant target is preceded by a movement of the trunk or a step towards the target. Even then the CNS is able to bring the hand to the remembered location of the previously seen target. Apparently, the step or trunk movement is adequately incorporated in the reaching movement.

The various actions described above reflect a rather complex series of processes, since they require the integration of information from different sources: first the reconstruction of the 3-D position of the object from the 2-D retinal images of the two eyes, second the storage of this 3-D target position relative to the body, and third updating the object's position relative to the subject for any movements of the body in space. Finally an appropriate set of muscles must be activated to bring the hand to the remembered position. Bringing the hand to a position in 3-D space can be achieved with various postures of the arm, which is referred to as being *kinematically redundant*, and forms yet another challenge to the CNS.

This thesis describes studies on the perception and storage of the 3-D location of visual targets and on the (visual) information that is needed to accurately reach a target position that was previously viewed (Chapters 2 and 3). Furthermore, we describe analyses of various models for the reduction of degrees of freedom in the execution of reaching movements towards the remembered 3-D target position (Chapters 4 and 5).

In this introduction we will first discuss the integration of the various signals in eye-hand coordination and the practical difficulties that the CNS has to cope with in driving a kinematically redundant limb. We will discuss various models for the control of arm movements. This section is followed by a description of the basic formalisms to describe and analyze arm, eye and head movements.

EYE-HAND COORDINATION

One of the main problems in the coordination of a hand movement toward a visual target is related to the integration of visual, proprioceptive and other sensory information. These sensory inputs are all represented in different frames of reference, and integration of these inputs is necessary for the preparation, planning, and execution of the movement. Postural information about the orientation of the arm is easiest described relative to the shoulder, whereas the coding of visual information will initially be in retinal coordinates. This visual information has to be combined with information about eye and head position in order to determine the target position relative to the body. Next, a pointing or grasping movement to this position requires a specific muscle activation pattern that brings the hand from the initial position to the target. Obviously, both visual information about target position and information about head and arm orientation contribute to the final motor plan that drives the finger to the right position, each in a different frame of reference.

It is now generally accepted that the position of a visual target is perceived in a viewer-centered frame of reference (e.g. Soechting et al. 1990; McIntyre et al. 1997; Henriques et al. 1998; Medendorp and Crawford 2002a). This implies that the main coordinates are given by azimuth, elevation and distance of the target relative to the subject, as is indicated in Figure 1.1.

When the 3-D position of a target is represented in three separate coordinates, the errors along these independent coordinate axes are assumed to be uncorrelated. Therefore, many studies on the frames of reference used for reaching to remembered visual targets, analyzed the orientation of reaching errors (Soechting and Flanders, 1989; Berkinblit, 1995; McIntyre, 1997; Messier and Kalaska, 1997). If one can find the directions of the covariance matrix for the pointing errors, the eigenvectors of the covariance matrix are thought to reflect the independent coordinate axes of the frame of reference. Furthermore, the differences in errors in reaching between different visual conditions may indicate how and to what extent visual information contributes to the task.

Based on the errors that subjects make in different reaching tasks, several hypotheses have been put forward on how the CNS stores the parameters of the target position. Some suggested that movements are coded in terms of vectorial

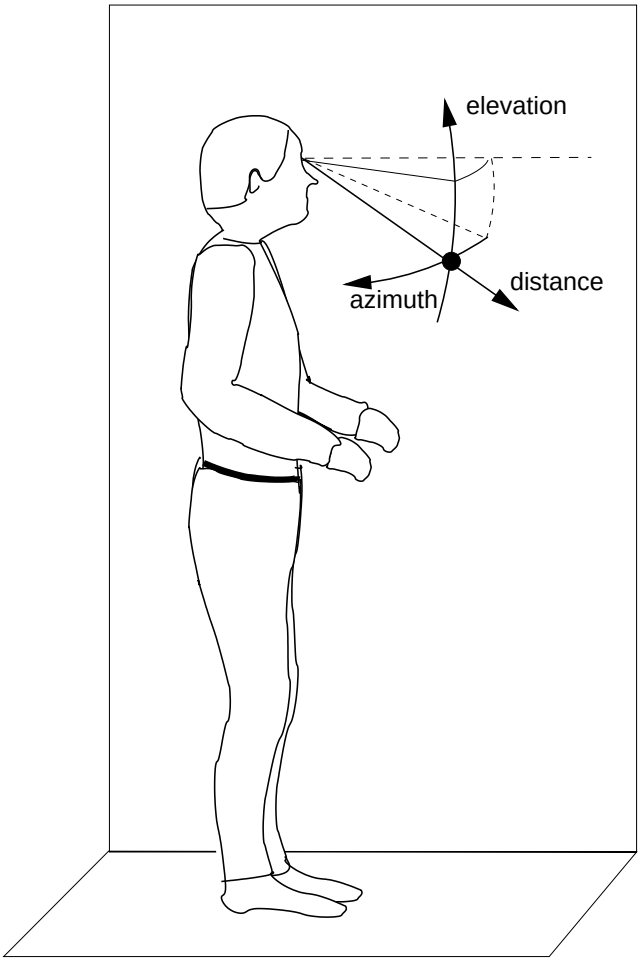

FIGURE 1.1: Describing a position in spherical coordinates relative to the subject. A position in 3-D space described in relative to the subject's cyclopean eye in azimuth (rotations about a vertical axis, elevation (rotations about a horizontal axis) and distance from the cyclopean eye.

displacement from the initial position (Messier and Kalaska 1997;Vindras et al. 1998; and Gordon et al. 1994), which was supported by findings of Georgopoulos et al. (1984), who provided evidence that cells in the motor cortex specify the parameters of the target position separately for distance and direction. Other studies interpreted errors in pointing as evidence for movement planning in a shoulder-centered frame of reference (Soechting and Flanders 1989; Berkinblit et al. 1995), in a viewer-centered frame of reference (e.g. McIntyre et al. 1997), or in both a shoulder-centered and a head-centered frame of reference (Soechting et al. 1990; McIntyre et al. 1998).

Obviously, the transformation from a target position defined in viewer-centered coordinates to a motor output signal to the arm muscles introduces a combination of errors attributed to different stages in the sensori-motor transformation. The relative contributions of the different stages, however, may vary for different experimental conditions.

Many studies have shown that the accuracy of reaching depends on binocular gaze direction (see e.g. Henriques et al. 1998; Van Donkelaar and Staub 2000). These authors have shown that when gaze is directed away from the target position, the reaching movement tends to be attracted in the direction of gaze. This is

interpreted as evidence that reaching movements are coded in a retinal frame of reference. But so far, no study has tested the effect of vision on the reaching errors in different visual feedback conditions. Therefore, in Chapters 2 and 3 we present studies on the interaction between 3-D binocular gaze and arm movements towards remembered visual targets, in different visual feedback conditions. We try to identify the parameters that are used by the CNS for the storage of a target position and for the execution of a reaching movement, and the frame of reference used to code the target position.

An even more complex task concerns the updating of an internally stored target position for a displacement of the body in order to preserve a correct representation of the target position relative to the subject. Incorporating the step to make the proper hand movement requires that the subject adequately combines egocentric and allocentric information about target position and step displacement (see Medendorp et al. 1998). In Chapter 3 we studied the contribution of different inputs to the CNS that are of interest when a reach is preceded by a step. We investigated the relation between the errors in pointing, binocular gaze and the step displacement in order to test how the step is incorporated in reaching and to what extent binocular gaze is of influence.

MODELS ON ARM MOVEMENT COORDINATION

When the target for a reaching movement of the hand is stored, the next difficulty is to define the appropriate posture of the whole arm, which brings the hand to the right position. In a task where the only objective is to bring the hand to some position in 3-D space, there will be many arm postures that satisfy this requirement: the arm is *kinematically redundant*. Every time a certain position must be reached, the CNS has to select one movement trajectory and one final posture from the numerous options that meet the task requirements. Although it is possible to choose a different trajectory and arm posture each time, several studies have shown that the kinematics of arm postures are quite consistent and reproducible within and across subjects (e.g. Straumann et al. 1991; Soechting et al. 1995). This indicates that the CNS has found a way to overcome the problem of kinematical redundancy and that the CNS may define the desired end-posture by more parameters than just the 3-D target position. Therefore, several studies have tried to describe this reduction of degrees of freedom by formulating criteria that might be used by the CNS to reduce the number degrees of freedom for arm movements (e.g. Straumann et al. 1991; Hore et al. 1992; Soechting et al. 1995).

Beside postural flexibility at the end point of a movement, the many degrees of freedom of the arm also allow many different movement trajectories, which all bring the hand from the initial position to a given end position. Yet, the path of the index finger during a reaching movement has been reported to be very consistent from trial to trial (Georgopoulos et al. 1981; Soechting and Lacquaniti 1981), which

has led some studies to propose dynamics-based models for arm movements (e.g. Uno et al. 1989; Harris and Wolpert 1998).

The fact that movement kinematics and dynamics of movement trajectories are consistent within and between subjects has raised the question to what extent movement kinematics and movement dynamics are related. One possibility might be that movements are planned at a kinematic level (e.g. in joint coordinates or in extrinsic coordinates) and that, once such a plan exists, the forces to produce the desired trajectory of movement kinematics are generated. This class of models is usually referred to as *posture-based* models. One particular model from this type is Donders' law, which was originally proposed to describe eye movements. It states that torsion of the eye is uniquely determined for each 2-D gaze direction (Donders 1848; Tweed and Vilis 1987). Later studies have reported that Donders' law is also obeyed for head and arm movements (Straumann et al. 1991; Hore et al. 1992; Miller et al. 1992). These studies all evaluated Donders' law for arm and head orientations at the end of a movement and showed that in many situations Donders' law holds for static arm and head orientations. But until now, no one has tested whether Donders' law also holds for the dynamics of arm and head movements. This question is addressed in Chapter 4, where we tested whether the 3-D orientation of the arm or head for a certain 2-D pointing or heading direction is the same during movements and at rest.

If movement trajectories are not the consequence of a posture-based model, it may be the other way around. In this view movement trajectories are the result from an optimization process or some dynamical constraints and the kinematics are the result of movement dynamics. An example of this class of models is the *minimum work model* (Soechting et al. 1995). This model assumes that a movement trajectory is chosen such that the amount of work that must be done to transport the arm from the starting posture towards a target is minimal. According to the minimum work hypothesis, the dynamics and kinematics follow tightly connected from the optimization criterion given the movement time, the initial posture of the arm, and the final position of the hand. There are many models of this type, which hypothesize that the CNS optimizes some constraint, for example: the *minimum torque-change model* (Uno et al. 1989), the *minimum commanded-torque-change model* (Nakano et al. 1999), the *minimum variance model* (Harris and Wolpert 1998) and the *stochastic optimal control model* (Todorov and Jordan 2002). Obviously, the models mentioned above cannot all be correct. Therefore, in Chapters 5 we performed a quantitative comparison, in order to reveal whether a single model can provide a good fit to the data or whether the central nervous system might use multiple criteria, with each criterion suitable for one or a small set of contexts (see e.g. Haruno et al. 1999). In the latter case it might be that a model gives a good performance for a particular set of movements or movement instructions, but fails for another.

GENERAL ANATOMY OF THE ARM

Orienting the arm in space is a complex process, since the arm has many degrees of freedom, which allow various different postures of the arm. Moreover, the many muscles that move the shoulder, the elbow and the wrist consist of agonist and antagonist muscles, which allow different combinations of muscle activation to result in the same forces to the upper arm, forearm and hand, and to lead to the same postures. In this thesis, however, we have focused mainly on the kinematic properties and on the role of multiple degrees of freedom involved in arm movements.

If we ignore rotations in the wrist, the arm's orientation is defined by 5 rotational degrees of freedom: two in the elbow (flexion / extension (ϕ) and pronation / supination (ξ)), and three in the shoulder (elevation (θ), azimuth (η) and torsion (ς)), which are indicated in Figure 1.2. In this thesis the orientation of the arm will be described in terms of the joint angles in the shoulder and the elbow. Since pronation / supination of the forearm does not effect the location of the hand in space, we will focus only on the three rotational degrees of freedom in the shoulder, and flexion/extension of the elbow.

The CNS perceives the orientation of the arm by various sensory inputs. An important source of input is *proprioceptive information* of the arm, which mainly consists of signals from various muscle receptors that relate to the amount of stretch and stretch velocity of the muscle. In addition, thee are signals from the many tactile sensors in the skin. Furthermore, *efference copies,* which are copies of the efferent motor commands to the arm muscles, and vision of the arm can be used to derive the arm's orientation. Depending on the task and the availability of input signals, the CNS may rely on different combinations of these types of inputs (see e.g. Van Beers et al. 2002).

Orienting the eye and head

Directing *binocular gaze* (the 3-D viewing position of the two eyes) towards an object in 3-D space requires a close cooperation between the orientation of the eyes in the head and the orientation of the head in the world. The orientation of each eye in the head is established by six extra-ocular muscles, which are arranged in more or less antagonistic pairs of muscles, which rotate the eye in three directions. This gives the eye three rotational degrees of freedom, for horizontal, vertical and torsional rotations. In order to direct the eye towards an object, only two degrees of freedom are needed (the horizontal and vertical directions) since torsion about the line of sight does not change gaze direction. Torsion is not relevant for gaze direction, but is important in order to reduce retinal slip during head movements, which usually have rotational components.

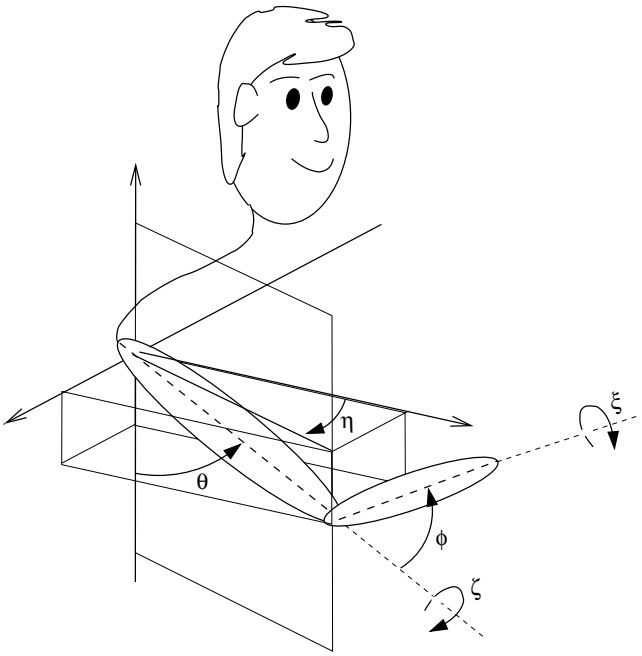

FIGURE 1.2: Definitions of joint angles relative to a shoulder-centered frame of reference. Elevation of the upper arm is indicated by θ, azimuth of the upper arm by η, and ς gives the torsion of the upper arm. Flexion of the elbow is indicated by ϕ and pronation/supination of the forearm is given by ξ.

For the control of eye position in the head, the CNS is thought to use both visual input from the retinas of the two eyes and extra-retinal inputs such as efference copies (e.g. Carpenter 1988; Von Helmholtz 1867). The contribution of efference copies to our perception of the spatial orientation of the eyes is usually demonstrated by pushing the eye aside with the finger, which, unlike active eye rotation, does cause a shift of the perceived world.

The orientation of the head is the result of complex rotations of combinations of vertebrae, which are controlled by over 20 pairs of muscles, which can orient the head in almost every direction in 3-D space. The CNS perceives the orientation of the head in space mainly through the vestibular system, which consists of the semicircular canals and the otolith organs, which both are located in the inner ear. Together, the canals and otolith organs provide information about rotational and translational movements of the head, respectively, and about the orientation of the head relative to gravity; The semicircular canals respond to angular acceleration, whereas the otolith organs provide an afferent signal that is related to both linear acceleration and gravity. Normally, visual information provides additional information about displacements of the head relative to the world-fixed visual environment, and helps to overcome the ambiguity in the otolith signals regarding the origin of the signals (acceleration of the head vs. change in orientation relative to gravity). In complete darkness however, when visual information is absent, the CNS has to rely mainly on the vestibular signals to derive the orientation of the head in space.

Describing orientations

Generally, the kinematics of a rigid body in space is quantified by six parameters: three to describe the position of an arbitrary point of the object, and three to describe the orientation of the object relative to this point. For studies on the human arm, the shoulder is often chosen to serve as an origin, and the joint angles described in Figure 1.2 are used to describe the arm's orientation relative to the shoulder. Beside a representation in terms of joint angles there are other ways to describe the orientation of the arm, such as rotation matrices, Euler angles or rotation vectors (see e.g. Van Opstal 1993; Haslwanter 1995). These various representations have different advantages in specifying the orientation, and they are formally equivalent. The rotation matrix is very useful to describe the rotation of an object, but it requires a redundant set of nine matrix-indices to represent a rotation in 3-D. When using Euler angles, the rotation is decomposed into three separate rotations about specific axes. However, this description requires the definition of a coordinate system in which the consecutive order of the separate rotations is settled, because the end-orientation after multiple rotations in 3D depends on the order of the rotations (*non-commutativity* of rotations in 3-D space).

Depending on the requirements of the analysis or calculus one intends to perform, one of these representations for the orientation of the arm will be the most useful. For the analyses described in this thesis, the notation of *rotation vectors* was chosen. A rotation vector represents the rotation that brings the object from a predefined orientation (*reference orientation*) into the current orientation. The rotation vector's orientation indicates the axis around which the object is virtually rotated, and its length is related to the rotation angle around this axis that brings the object in the current orientation:

$$\vec{r} = \tan\left(\frac{\theta}{2}\right) \vec{n} \qquad (1.1)$$

where $\vec{n}$ represents the unit vector of the rotation axis in 3D, and θ is the angle of rotation along that axis. This is illustrated in Figure 1.3, which shows several 3-D orientations of the same hand that follow from the orientation of the central hand after a rotation of 90º around axes that lie in the plane of the figure.

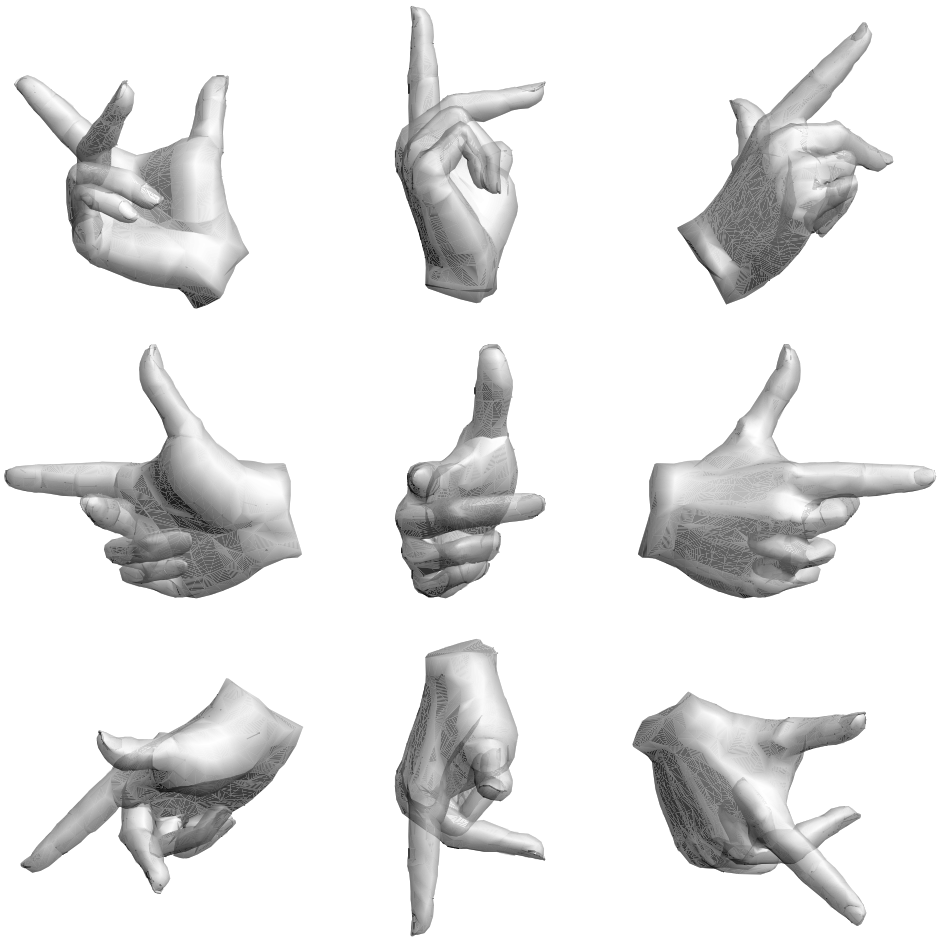

FIGURE 1.3: Describing orientations by a rotation vector relative to a reference orientation. All hand orientations at the border of the figure follow from the reference (central) orientation after a rotation of 90º around axes that lie in the plane of the figure. The corresponding rotation vector will have a length of tan(90º/2) =1.

CHAPTER 2

THE INTERACTION BETWEEN GAZE AND POINTING TOWARDS REMEMBERED VISUAL TARGETS

INTRODUCTION

One of the main problems in understanding human motor control is related to the frames of reference, which are used for the preparation, planning, and execution of movements. Visual information about targets in three-dimensional (3-D) space is initially coded in retinal coordinates. The visual information in retinal coordinates has to be combined with information of eye and head position to determine target position relative to the body. Finally, a pointing or grasping movement to a target requires a specific muscle activation pattern that brings the hand to the target. Obviously, both visual information about target position and proprioceptive information about arm position contribute to the final finger position, each in a different frame of reference. To gain more insight in the frames of reference that may be used, many studies have focused on movements of the hand to match the position of visible or remembered visual targets. In previous literature, such movements are commonly referred to as *pointing* movements. In this study we will use this term accordingly, although the term *pointing* may be somewhat misleading for the actual matching task.

Most studies on pointing toward remembered visual targets have in common that they showed that the distribution of finger positions for pointing to a remembered target is characterized by an ellipsoid with the long axis of the distribution oriented toward the subject. This has been interpreted as evidence for the hypothesis that the central nervous system (CNS) specifies the parameters of the endpoint of the movement separately for distance and direction (Georgopoulos et al. 1984; Flanders et al. 1992; Gordon et al. 1994), that the movement is planned in terms of displacement from the initial position (Messier and Kalaska 1997; Vindras et al. 1998), or as evidence for movement planning in a viewer-centered frame of reference (e.g. McIntyre et al. 1997). Other studies, however, interpreted errors in pointing as evidence for movement planning in a shoulder-centered frame of reference (Soechting and Flanders 1989, Berkinblit et al. 1995), or in both a

Adapted from: M.A. Admiraal, N.L.W. Keijsers, C.C.A.M. Gielen,
J. Neurophysiol. 90: 2136-2148, 2003.

shoulder-centered and a head-centered frame of reference (Soechting et al. 1990, McIntyre et al. 1998). The different results regarding the variability in the orientation of the ellipses in these studies are most likely explained by differences in the experimental conditions with which different studies approached the issue: in some studies subjects had no visual information whatsoever on the environment, nor on their arm (McIntyre et al. 1997), whereas in other studies subjects had feedback on their arm (Berkinblit, et al. 1995) or on both the arm and the visual environment (Soechting and Flanders 1989 and McIntyre et al. 1998). However, because none of these studies tested subjects for pointing in all these different experimental conditions, it is not clear to what extent the different contributions of information about finger position and about target position relative to the visual environment could explain the different results. To investigate the effect of vision of the finger and the environment on the pointing errors and in particular the effect of visual feedback of the finger, we have measured pointing movements in three visual conditions: 1) complete darkness with visual feedback of the finger position; 2) complete darkness without visual feedback on the position of the index finger; and 3) vision of the index finger along with vision of a well-defined visual environment. A previous study by Van Beers et al. (2002) demonstrated that the contributions of visual and proprioceptive information may vary, depending on the experimental conditions. The first aim of this study was therefore, to compare the distributions of pointing errors in each of the 3 conditions, to see whether the different results of previous studies could be explained by different contributions of visual and proprioceptive information in different experimental conditions. In particular, we tested whether the error distributions in each condition were oriented toward a single point, which might be interpreted as the center of some frame of reference for pointing (e.g. viewer-centered or shoulder-centered) and whether differences in the experimental conditions would change the location of any such point.

Several studies (Bock 1986; Enright 1995; Henriques et al. 1998; Medendorp and Crawford 2002a) have stressed the importance of fixation of gaze to a target on pointing accuracy by demonstrating that pointing errors increase when gaze deviates from the target position. This observation adds another complicating factor to the interpretation of the error ellipses that have been obtained in previous studies. Eye position was not measured in most of the studies on pointing to remembered targets and fixation might very well have been different in conditions with and without visual feedback about the environment. If pointing errors depend on gaze and if gaze is different with and without visual feedback on the finger and the environment, different orientations of error ellipses might also be attributed to differences in gaze.

Therefore, the second aim of this study was to compare the errors in pointing and in gaze as a function of time in the period from target onset until completion of the pointing movement, and to look for the presence (or absence) of a correlation between constant and variable errors of 3-D gaze and of 3-D finger position during pointing.

METHODS

In this study we performed two experiments. In the first experiment we measured movements of the arm during pointing toward remembered visual targets. In the second, we simultaneously measured pointing movements of the arm and binocular eye movements to determine 3-D gaze.

Fifteen subjects (aged 21-49 years) participated in these experiments. Ten subjects participated in the first experiment and six subjects participated in the second experiment. One subject (RK) participated in both experiments. All subjects had normal or corrected-to-normal vision and all gave informed consent. The experimental protocol was approved by the Medical Ethical Committee of the University of Nijmegen. None of the subjects had any known history of neurological sensory or motor disorders. All subjects were right-handed, except for subject MA, who participated only in the second experiment. Pointing movements were performed with the right hand, unless explicitly indicated otherwise. Three subjects (MA, NK and SG) were familiar with the aim of this study. Their results were not different from those of the other subjects.

Experimental paradigm

Subjects were standing in a completely dark room. An L-shaped obstacle was attached on the floor to offer the subject a reference to maintain the correct location in the otherwise dark room in all three test conditions. Seven red light-emitting diodes (leds) were attached on the vertices of two 30 x 30 x 30 cm^3 cubes, next to each other, about 25 cm in front of the subject (see Figure 2.1). Each of these seven leds served as a target for pointing movements in the first experiment. Targets 1, 4, and 5 were used in the second experiment.

The onset of the target marked the start of a trial. After 1 s the target led was switched off and the cubes with targets were canted away. Two seconds after target disappearance an auditory signal notified the subject to start the pointing movement to the remembered target. Subjects were instructed to wait for the auditory signal before positioning their index finger at the remembered target position, and to keep it at the position of the remembered target for at least 0.5 s. Subjects could freely move their head and eyes and no explicit instruction was given about where to direct gaze.

Three visual feedback conditions were tested: pointing in complete darkness (DARK), pointing with feedback by means of a red led on the tip of the index finger that was visible at all times (FINGER), and pointing in the presence of an illuminated cubic frame with a continuously lit red led attached on the tip of the index finger (FRAME). In the latter condition, a well-defined visual environment was shown to the subject by means of illuminated optic fibers along the edges of a cubic frame of 90 x 90 x 90 cm^3 (see Figure 2.1). The surface of the optic fibers was roughened by sandpaper and red leds at the long ends of the optic fibers gave the

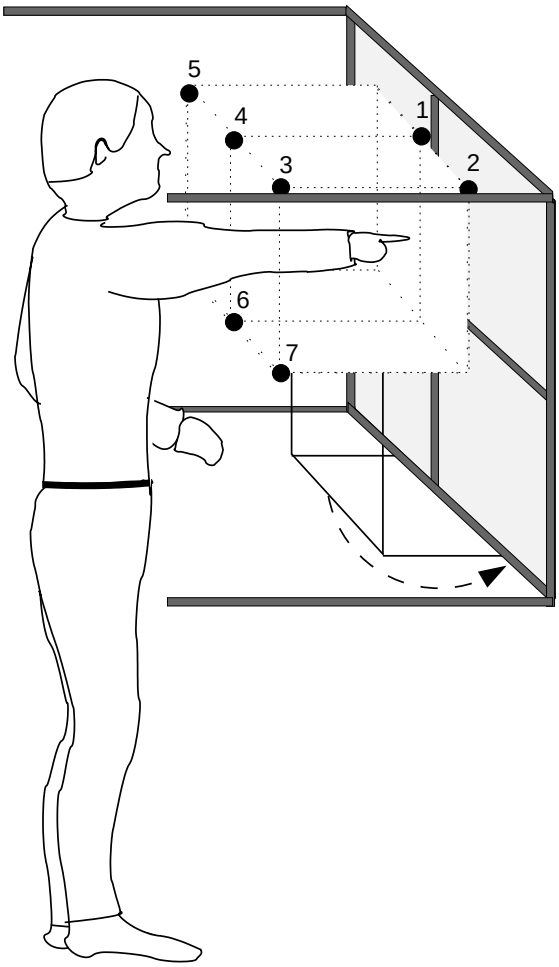

FIGURE 2.1: Schematic overview of the setup. In the first experiment, the subject was standing about 40 cm from the center of the 30x60x30 cm frame, i.e. 25 cm from the front of the frame with the seven targets. Targets (black dots) were located 15 cm above and below the shoulder, and 15 cm to the right (targets 2, 3, and 7), 15 cm to the left (targets 1, 4 and 6) and 45 cm to the left (target 5) of the shoulder, such, that the workspace of the right shoulder ranged from -30 to +60 degrees in azimuth, from -30 to +30 degrees in elevation, and from about 30 to 55 cm in distance. After target disappearance the frame was canted away (arrow). In the second experiment the subject stood right in front of target 4 and the framework was elevated, such that the upper targets were at eye level. Solid gray lines indicate the 90x90x90 cm frame of optic fibers, which was illuminated in the FRAME condition.

optic fibers a red color. The frame was visible at all times in the FRAME condition. All targets were within this illuminated cubic frame, well within reaching distance from the subject.

In the first experiment, we investigated pointing movements without measuring gaze, and tested pointing movements to the seven targets in each of the three visual feedback conditions. The visual feedback conditions were tested in pairs (DARK-FINGER and FINGER-FRAME). Measuring two feedback conditions took about one hour, and measuring all three feedback conditions in one experimental session would exceed the maximum amount of time that the subjects could remain concentrated. Four subjects participated in both pairs of conditions, and four other subjects participated in either the DARK-FINGER pair or the FINGER-FRAME pair. As a result, we tested six subjects in the DARK and in the FRAME condition and all eight subjects were tested in the FINGER condition.

In this experiment, we also examined the influence of the effector arm (left or right) for pointing to targets in the same workspace relative to the shoulder of the

pointing arm. Therefore, we also had subjects to point with the left arm in the FINGER condition. Targets were presented at mirror-symmetric locations relative to the left shoulder. Four subjects performed pointing movements with the left and right arm (LEFT-RIGHT pair) and two subjects performed pointing movements with the left arm only (LEFT ONLY). This resulted in a total of six subjects performing pointing movements with the left arm in the FINGER condition. Two of the subjects who pointed in the LEFT-RIGHT condition pair had not participated in the DARK-FINGER or FINGER-FRAME pairs. Therefore the total number of subjects that performed pointing movements with the right arm in the FINGER condition increased to ten. Six subjects were tested twice in the FINGER condition for pointing with the right arm (see Table 2.1).

	FINGER (right)	*DARK right)*	*FRAME (right)*	*FINGER (left)*	*COIL (FRAME-FINGER-DARK)*
Subject					
AT	2	1	1		
DL	1		1		
JL	2	1	1	1	
MV	2	1	1		
NK	2		1	1	
WV	2	1	1		
FH	1	1		1	
MK	2	1		1	
FW	1			1	
RK	1			1	1
MA					1
BB					1
HN					1
SG					1
BA					1
Total	10(16)	6	6	6	6

TABLE 2.1: Number of times of participation per condition by each subject. At least six subjects participated in each condition. Due to pair-wise testing of the three feedback conditions, six subjects participated twice in the FINGER condition for pointing with the right hand.

The targets were presented in a randomized order in 16 blocks of 20 trials each. In each block, only one visual feedback condition was tested. For each of the visual feedback conditions, each target was presented 20 times, except for the target that was closest to the subject's eyes (target 4), which was presented 40 times. A block with 20 trials typically lasted about 3 minutes, and after each block, room lights were switched on for about 1 minute to avoid dark adaptation.

In the second experiment we measured pointing movements and binocular eye movements using the search-coil technique. In this experiment, subjects were tested in each of the three conditions (DARK, FINGER, and FRAME) in one experimental session. Since the duration of these experiments had to be restricted to 45 minutes (because of the limited time available to wear the search coils without discomfort), only targets 1, 4, and 5 were used, which were presented ≥13 times each in each condition. All three targets were at eye level. Targets were presented in a randomized order in six blocks of 20 trials each. In each block, only one visual feedback condition was tested. Blocks with different visual feedback conditions were tested in randomized order.

Experimental setup

The position of several segments of the subject's body and the position of the targets were measured with an Optotrak 3020 system (Northern Digital, Ontario, Canada), which measures the 3-D position of infrared, light-emitting diodes (ireds) with a resolution better than 0.2 mm within a range of about 1.5 m^3. The Optotrak system was mounted on the ceiling above the subject at a distance of about 2.5 m to the right of the subject, tilted downward at an angle of 30º relative to the ceiling. When pointing movements with the left arm were measured, the subject and the framework with targets were rotated 180º, for better visibility of the pointing arm to the OPTOTRAK system. The position of ireds was measured with a sampling frequency of 100Hz.

Ireds were placed on the subject's shoulder (*acromion*) and elbow (*epicondylus lateralis*). The position of the tip of the index finger was measured by means of an ired attached to a thimble on the index finger. This thimble also contained a visible red led that provided the subject with feedback on finger position in the FINGER and FRAME conditions. When gaze was measured, subjects were wearing a helmet with six ireds, which were attached in such a way that at least three ireds were visible for the OPTOTRAK system at all possible head orientations. This was necessary to calculate 3-D head orientation at all times, such that eye position could be reconstructed from head position (see following text).

Gaze was measured using the scleral search-coil technique (Collewijn et al. 1975) in a large magnetic field system (Remmel Labs). This system consists of a cubic frame of welded aluminum of 3 x 3 x 3 m^3, which produced three orthogonal magnetic fields at frequencies of 48, 60, and 80 kHz. During these experiments subjects were tested such that the search coils were close to the center of the large magnetic field system. Care was taken that the calibration of the eye coil signals was performed in the same region of the magnetic field where the actual measurements took place. During the calibration procedure subjects fixated a series of red LEDs attached to a board at a distance of 90 cm in front of the subject. The LEDs were arranged at three circles of different radius (15, 27.5 and 37.5º),

concentric around the straight-ahead direction. With this setup, calibration errors (defined as twice the SD) were typically about 0.5° in azimuth and 1° in elevation on average; resolution was <0.04°. As a result, the errors in 3D-gaze position - resulting from calibration errors in the orientation of the two eyes in space - were on average about 0.6 and 1.1° in azimuth and elevation, respectively, and 3 cm in radial distance from the cyclopean eye.

Two PCs controlled the experiment, one of which was equipped with hardware and software for the collection of the search-coil data and with software for the stimulus presentation. The second PC contained hardware and software to collect the ired data from the OPTOTRAK system, and was controlled by the first PC to synchronize the ired data collection (second PC) with the collection of the search-coil data (first PC). Coil signals were sampled at 500Hz. In off-line analyses, the coil signals were resampled at a 100Hz frequency by cubic spline interpolation.

Data analysis

We distinguish two types of pointing errors: the *constant error*, which is the distance between the LED position of a target and the average of all pointing positions toward that target, and the *variable error*, which reflects the distribution of the pointing positions toward a target relative to the average pointing position to that target. *Pointing position* is defined as the position of the ired on the tip of the index finger at the end of the pointing movement toward the target. The distribution of the pointing positions for a target i is described by the 3-D covariance matrix S_i:

$$S_i = \frac{\sum_{j=1}^{n} \pi_j^i \left(\pi_j^i\right)^T}{n-1} \qquad (2.1)$$

Where n is the number of trials to target i and $\pi_j^i = p_j^i - \bar{p}^i$ is the deviation of the finger position in trial j to target i relative to the mean pointing position $\bar{p}^i$ to target i. The three orthogonal eigenvectors of the covariance matrix S_i describe the orientations of the variable errors. The corresponding eigenvalues of the matrix give the size of the variable error along the eigenvectors. These eigenvalues of the covariance matrix S_i can be scaled to compute the limits that contain 95% of the data (see McIntyre et al. 1998 and Morrison 1976). A χ^2 test was used to decide whether the three eigenvalues of the covariance matrix were statistically different (see Barlow 1989). In all figures we display only contours of the 95% confidence ellipses when one of the eigenvalues is significantly larger than the other two ($P<0.05$). The eigenvector that corresponds to the largest eigenvalue will be referred to as the *main axis* of the distribution. We derive the accuracy of the main axis by means of a bootstrap method (see e.g. Mooney and Duval 1993). From the 20 data points for each target, we drew a random sample of 1000 data points. For this artificial data set of 1000 points we calculate the 3-D covariance matrix, and determined the corresponding main axis. This procedure was repeated 500 times for

each target, which resulted in 500 main axes per target. From the distribution of the 500 main axes we estimated the accuracy of the orientation of the ellipsoid.

Intersection point of confidence ellipsoids

Assuming that the ellipsoids for all targets are oriented toward one single point in space, one can find this point by estimating the intersection point of the main axes of the ellipsoids. We determined the accuracy of the orientation of the main axis of each ellipse by a bootstrap method. Because the orientation of the main axes can be determined only up to certain accuracy, there will hardly ever be one single position in 3-D at which all main axes intersect exactly. Therefore we have used a maximum log-likelihood method to determine the most likely position of the hypothetical intersection point. Finding the most probable intersection point in 3-D space given the pointing data set (D) corresponds to maximizing $\log p(\vec{x}|D)$, where $p(\vec{x}|D)$ represents the probability that the intersection point is at position $\vec{x}$, given the data set D. Finding the most probable intersection point for multiple data sets D_i, corresponding to the targets i, is equivalent to maximizing the product of the probabilities, according to

$$\max_x \log\left(\prod_i p(\vec{x}|D_i)\right) = \max_{\vec{x}} \sum_i \log\left(p(\vec{x}|D_i)\right) \quad (2.2)$$

We verified that the pointing responses could be considered to be normally distributed, using a Jarque-Bera test for goodness of fit ($p<0.01$, see Judge et al. 1988). For a normal distribution, $p(\vec{x}|D)$ is proportional to

$$p(\vec{x}|D) \propto e^{-(\vec{x}-\vec{\mu}_i)\Sigma_i^{-1}(\vec{x}-\vec{\mu}_i)'} \quad (2.3a)$$

and thus

$$\log\left(p(\vec{x}|D)\right) \propto -(\vec{x}-\vec{\mu}_i)\Sigma_i^{-1}(\vec{x}-\vec{\mu}_i)' \quad (2.3b)$$

where $(\vec{x}-\vec{\mu}_i)$ corresponds to the distance of position $\vec{x}$ relative to the main axis of the ith distribution $\vec{\mu}_i$. Σ_i is the covariance matrix describing the SD of the data distribution for target i. When the data sets D_i are normally distributed, maximizing the product of probabilities thus corresponds to minimizing

$$\min_{\vec{x}} \sum_i (\vec{x}-\vec{\mu}_i)\Sigma_i^{-1}(\vec{x}-\vec{\mu}_i)' \quad (2.4)$$

The expression $r_i = (\vec{x}-\vec{\mu}_i)\Sigma_i^{-1}(\vec{x}-\vec{\mu}_i)'$ is known as the *Mahalanobis distance* (see Duda and Hart 1973). The most probable intersection point $\vec{x}$ given the data corresponds to the minimum of the sum of Mahalanobis distances. The basic idea behind this method is schematically displayed in 2-D in Figure 2.2:

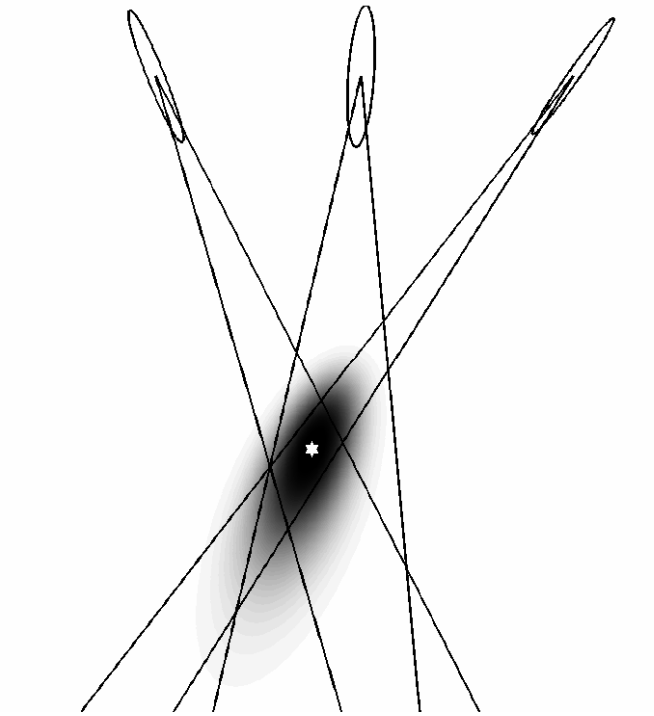

FIGURE 2.2: Determining the most likely intersection point. Three ellipses represent the hypothetical pointing error distributions for three targets. Accuracy of the main axis direction is indicated with a cone of confidence along the main axis. The probability of finding an intersection point of the three main axes is represented in grey-scale. The star indicates the position of the most likely intersection point of the main axes of these three error ellipses.

For three targets we show hypothetical 2-D error ellipses. For each error ellipse, the probability of finding an intersection point decreases with distance relative to the main axis for that error ellipse. This probability distribution, orthogonal to the main axis, corresponds to a normal distribution. The SD of this normal distribution depends on the ratio between the largest eigenvalue of the covariance matrix S_i and the smaller eigenvalue, and on the distance along the main axis relative to the center of the error ellipse. The most probable location for the intersection point corresponding to the minimum of the sum of Mahalanobis distances is indicated by a star.

To study the relation between gaze and pointing, we use the covariance between pointing position at the end of the pointing movement and gaze, which changes as a function of time:

$$\rho(t) = \frac{\sum_i \left(\left(g_i^j(t) - \overline{g^j(t)} \right) \left(p_i^j - \overline{p^j} \right) \right)}{\sqrt{\sum_i \left(g_i^j(t) - \overline{g^j(t)} \right)^2} \sqrt{\sum_i \left(p_i^j - \overline{p^j} \right)^2}} \qquad (2.5)$$

where $g_i^j(t)$ represents gaze in trial i for target j as a function of time. p_i^j represents the pointing position for trial i for target j. $g^j(t)$ and p^j represent the mean gaze as a function of time for target j and the mean pointing position for

target j, respectively. Note, that gaze is a function of time, whereas pointing position p is not. Therefore, any variations in the covariance between gaze and pointing in time are a consequence of changes in gaze as a function of time.

RESULTS

In the analysis of pointing movements to remembered target positions we will mainly focus on the constant and variable errors of the pointing movements and on the relation between these errors and 3-D gaze position as a function of time after target onset. First we will focus on the pointing movements for the three visual conditions (FINGER, DARK, and FRAME).

Figure 2.3 shows the main results for a typical subject (MV) when pointing with visual feedback of the fingertip (FINGER condition, Figure 2.3, A and B), in the absence of visual feedback (DARK condition, Figure 2.3, C and D), and with both vision of the environment and feedback of the fingertip (FRAME condition, Figure 2.3, E and F). The top panels show top views on the 3-D position of the fingertip (Figure 2.3, A, C and E), and the lower panels show side views (Figure 2.3, B, D and F). In each panel we have also drawn a fictive subject to indicate the position of the subject relative to the targets.

As described in Methods, we distinguish between a constant error and a variable error. Figure 2.3, A and B shows that with vision of the tip of the index finger (FINGER condition) the constant errors are on average about 5 cm (range 3 to 8 cm for the different target positions). These constant errors are representative for all subjects: averaged over all subjects and all targets, the constant error is 5 cm (SD= 2 cm).

Figure 2.3, A and B shows that the variable error is in general largest along an axis that is oriented toward the subject. Variable errors along the two minor axes of the ellipse are about the same in size, and are much smaller than errors along the main axis. As a result, the distribution of pointing positions has a significant orientation for most targets, and the distribution is indicated by an ellipse (see Methods).

Lack of vision of the tip of the index finger (DARK condition) leads to larger pointing errors than in the FINGER condition. Both constant and variable errors increase compared to that in the FINGER condition (compare Figure 2.3, C and D and Figure 2.3, A and B, respectively). The average constant error in Figure 2.3, C and D is about 7.5 cm (range 4 to 11 cm for different target positions). The constant error is mainly in the radial direction from the subject toward the target. Over all subjects, the average constant error is about 9 cm (SD= 4 cm), but pointing errors

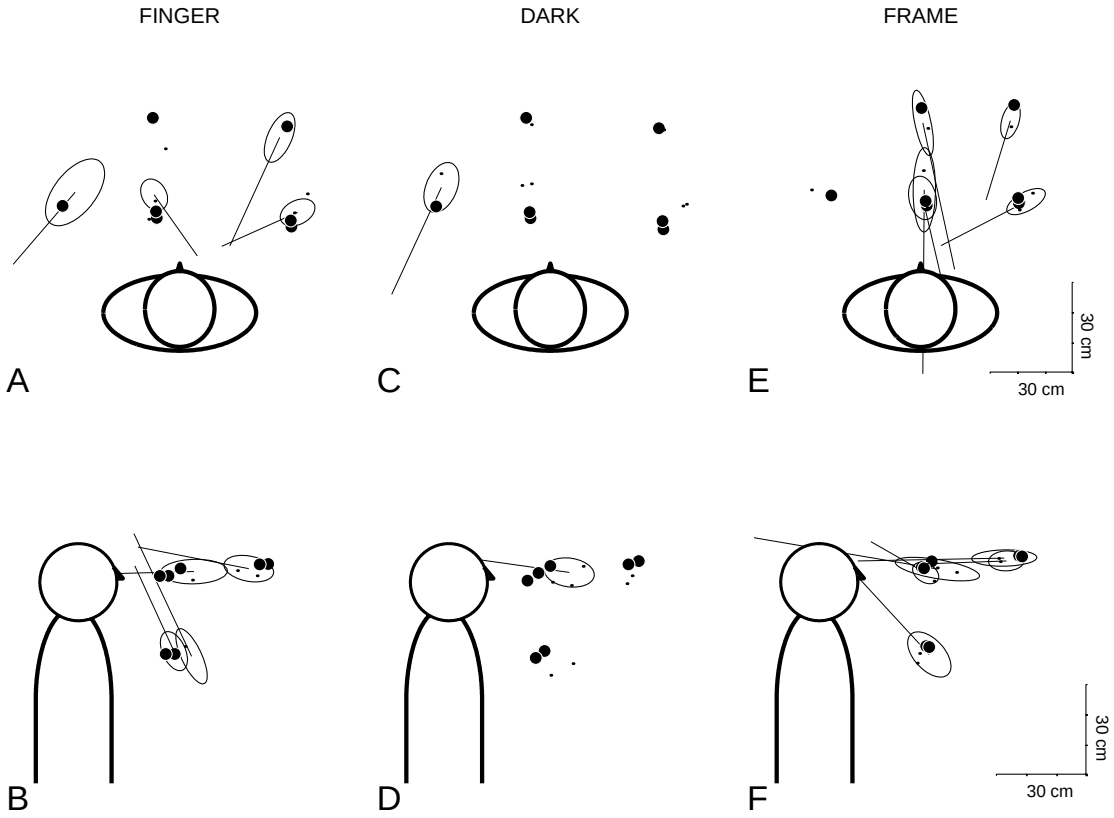

FIGURE 2.3: Typical example of pointing responses. Pointing responses for subject MV in the FINGER (panels A and B), DARK (panels C and D) and FRAME condition (panels E and F). Top panels show a top view of the subject and the data, lower panels show a side view. Large black dots represent the target positions, small dots show the individual pointing responses toward the targets. Ellipses show the 95% confidence distribution of the pointing responses, and are drawn only when the distribution has a significant orientation. Lines emerging from the ellipses indicate the direction of the main axis.

up to about 15 cm were observed. Averaged over all subjects, the constant error is significantly larger in the DARK condition than in the FINGER condition ($t=5.79$; $p<0.05$).

Similarly, the variable error is significantly larger in the DARK condition than in the FINGER condition ($t=6.05$; $p<0.05$). This is mainly caused by a large increase of errors in azimuth and elevation direction. Errors in distance are not significantly different from those in the FINGER condition. Because of the increased error in azimuth and elevation, the variable error is about the same in all directions for most target positions in the DARK condition. Fitting an ellipse to the data did not usually produce an ellipse with a clear orientation. For the data in Figure 2.3, C and D the orientation for the variable error is significant only for the leftmost target.

Figure 2.3, E and F shows data for pointing toward remembered targets with vision of the index finger and with vision of an external frame. In this condition (FRAME) the average constant error for this subject is about 4 cm, ranging from 3 to 6 cm. Averaged over all subjects, the constant error in the FRAME condition is 4 cm (SD= 2 cm). This is significantly smaller than that in the other two conditions ($t=7.08$ and $t=2.48$; $p<0.05$, for DARK and FINGER, respectively).

The variable error is also smaller than in any of the other two conditions. This effect is significant across subjects ($t=5.91$ and $t=3.00$; $p< 0.05$, compared with DARK and FINGER, respectively). The decrease in variable error is found especially along the axes in which the variability was already smallest (azimuth and elevation). Because the variability along the long axis of the distribution decreases relatively little, this results in a more pronounced orientation tuning of the 95% confidence ellipses.

Thus constant errors decrease when visual feedback of the finger is provided, and decrease even further when additional feedback of the environment is presented by means of the illuminating frame. Providing visual feedback also results in a decrease in variable errors, mainly in azimuth and elevation direction, and hardly in radial distance.

Frames of reference for pointing movements

Figure 2.3 shows pointing responses toward seven targets for one subject in three conditions. For the DARK condition most ellipses do not deviate significantly from a spherical distribution. For the FINGER and FRAME conditions, most ellipses do have a long axis with a clear orientation, usually oriented toward the subject. Therefore the analysis to test various hypotheses regarding the frame of reference for pointing, based on the search for a common origin of the main orientations of the variable error distributions, was limited to the FINGER and FRAME condition.

Using the maximum likelihood estimation procedure (see Methods) we determined the location of the most likely intersection point of all long axes of the error ellipses for each subject. The results of this analysis are shown in Figure 2.4. For each of the subjects, the point that most likely serves as the intersection point of all ellipses is indicated by a star. The circle indicates the most likely intersection point for the data shown in Figure 2.3. We tested six subjects in the FRAME condition (Figure 2.4, A and B), and ten in the FINGER condition (Figure 2.4, C and D). Although the inter-subject variability in the location of the intersection point is rather large, all subjects seem to show a most likely intersection point close to or in front of the eyes for both conditions.

Some studies in the past have suggested that the distributions of pointing errors are directed toward the shoulder (Soechting and Flanders 1989) or toward a position

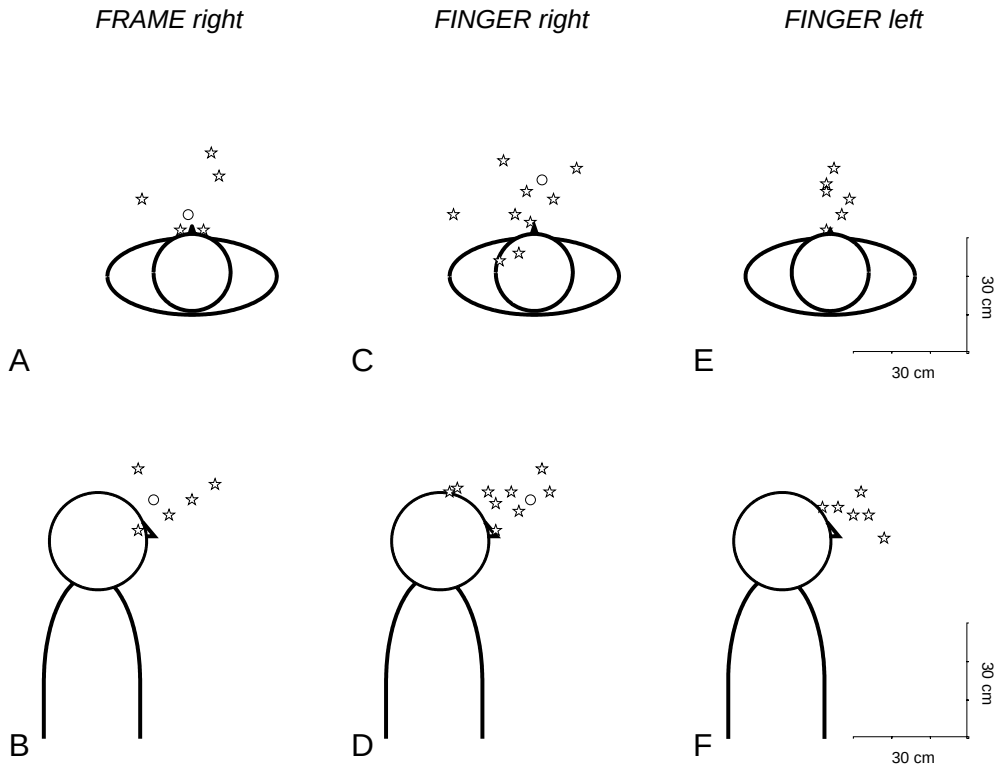

FIGURE 2.4: Most likely intersection points. Top views and side views (panels A, C and E, and panels B D and F, respectively) on the most likely intersection points (stars) for all subjects, for the FRAME condition (left hand panels) and FINGER condition for pointing with the right hand (central panels), and for pointing with the left hand (right hand panels). The most likely intersection point for the subject from Figure 2.3 is indicated in panels A-D with a circle. Six subjects participated in the FRAME condition and six in the FINGER condition for pointing with the left hand. Ten subjects participated in the FINGER condition for pointing with the right hand. Six of these subjects participated twice in this condition, and for these subjects the average of the two intersection points is displayed in this figure.

between the head and the shoulder (Soechting et al. 1990). The left and central panels of Figure 2.4 show that the most likely intersection points of the subjects in our study do not lie close to the right shoulder in either condition. To test whether the location of the intersection point is affected by the pointing arm, we asked six subjects to point with their left arm instead of the right arm in the FINGER condition. Figure 2.4 (right panels) shows a top view and a side view of the most likely intersection points for these six subjects. Clearly, the intersection points lie close to the subjects' head and the locations of the intersection points for pointing with the right versus the left arm are not very different.

Table 2.2 shows the coordinates of the most likely intersection points relative to the cyclopean eye for all subjects who pointed with either the left or the right arm in the FINGER condition. A statistical analysis showed that the sideward location of the intersection point was not significantly different for pointing with the left or the right arm ($t=1.36$, $p=0.19$). For both arms the intersection point seems to lie just in front of the cyclopean eye.

	A			B		
subject	X (cm)	Y (cm)	Z (cm)	X (cm)	Y (cm)	Z (cm)
FH				7	8	-1
JL				-1	-4	1
FW	5	-1	-6	1	13	-8
MK	7	7	2	-1	7	4
NK	7	-7	2	-1	13	-4
RO	8	13	2	2	-1	-2
AT	5	-9	2			
AT	5	3	6			
DL	-11	-13	10			
FH	-3	-8	5			
JL	15	10	7			
JL	27	-10	-3			
MK	1	11	8			
MV	-1	-5	4			
MV	-3	-15	0			
NK	-3	-15	-8			
WV	8	-20	-7			
WV	6	-8	17			
mean (sd)	4 (9)	-7 (10)	3 (7)	1 (3)	6 (7)	-2 (4)

TABLE 2.2: Position of most likely intersection points for pointing with the right arm (A) and with the left arm (B), relative to the cyclopean eye. Positive x-direction: leftward, positive y-direction: backward, positive z-direction: upward. When subjects were tested twice in the FINGER condition for pointing movements with the right arm, both data are included.

The relation between gaze and pointing position

To investigate to what extent pointing and gaze are related, binocular gaze was measured. In these experiments only a subset of the targets was tested in each of the three feedback conditions, because of the limited time available to wear the search coils. Nevertheless, the results provide evidence for a relation between pointing and gaze as a function of time, as will be illustrated below.

Figure 2.5 shows gaze at three different moments in time relative to target onset for the three visual conditions FINGER (Figure 2.5, A-C), DARK (Figure 2.5, D-F) and FRAME (Figure 2.5, G-I), for subject BB. The data are shown at 0.9 s after target onset (when the subject fixates the visible target, left panels); 2.9 s after target onset, which corresponds to 1.9 s after target offset (just before movement onset, middle panels); and 4.9 s after target onset (when the fingertip points at the remembered target position, right panels).

Figure 2.5, A, D and G shows that subjects fixate close to the target in almost all trials, when the target has been visible for 0.9 s. In the FRAME condition, subjects sometimes fixate at a point between the target and the back plane of the visible frame. At the end of the delay period, 1.9 s after target disappearance (Fig 2.5, B, E and H), gaze has drifted away from the target in a radial direction to a larger distance from the subject in all three conditions, but most clearly in the FRAME condition. During this drift period, the direction of gaze remains almost the same (i.e. any changes in azimuth and elevation are small). The amplitude of the drift at the end of the delay period depends on visual feedback of the environment. The amount of drift is about the same in the FINGER and DARK conditions, but is considerably larger in the FRAME condition (compare Figure 2.5, B and E and Figure 2.5H).

Figure 2.5, C, F and I (right side) shows gaze at the time when the subject is pointing to the remembered target position. In these panels, the variability and location of the corresponding pointing positions are indicated by the error ellipses, which capture 95% of the pointing positions. Figure 2.5, C, F and I shows that gaze is much more variable at the time of pointing than at the time of fixation to the visible target (Figure 2.5, A, D and G). Gaze and pointing seem to overlap quite well for the FINGER condition, but less so for the DARK and FRAME conditions (Figure 2.5, F and I), where gaze locations at the time of pointing are farther away from the subject than the corresponding pointing positions.

In Figure 2.5 we showed that gaze does not remain fixated to the target position throughout the trial, but changes during the delay period. To test whether errors in gaze (at some period in time) and pointing position are related, we analyzed the constant and variable errors in gaze as a function of time in relation to the constant and variable errors in pointing.

Figure 2.6 shows the constant errors in gaze averaged over all subjects, for each of the three targets. Similar to the constant error in pointing position (see Methods), we define the constant error in gaze as the deviation of mean gaze position from the target position. Because the average gaze position changes during a trial, the constant error in gaze also changes in time. The constant error in pointing position does not change during one trial, given that by definition the pointing position is the mean position of the tip of the index finger at the end of each pointing movement. The constant pointing error is indicated by a horizontal line in order to simplify a comparison with the constant error in gaze.

Figure 2.6 shows that the constant gaze errors in elevation (θ, right column) show a more or less constant offset, slightly above (target 1) or below (targets 4 and 5) the target. These small deviations of about 2º or less may represent incorrect fixation to the target by the subjects, but they could also be attributed to small errors in calibration of 3-D gaze position (see Methods). The most interesting effects are found for radial distance relative to the cyclopean eye (R) and azimuth angle (φ), which are displayed in the left and middle columns, respectively.

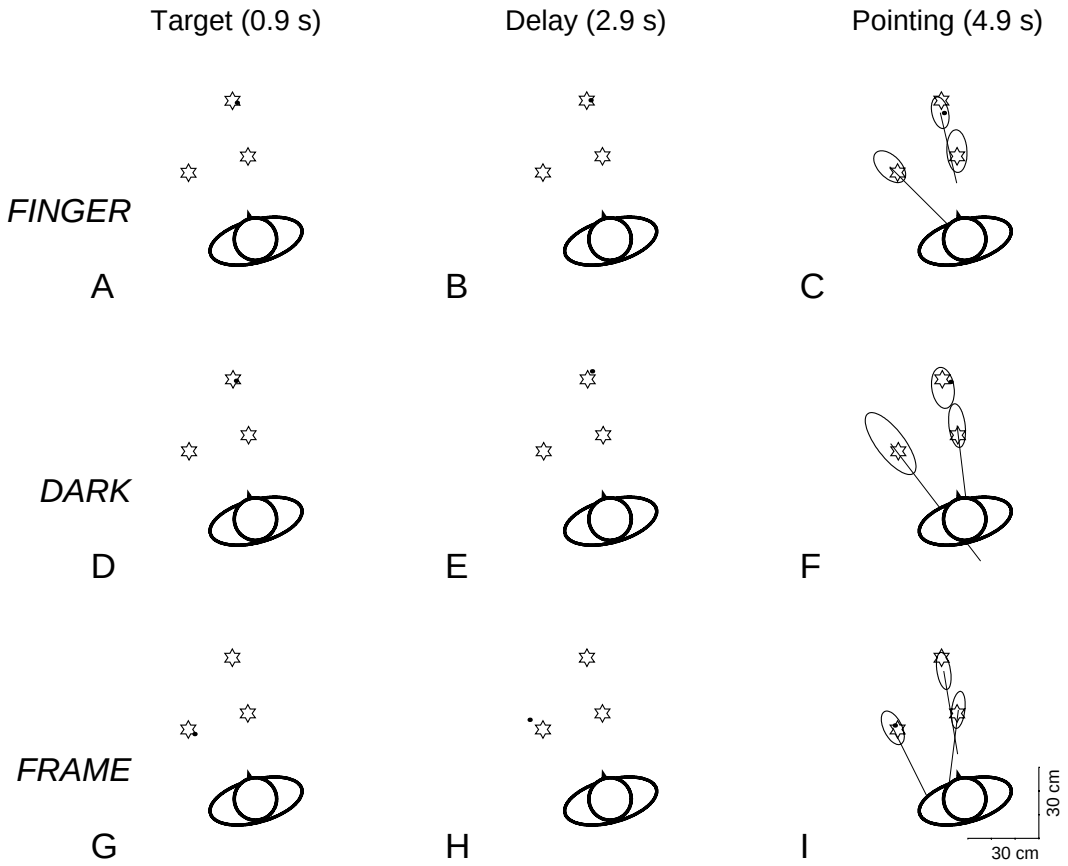

FIGURE 2.5: Gaze in time. Top views of gaze at different moments in time for subject BB: at the time of target presentation (panels A, D and G), at the end of the delay time (panels B, E and H) and at the time of pointing (panels C, F and I), for the FINGER (top row), DARK (middle row) and FRAME condition (bottom row). Stars indicate the target locations and small dots represent the gaze positions for all trials to that target. In the panels at the right hand side, ellipses indicate the 95% confidence levels of the distribution of the corresponding pointing positions. Lines emerging from the ellipses indicate the orientation of the distribution and are only plotted for elliptical distributions that have a significant orientation.

In all conditions, the average radial distance of gaze at the end of target presentation lies within 2 cm from the target, except for the most distant target (target 1), for which gaze falls short by about 5 cm. After target disappearance gaze distance increases for all three targets and in all conditions, compatible with the drift in gaze described earlier in Figure 2.5. The amount of drift away from the subject and the duration of this gaze drift are different in the three conditions.

In complete darkness (FINGER and DARK conditions, Figure 2.6, A and D) gaze distance at the end of target presentation matches the target's radial distance well. During the 2-s delay period, gaze slightly drifts away from the subject by about 3 to 10 cm. When the finger is visible during pointing (FINGER condition), gaze returns back to the radial distance of the initial gaze position when the pointing movement starts, such that gaze and pointing position match quite closely when the subject points at the target (compare the traces for gaze error and the corresponding horizontal line for pointing error in Figure 2.6A).

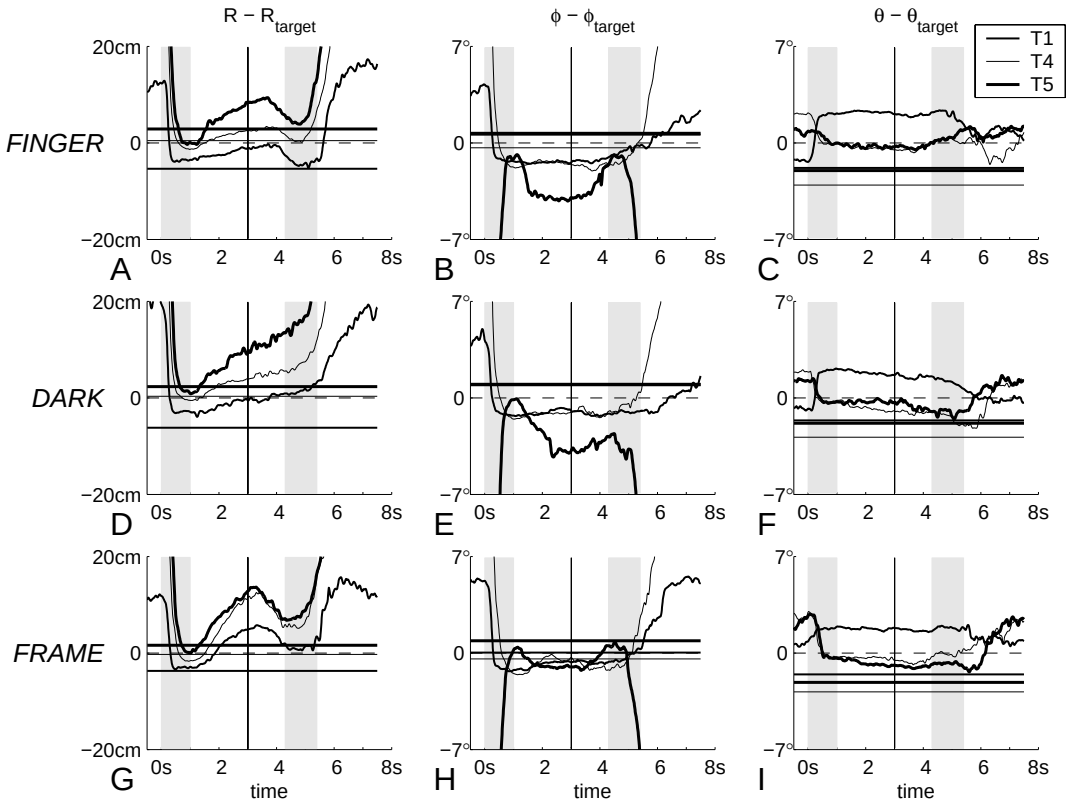

FIGURE 2.6: Constant errors of pointing and gaze in time. Constant errors are displayed for the average pointing position (solid, horizontal lines) and gaze in time for three targets: target 5 (bold lines), target 1 (medium lines) and target 4 (thin lines). The constant errors are displayed for radial distance (R, left column), azimuth (φ, middle column) and elevation (θ, right column) separately, for the FINGER (top row), DARK (middle row) and FRAME conditions (bottom row). The dashed line corresponds to a perfect reproduction of the target position. Vertical grey bars represent the interval of target presentation (0.0s. < t < 1.0s.) and the interval of pointing (4.3s. < t < 5.4s.). The vertical line at t=3s indicates the auditory tone that indicated the end of the delay period.

In the DARK condition when the finger is not visible during pointing (Figure 2.6D), gaze distance relative to the cyclopean eye does not return to the target distance, nor to the pointing distance (horizontal lines in Figure 2.6D). The average pointing error in radial distance in the DARK condition is much smaller than the average error in gaze at the time of pointing (on average about 2 versus 7 cm, respectively).

Figure 2.6G shows the constant errors in radial distance for the FRAME condition: gaze distance corresponds well to the target distance at the end of target presentation. When the target disappears, gaze rapidly drifts away from the subject in the radial direction. Figure 2.6G shows that gaze moves back toward the target position after the cue to start the pointing movement. However, at the time of pointing the decrease in gaze distance does not completely compensate for the drift in the delay period (as it did for the FINGER condition), and thus gaze does not correspond to the target distance, nor to the pointing distance, which is close to that of the target.

For constant errors in azimuth (Figure 2.6, middle columns), there is a clear distinction between targets 1 and 4 and target 5. For targets 1 and 4, which lie at eye level almost straight in front of the subject (see Figure 2.1), gaze errors in azimuth direction are small (less then 2º from the target) in all three conditions (Figure 2.6, B, E and H). Gaze azimuth remains almost constant from target offset until the end of pointing. For target 5, however, which lies about 30º eccentric to the left at eye level (see Figure 2.1) there are clear differences between the three feedback conditions: At the end of target presentation, gaze azimuth corresponds within 2º from the target position in all 3 conditions. After target disappearance, however, gaze drifts by about 3º to the right of target 5 (decrease in azimuth, corresponding to a more straight-ahead direction) in the FINGER and DARK conditions (Figure 2.6, B and E). Similar to the effects described above for gaze distance, drifts in azimuth are compensated in the FINGER condition at the time of pointing, such that gaze direction returns to the target direction. In the DARK condition, gaze direction remains to the right of the target. In the FRAME condition, the visual feedback of the environment seems to prevent large drifts in azimuth for all targets (see Figure 2.6H).

To summarize, as long as the target is visible, gaze is directed toward the target. After target disappearance gaze tends to drift away from the subject in the radial direction. In the DARK and FRAME conditions gaze remains too far from the cyclopean eye, relative to the target, whereas in the FINGER condition gaze almost completely returns at the time of pointing. In the FINGER condition, pointing errors correspond closely to gaze errors, which is not surprising given that the finger is visible during pointing. In the DARK, pointing errors are smaller than gaze errors, mainly because gaze errors are primarily attributed to drift from the target position. In the FRAME condition pointing errors are small, but gaze is directed to a position between the pointing position and the visual background.

To study the effect of variable errors in gaze on the variability of the pointing positions or vice versa, we compared gaze in time with the corresponding pointing position. There is only one pointing position per trial, but gaze may vary in time. Therefore we tested whether there is a moment in time when the variability in gaze is closest related to the variability in pointing position (see Methods).

Figure 2.7 shows the covariance between the pointing position and gaze position as a function of time, averaged over all six subjects. The average covariance for radial distance (R), azimuth (φ) and elevation (θ) is shown in the left, middle and right panels, respectively. We tested whether the time when the highest covariance was reached, was related to a specific stage in the delayed pointing task. Therefore, we focus on two time intervals: the interval of target presentation (from 0 to 1 s) and the interval during which the finger points to the target (on average from 4.3 to 5.4 s after target onset). These intervals are indicated by gray bars in Figure 2.7.

All three feedback conditions show a similar increase in covariance from target offset toward the time of pointing (see the bold lines in Figure 2.7, indicating the

values of the covariance averaged over all subjects). This increase toward the time of pointing was found for all subjects. The peak value of the covariance was reached at slightly different times in the interval between 4.3 and 5.4 s after target onset for different subjects. Therefore, the peak value of the average covariance shown in Figure 2.7 is about 25% smaller than the average of the peak values of all subjects. To overcome this problem of inter-subject timing differences, we counted the number of subjects that show a significant covariance ($p<0.05$) somewhere within the interval of target presentation (0-1 s), and the number of subjects having a significant covariance within the pointing interval (4.3 to 5.4 s). These numbers are displayed in the gray bars for each of the specific time intervals. Note that the number of subjects showing a significant covariance in the pointing interval is always at least equal to, but in general larger than, the number of subjects with a significant covariance during target presentation. We found that for almost all subjects, the largest covariance is reached in the pointing interval.

In the FINGER condition (Figure 2.7, A-C), the average covariance exceeds a 5% significance level for all three coordinates (radial distance, azimuth and elevation) at the time of pointing. Moreover, Figure 2.7, A-C shows that the covariance increases gradually toward the time of pointing, indicating that the variability in pointing resembles the variability in gaze at a time, well before the time of pointing. This means that the variability of the pointing position in radial, azimuth and elevation direction can be explained (at least partly) from the variability in gaze at the time of pointing. When the subjects are considered individually, all subjects show a significant covariance in all 3 coordinates in the FINGER condition at the time of pointing ($p<0.05$), except for one subject, who shows a significant covariance for the two directional components (azimuth and elevation, $p< 0.05$), but not for radial distance ($p=0.18$).

For the DARK and FRAME conditions (Figure 2.7, D-F and G-I, respectively), the covariance between pointing position and gaze is less pronounced: at the time of pointing the average covariance is significant for azimuth and elevation ($p<0.05$). The average covariance for radial distance, however, increases toward the time of pointing, but does not reach a significant value ($p=0.06$ and $p=0.11$ for DARK and FRAME, respectively).

As indicated by the numbers in the gray bars in Figure 2.7, D-F (DARK condition), all six subjects show a significant covariance at the time of pointing for the azimuth direction, but only four subjects also have a significant covariance for radial distance and elevation at the time of pointing. The high correlation between gaze and pointing in the FINGER condition is not surprising because of visual feedback. However, all subjects also show a significant covariance between pointing and gaze at the time of pointing in the DARK condition in at least two of the three spatial parameters. Thus, covariance at the time of pointing is also present without visual feedback of the finger during pointing.

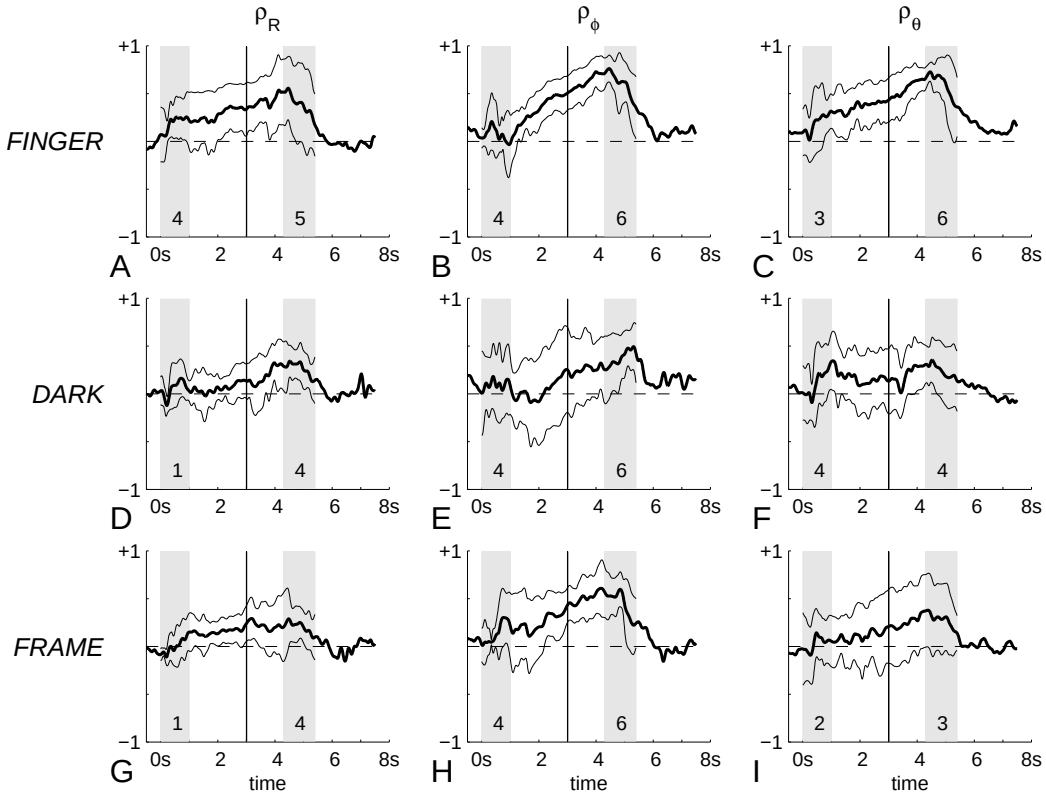

FIGURE 2.7: Covariance of pointing position and gaze in time. Covariance of pointing position and gaze in time -averaged over all subjects- is represented by a bold line. The thin lines indicate the standard deviation around the mean. Correlations are calculated for radial distance (R, left columns), azimuth (φ, middle columns) and elevation (θ, right columns), for the FINGER (top row), DARK (middle row) and FRAME condition (bottom row). Thin lines represent the standard deviation (1 SD). Vertical gray bars represent the interval of target presentation (0s < t < 1s) and the interval of pointing (4.3s < t < 5.4s). The vertical line at t=3s indicates the auditory tone that indicated the end of the delay period. The numbers in the gray bars indicate the number of subjects that show a significant covariance ($p<0.05$) within the interval.

For the FRAME condition (Figure 2.7, G-I) three subjects show a significant covariance for all three coordinates at the time of pointing ($p<0.05$). The remaining three subjects show a significant covariance in azimuth ($p<0.05$), but only one of them also shows a significant covariance in radial distance ($p<0.05$).

In all conditions, we found subjects that have a significant covariance between pointing and gaze at the time of target presentation (see the numbers in the gray bars that indicate the time of target presentation). In most of these cases, the covariance was smaller at the time of target presentation than it was at the time of pointing.

In summary, Figure 2.7 shows that the variability in pointing position is related to the variability in gaze at the time of pointing and often already at the time of target presentation. This relation is most prominent for the FINGER condition, but is also present in the DARK and FRAME condition.

DISCUSSION

In this study we have investigated the accuracy of gaze and pointing movements toward remembered visual targets in 3-D space. The results demonstrate that the presence or absence of visual feedback of the finger and of the environment has a large effect on the variable and constant errors of pointing. Moreover, we found that the variability in the final position for the pointing movement is to a large extent related to the variability gaze. Like pointing position, gaze is not always directed to the target position but may differ quite considerably from the target position depending on visual feedback conditions. We will first discuss the relation between pointing and gaze and its implications for pointing accuracy. After that, we will discuss the interpretation of the condition-specific constant and variable errors in pointing.

Gaze versus pointing

We found a significant correlation between the variable errors in pointing and in gaze at the time of pointing. This covariance between gaze and pointing could suggest three possible explanations. The first explanation could be a common command signal to drive gaze and pointing toward the same target position.

Other explanations might be that gaze affects pointing or that pointing serves as a target for gaze. Obviously, these explanations do not exclude each other. We will consider the implications of each of these hypothetical explanations in the context of our experimental results to investigate which explanations are consistent with the data.

The three possible explanations are schematically illustrated in Figure 2.8. At the time of target presentation, the orientations of the head in space (Hs), the eyes in the head (Eh) and the target on the retina (Tr) are available to calculate the perceived target position, which is stored during the delay period [Internal Target Representation, (ITR)]. This ITR is used as target for the pointing movement (path A), and can also be used to guide the eyes to keep gaze at the remembered target position (path B). Evidence for such a common command signal for the eyes and the hand has been presented before by several studies, which reported that eye and hand movements show similar characteristics in tasks like choosing between two targets (Gielen et al. 1984) or anticipating target displacements (Frens and Erkelens 1991). Our data provide additional evidence in favor of a common drive of gaze and pointing because of the -for many subjects- significant correlation between pointing position and gaze, when the target is visible (see Figure 2.7).

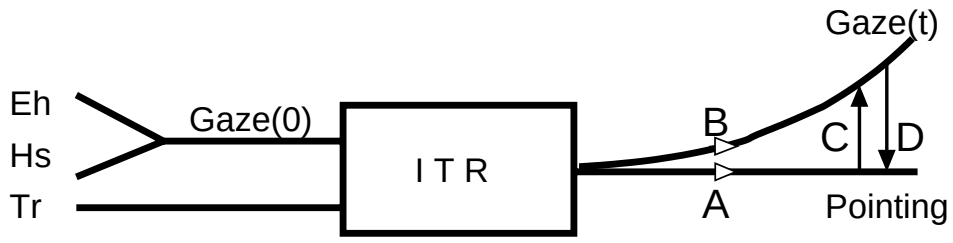

FIGURE 2.8: Possible pathways to describe the transformation of retinal information to the pointing position. Eye-in-Head (Eh) and Head-in-Space (Hs) determine gaze during fixation (Gaze(0)). Target position on the retina (Tr) and gaze during fixation determine the Internal Representation of Target position (ITR). The ITR provides a common signal to drive the arm toward the remembered target position (path A) and to drive gaze (path B). Path C represents a hypothetical pointing signal, which is used to direct gaze, and path D represents a hypothetical gaze signal, which is used to adjust the accuracy of pointing.

If the covariance between gaze and pointing were attributable only to a common command signal to the motor systems for gaze and pointing, one would expect that the gradual drift in gaze in the delay period should deteriorate the covariance between pointing and gaze. This is obviously not the case, as is shown in Figure 2.7, which shows that the covariance increases, rather than decreases with time. A possible explanation might be, that the gradual drift in gaze reflects a drift of the ITR, which then should result in a constant error in pointing, proportional to the drift of gaze. Figure 2.6 clearly shows that this effect is not found at the end of the delay period: In general, the constant error in gaze is much larger than the constant error in pointing. Therefore, a common drive cannot be the only explanation for the results reported in this study.

Because various studies have shown that deviations of gaze from the target will affect pointing accuracy (e.g. Biguer et al. 1984; Bock 1986; Enright 1995; Van Donkelaar and Staub 2000; Henriques et al. 1998) one could argue that gaze accuracy affects the accuracy of pointing. Recently Neggers and Bekkering (2001) have demonstrated a strong linkage between eye movements and pointing movements. Subjects were instructed to make a pointing movement and a saccade toward the same target. When the saccade had reached the target (but when the corresponding pointing movement was not yet completed), a new saccade target was presented. Subjects had to initiate a second saccade toward this new target, but the pointing movement had to stay directed toward the initial target. Neggers and Bekkering showed that the second saccade, away from the pointing target, was delayed until the pointing movement was nearly completed. These results were interpreted as evidence that gaze is used to improve accuracy of the ongoing pointing movement, in addition to a common command signal for eye and arm movements. This is in line with the conclusion obtained by Soechting et al. (2001), who reported that gaze position provides the target signal for hand movements to targets moving behind a moving background (Duncker Illusion).

Other evidence for gaze defining the target for pointing movements was presented by Kröller et al. (1999), who tested whether adaptive changes in saccadic amplitude influence pointing accuracy of the unseen hand, in a double-step adaptation paradigm. In the adaptation session, subjects had to make a saccadic eye movement toward a visual target on a 2-D table. During the saccade, the visual target jumped either backward or onward, thus shortening or lengthening the amplitude. This introduced an artificial post-saccadic error, which led to a corrective saccade. After the adaptation period, the saccadic system incorporated the corrective saccade in the first saccadic movement. When saccadic adaptation was achieved, subjects were asked to perform movements toward the same visual targets with the unseen hand instead of with gaze. The adaptation transfer from the saccadic system to the hand-pointing movement was most prominent, though not complete, when accompanying eye movements were allowed, but only when the adaptation concerned shortening of the saccadic amplitude.

The third alternative explanation, that gaze depends on pointing, is less likely: subjects can quite well look at remembered targets irrespective of finger position.

Evidence in favor of a role of gaze at the time of pointing on pointing accuracy was found in various studies, in which gaze and pointing position were dissociated. Bock (1986) and Enright (1995) showed that the pointing movement tends to overshoot the target distance relative to the gaze location, when gaze is not directed toward the location of the remembered target for the reaching movement. A similar finding was reported by Henriques et al. (1998, 2000), who studied pointing errors toward a remembered target, which was presented while gaze was directed in various horizontal and vertical peripheral positions not coinciding with the target. Subjects were found to overshoot the magnitude of the retinal eccentricity of the target, both in horizontal and vertical directions. Medendorp and Crawford (2002a) showed that a similar overshoot occurs when subjects are allowed to foveate a visual target but have to make a saccade in the delay period before pointing. In this paradigm, the pointing responses still indicated an overestimation of the retinal eccentricity of the target relative to gaze at the time of pointing. Therefore, the authors concluded that the target position is updated for gaze at the time of pointing, which was interpreted as evidence that target position is stored in retinocentric coordinates. A similar question was addressed by Pouget et al. (2002) who investigated whether the remembered position of a reach target is also stored in a retinocentric frame of reference for targets of other modalities (i.e. auditory, proprioceptive and imaginary targets). They found that when gaze was not directed to the target position, subjects largely overshot the retinal eccentricity of the target, irrespective of target modality.

If fixation away from the target leads to overshoot of the retinal position of the target, one would expect a negative correlation between variability in gaze and pointing in the present study, where gaze drifts away from the target in the delay period. This is not in agreement with our data, which clearly show a positive

correlation between pointing and gaze. Positive correlations have also been reported in other studies (see e.g. Flanders et al. 1999 and Soechting et al. 2001). One of the main differences between these studies and the ones that report overshoot of the target and a corresponding negative correlation is that in the latter studies, subjects deliberately fixated away from the target, whereas in our study (as in the studies by Flanders et al. 1999 and Soechting et al. 2001), subjects were not aware of the off-target fixation. None of our subjects was consciously aware of the drift in the delay period. One subject explicitly mentioned that he tried to use the strategy to rigidly fixate the remembered target in the DARK and FINGER conditions, to "anchor" the visual target in the otherwise dark environment. The results of this subject were not different from those of the other subjects, which indicates that the drift in gaze occurs unconsciously, even when a strategy is adopted to maintain gaze at the remembered target. When the remembered target position is stored relative to gaze, as suggested by, for example, Henriques et al. (1998), and when subjects are not consciously aware of the drift in gaze, the remembered target position is presumably not updated for the drifted gaze position at the time of pointing. Consequently, one will find a positive correlation between gaze and pointing, which is what we found.

Gaze drifts during delay period

From previous studies it is known that when subjects are left in complete darkness for a few minutes, gaze tends to shift toward a preferred distance, which varies between subjects from about 40 to 80 cm relative to the cyclopean eye, and slightly changes with gaze direction (*dark vergence*, Heuer et al. 1989). Gaze shifts in complete darkness, which occur already a few seconds after the disappearance of a visual target, were also described by Medendorp et al. (2002b). These authors tested the stability of gaze to a remembered target during active head movements. They found that the correspondence between target position and gaze gradually deteriorates after the visual target disappears, both for direction and for radial distance. Medendorp et al. presented a target at 20 cm from the cyclopean eye, and found that gaze distance starts to increase almost immediately after disappearance of the visual target, which is in agreement with our observations. We conclude that subjects do try to maintain gaze on the target, but fail to do so.

In the FRAME condition we found larger gaze drifts in radial distance than in the DARK and FINGER condition, and hardly any drift in direction (see Figures 2.5 and 2.6, middle columns). For the FRAME condition one might expect that it would be easier to maintain fixation at the remembered target position: the visual environment provides a reference that might assist the subject to correct for any unintended gaze drift. On the other hand, one might argue that because the visual environment provides a reference frame to store the remembered target position, precise fixation may not be that important, given that the visual frame serves as an "anchoring point" for the remembered target. Our results provide evidence for the latter because at the time of pointing gaze has not returned completely to the target

position and, nevertheless, the pointing performance is more accurate than without the frame. More evidence for the latter interpretation was provided by Blouin et al. (2002), who showed that the definition of gaze direction after several saccades in the dark is more accurate when there is visual stimulation of the retina, than when there is no visual information whatsoever. This effect is irrespective of whether the visual stimulation caries spatial information. In the FINGER condition we found that vision of the index finger resulted in a correction of the radial drift in gaze. Following the reasoning of Blouin et al., this corrective movement of gaze may be the response to a more accurate definition of gaze direction attributed to visual stimulation of the retina by the tip of the index finger.

Frames of reference

Many authors have studied pointing movements toward remembered targets. However, the conclusions of these studies have not always been congruent. Some studies concluded that subjects make pointing movements to remembered visual targets in an illuminated environment in a viewer-centered frame of reference, usually with respect to the head or the cyclopean eye (e.g., McIntyre et al. 1997; Soechting et al. 1990). Other studies suggested that pointing movements are executed in a shoulder-centered frame of reference (e.g., Soechting and Flanders 1989), or both a shoulder-centered and a head-centered frame of reference, for pointing movements in the dark (Soechting et al. 1990; McIntyre et al. 1998). These studies all describe pointing movements to remembered visual targets, but they tested subjects under different visual conditions. The question arises whether these different conditions can explain the different observations.

Previous work on the effect of vision on the accuracy of pointing movements on a 2-D table was reported by Carlton (1981), who showed that vision of the pointer (a hand-held stylus) was the most important requirement for accurate pointing, irrespective of visibility of the environment or the target. When the hand is not visible, continuous vision of the target improves the pointing performance of the hand, indicating that the CNS is able to correct pointing movements of an unseen hand during the execution (Prablanc et al. 1986; Adamovich et al. 2001).

Elliott and Madalena (1987) showed that subjects are able to accurately use a visual representation of the target in the control of aiming movements only shortly after visual occlusion. For pointing movements after delays of 2 s or longer, the pointing errors increase significantly, attributed to the decay of such visual representation.

Soechting et al. (1990) tested pointing movements toward remembered targets in the *Dark*. Unlike in our study, the room lights were on when the target was presented in the *Dark* condition of their study. They tested the average orientation of the *total error* (constant and variable error taken together) between pointing position and target position, under the assumption that errors are largest in radial distance, and much smaller in direction. For pointing in the dark, they found that the

total errors are best described relative to an origin located between the head and the shoulder. They also analyzed pointing movements when the room lights remained on after target presentation. In this *Light* condition they found that total pointing errors were best described relative to a position close to the subject's eyes. From these results they concluded that there exists both a head-centered and a shoulder-centered representation of target location in the CNS, and that for pointing in the dark, the CNS includes the shoulder-centered representation.

The FRAME condition in the present study is similar to the *Light* condition in the study by Soechting and colleagues. In this condition we find that orientations of the variable errors are best described as originating from a center close to the subject's head. However, in the DARK setup, we did not find that the variable errors originate from a distinct origin at or near the head or the shoulder or in between. Differences between the results of Soechting and Flanders and the findings of our study may well result from differences in the approach to estimate the orientation of the pointing errors. The analysis by Soechting and Flanders was based on the total error whereas we analyzed the variable and constant errors separately. The two approaches will lead to the same conclusions, when the constant errors are mainly in radial distance. In our study, however, we found moderate constant errors also in direction, especially in the DARK condition (2º in the FINGER and FRAME conditions and 4º in the DARK condition), and these may result in different origins for the variable errors and for the total errors.

McIntyre et al. (1998) tested movements toward remembered targets performed in the dark and in a dimly lit room, apparently similar to our DARK and FRAME conditions. They found that, with vision of the environment and the arm, the distributions of variable pointing errors are oriented toward the subject's head. McIntyre and colleagues also tested the *local distortion*, which described the fidelity with which the relative spatial organization of targets within a small workspace region (on a sphere of 22-mm radius) is maintained in the configuration of final pointing positions. They found that the pointing positions reflected a contraction of the target configuration along an axis that was oriented toward a position between the subject's head and the shoulder. They interpreted the orientation of the variable errors and that of the local contraction as indicative for the use of both a viewer-centered and a shoulder-centered frame of reference. However, there may be alternative explanations.

Carrozzo et al. (2002) showed that the configuration of the targets influences the orientation of variable pointing errors, even though the targets were never presented simultaneously. Gentilucci et al. (1996) showed that the manifestation of such allocentric effects is strengthened by a delay between the visual stimulus and the motor response. In our study we used a delay period of 2s, which suffices for allocentric effects to occur. Nevertheless, we found no effects on the variable errors related to our target configuration. This may be attributed to the fact that our target configuration was more complex than the configuration used by Carrozzo and colleagues, in which the targets were located on a straight line. In the setup in which the subjects were provided with the most allocentric information (FRAME), one

might expect to find variable errors related to the illuminating frame. However, we found that the orientation of the pointing variability in the FRAME condition was largely related to gaze, instead of to the illuminated frame. A significant correlation between the variability in pointing and gaze was also found in the DARK and FINGER conditions. This may seem in contradiction to earlier findings of Prablanc et al. (1979), who tested gaze and pointing movements toward targets in 2-D, in a setup similar to that of our DARK condition. In their study, the target disappeared immediately after onset of the goal directed saccade. Therefore the target was not foveated and, moreover, the delay between target offset and the start of the pointing movement was much shorter than that in our study. Probably, the use of gaze for the definition of the pointing target, as is indicated by path D in Figure 2.8, takes place only when the target is actually foveated or when the target position has to be remembered for some time, as was the case in our study.

Another explanation for the distribution of variable errors was presented recently by Van Beers et al. (2002), who proposed an *optimal integration model* for the perception of position, which integrates information from different sensory modalities, weighted by their accuracy for each direction. They suggested that vision is more accurate for target direction than proprioception, but less so for radial distance. Therefore, errors in azimuth and elevation are thought to result from errors in vision and errors in radial distance supposedly result from errors in proprioception, which are larger than directional errors in vision. This might explain why the pointing errors in the FINGER and FRAME conditions are smaller in azimuth and elevation than in radial distance.

According to the suppositions of Van Beers et al. (2002) the CNS will use visual information for direction and proprioceptive information for distance, when the finger is visible (FINGER and FRAME conditions). When the finger is not visible (DARK condition), proprioceptive information will be used for both distance and direction. As a result, the variable errors in direction will be larger in the dark, given that the CNS has to rely on proprioceptive information, which is less accurate than visual information. This corresponds to almost spherical distributions of variable errors, just as we found for the DARK condition in the present study, and as reported previously by Desmurget et al. (1998). We found that providing visual feedback of the finger position (FINGER) decreases variable errors in direction. The large directional variability in the DARK condition resulted in almost spherical distributions, thus making it impossible to decide on the orientation of the variable errors. Moreover, when the accuracy of the visual information is increased by providing visual information about the environment (FRAME condition), we find that variable errors in direction decrease accordingly, which is also in agreement with the model proposed by Van Beers et al. (2002).

We have shown that the variability in pointing positions correlates highly to gaze at the time of pointing. This can be explained by a combination of 1) a common drive to the motor systems for gaze and pointing, and 2) an effect of gaze on pointing accuracy at the time of pointing. The eye-centered orientation of the

distribution of pointing positions found in previous studies may therefore reflect the effect of the variability in gaze (which is less stable in distance than in direction), in addition to possible internal reference frames used in processing and storage of the remembered target position.

CHAPTER 3

GAZE AFFECTS POINTING TOWARDS REMEMBERED VISUAL TARGETS AFTER A SELF-INITIATED STEP

INTRODUCTION

Reaching for nearby objects requires only an arm movement, which brings the hand to the object. However, when an object is at a distance that exceeds the length of the arm, a movement of the whole body or a few steps may be needed to reach the object. In such a case, the internal representation of target position relative to the subject must be updated for the movement of the body in order to preserve a correct representation of the target position relative to the subject. If the pointing movement is made towards a remembered visual target and when the body movement is made in total darkness, the task is even more complex, since the internal representation of object position relative to the body has to be updated for the body displacement without any visual feedback. Moreover, incorporating egomotion to make the proper hand movement requires that the subject adequately combines egocentric and allocentric information about target position and egomotion displacement.

The updating of a target position for a body movement has been addressed by several studies before. For example, Medendorp and colleagues (1999) investigated the accuracy of pointing movements to a remembered visual target after a step and the frames of reference that are involved in such a task. Their main conclusion was that subjects underestimate the size of the step, leading to systematic errors in reaching to the remembered targets. Based on the observed errors in reaching after a step, they concluded that the underestimation of the step was better described in Cartesian coordinates than in egocentric coordinates.

These results raise many questions regarding the underlying mechanisms for pointing. First of all, the study by Medendorp et al. (1999) did not measure eye movements. Since the accuracy of pointing depends on fixation (Henriques et al. 1998), it is not clear whether errors were due to errors in fixation to the remembered target during the delay period between stimulus presentation and pointing, or whether pointing errors are due to errors in the updating of target position relative to the subject during and after the step. Moreover, a firm conclusion regarding the use of egocentric versus world coordinates requires that subjects are tested in conditions

with various feedback conditions. We will elaborate on these questions in more detail below.

The issue of accuracy of fixation during egomotion has been studied from a different perspective by many studies on gaze control. Most of these studies investigated the role of the visual and vestibular system on gaze in subjects while they were rotated or translated passively (see e.g. Harris et al. 2000; Paige et al. 1998). Only few studies have investigated gaze control in subjects who made active movements. During active body motion, visual, vestibular, proprioceptive information, and possibly also corollary discharges are available to assist the control of gaze for target fixation. In a recent study Medendorp and colleagues (2002b) measured the quality of gaze control in subjects during head translations in complete darkness while subjects were instructed to fixate a visual or remembered visual target. In the latter condition the gain of the required changes in gaze - necessary to fixate the target- decreased, especially for near targets (e.g. 20 cm in front of the subject). This indicates that fixation position does not always match the real position of the remembered target during active movements in the dark.

These results on gaze control are relevant in the context of reaching to remembered visual targets, since several studies (e.g. Henriques et al. 1998; Van Donkelaar and Staub 2000) have shown that the accuracy of reaching to a remembered target depends on gaze direction. In addition, Flanders et al. (1999) have indicated a relationship between reaching and head orientation during ego-motion. These authors measured head orientation (not eye movements!) during a reach that included a step, and reported that the reaching errors were related to the variability in the orientation of the head. Based on these findings, Flanders and colleagues suggested that the orientation of the head might serve as a reference for the control of arm movements. In a recent study on binocular fixation during reaching towards remembered visual targets without a step, we have shown that binocular fixation, resulting from both the head orientation in space and the eye orientation in the head, affects the accuracy of reaching movements (see Chapter 2).

With this information in mind, we can define several hypotheses regarding the control of pointing and gaze to remembered visual targets and their interaction. A common input signal (i.e. visual information about target position) might provide input both to the oculomotor system to direct gaze to the remembered target and to the motor system to bring the hand to the remembered target. Any errors in this common input signal should cause a covariance in gaze and pointing accuracy. An alternative hypothesis, that gaze would affect the accuracy of pointing, would also cause a covariance between position of gaze and pointing. However, we can distinguish between these two hypotheses, since gaze can change in the delay period. If gaze changes during the delay period after offset of the visual target (i.e. when the common input does not change any more), the covariance between gaze and pointing due to a common input should *decrease* after target offset. However, if gaze affects pointing, changes in gaze in the delay period should give rise to a *gradual increase* of covariance in the period from target onset until the pointing movement. A third alternative could be that the stored target position is incorrectly

updated during the step. In that case, errors in stored target position relative to the body might increase in the delay period and will affect both gaze and pointing. We can discriminate between the hypothesis of a covariance between gaze and pointing due to the step and the hypothesis, that gaze affects pointing, by subtracting any covariance of gaze and pointing signal with the step signal from gaze and pointing. Any covariance, which is left after correcting for any covariance by the step, has to be due to an effect of gaze on pointing or the other way around.

Previous studies have shown that visual information of the environment may affect the perception of self-motion (Harris et al. 2000; Philbeck 2000; Panerai et al. 2002), and that vision of the environment, along with information from the vestibular system, helps the CNS to accurately direct gaze. Furthermore, visual feedback of the finger was shown to influence reaching accuracy (McIntyre et al. 1998). In order to investigate the various relevant frames of reference that are involved in pointing to a remembered visual target after a step, we have tested subjects in three visual feedback conditions: 1) DARK, without any visual feedback at any time; 2) FINGER, with visual feedback of the finger position during reaching; and 3) FRAME, with a visible environment and with visual feedback about finger position during the step and the pointing movement. In the DARK condition, subjects have to store the target position relative to the subject and they have to incorporate the step using proprioceptive information, vestibular information, or efference copies in order to update the remembered target position relative to the subject after the step. In the FRAME condition, subjects may be less dependent on updating of target position relative to the subject by using proprioceptive or vestibular information or efference copies, since they can remember the target position relative to the external visual environment. Therefore, we expect that pointing errors will be much smaller in the FRAME condition, than in the DARK condition if errors in pointing after the step are due to underestimation of the step, as suggested by Medendorp et al. (1999). Since an illuminated environment might provide enough light to make the finger visible to the subject, the FRAME condition might differ from the DARK condition in two aspects: the visible environment and the visible finger. In order to investigate the effect of vision of the finger, we included the FINGER condition. Since visual information is more accurate than proprioceptive information (Van Beers et al. 2002), differences in pointing accuracy in the DARK and FINGER condition reflect an effect of visual information of finger position on pointing accuracy.

In summary, the aim of this study was to investigate the updating of a remembered target position for egomotion. Since previous studies have suggested that errors in pointing after a step are due to underestimation of the step size, the first aim of this study was to investigate how the constant and variable errors of pointing depend on the size of a step in conditions of variable visual feedback. Secondly, there is evidence that deviations of binocular fixation from the target position affect the accuracy of pointing (see e.g. Henriques et al. 1998). Therefore, the second aim of this study was to measure gaze during and after the step and to explore whether and how the variable error in pointing covaries with the change of

gaze in time. Since gaze changes in time, we tested whether the covariance between fixation and pointing, if any, is strongest in the delay period near target offset or near pointing.

METHODS

Six subjects (aged 21-49 years) participated in this study. All subjects had normal or corrected to normal vision and none of the subjects had any known history of neurological, sensory or motor disorders. All subjects were right handed, except for subject MA. All subjects performed the pointing movements with the right arm. Two subjects (MA and SG) were familiar with the aim of this study. Their results were not different from those of the other subjects. The experimental protocol was approved by the Medical Ethical Committee of the University of Nijmegen and all subjects gave informed consent before the experiment.

Experimental setup

All experiments were performed in a completely dark room, and subjects were tested in three visual feedback conditions: pointing to a remembered visual target in complete darkness (DARK), pointing with visual feedback of finger position by means of a red light emitting diode (led) on the tip of the index finger which was visible at all times (FINGER), and pointing with a finger led and in the presence of an illuminated cubic frame of 90 x 90 x 90 cm^3 (FRAME). This frame formed a well-defined visual environment by means of illuminated optic fibers along its edges (see Chapter 2). In the present study, we shortened the length of the lower optic fiber at the right side of the cubic frame to avoid collision of the subject with the frame during the step. For symmetry, we also shortened the lower optic fiber at the left side of the cubic frame.

Three targets were used in the experiments, which were located within the cubic frame (see Figure 3.1). One (central) target was positioned 15 cm above, 15 cm to the right and 50 cm in front of the center of the cube's back plane. The other two targets (targets 2 and 3) were positioned 25 cm to the left and 25 cm behind the central target, respectively. The most distant target lay about 20 cm in front of the back plane of the cubic frame. The number of targets had to be restricted to three in order to keep the duration of the experiment under 45 minutes. The 45-minute period is roughly the limit to comfortably wear the search coils, which were used to measure eye movements.

Before each trial, subjects positioned their feet in a L-shaped obstacle, which was attached to the floor. This certified a unique and reproducible starting position of the subject for each trial. The subject's hand was relaxed with the arm pointing downwards along the body. Each trial started with the onset of one of the three

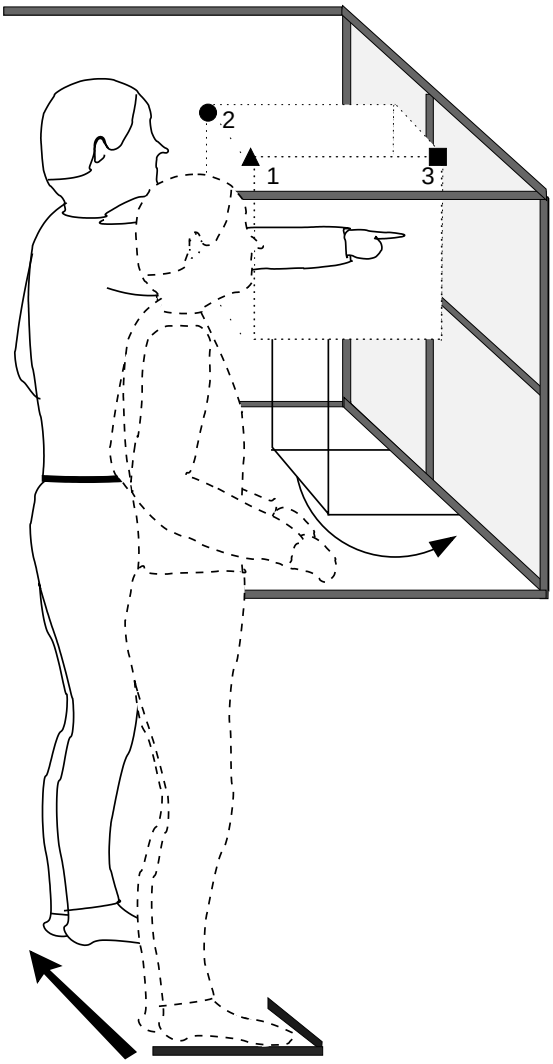

FIGURE 3.1: Experimental setup with the position of the subject before (dashed lines) and after (solid lines) the step. An L-shaped obstacle attached to the floor indicated the start position before the step. After the step, the subject stood with the cyclopean eye at a distance of about 25 cm in front of the position halfway between targets 1 and 2. Targets (black symbols) were located at a height of about 15 cm above the shoulder; target 2 (black dot) was placed 25 cm to the left relative to target 1 (black triangle), and target 3 (black square) was positioned 25 cm behind target 1. Thus the workspace of the right shoulder ranged on average from about 28 cm (targets 1 and 2) to 52 cm (target 3) in distance. Azimuth angles from the shoulder to the targets were on average -27º for target 1, +27º for target 2 and -14º for the most distant target 3 (negative azimuth angles indicate positions to the right). Since the size and direction of the step varied slightly between trials, the distances of the targets relative to the shoulder varied as well. After target extinction the framework was canted away (arrow). Solid gray lines indicate the 90 x 90 x 90 cm3 frame, which was illuminated in the FRAME condition.

target leds for a period of one second. The targets appeared in front of the subject with the center target about 50 cm to the left of the subject (see Figure 3.1). Immediately after disappearance of the target, the frame with targets was canted away, denying any visual or tactile feedback during pointing. The frame with targets was rotated downwards along a horizontal axis by approximately 135 deg bringing it behind the back-plane of the cubic frame and making the targets invisible to the subject even when the luminous cubic frame was on. Subjects were instructed to make a leftward step of about 50 cm immediately after target offset, which would bring the subject's cyclopean eye at a distance of about 25 cm in front of the position halfway between targets 1 and 2. Since different subjects made steps of different sizes (range about 10 cm), we positioned the L-shape obstacle for each subject individually, such that each subject would end at the intended position after stepping their average step size.

Usually subjects started to make a step about 500 ms after target offset, which provided enough time to remove the targets and which prevented any chance of hitting the frame during the step. Two seconds after target disappearance, an auditory signal cued the subject to start the movement placing the index finger at the remembered target position. Subjects were instructed to simply lift the arm and to keep the tip of the index finger at the pointing position for at least half a second. Then subjects returned to the starting position to prepare for the next trial.

Each feedback condition was tested in two blocks with 20 trials each. All three targets appeared in a quasi-randomized order in each block, which resulted in at least 13 trials per target. Blocks with different visual feedback conditions were presented in randomized order. A block of 20 trials typically lasted about three minutes, and after each block the room lights were switched on for about one minute to avoid dark-adaptation. Before the experiment, one block of test-trials was run to familiarize the subject with the procedure.

Experimental set-up

The position of various segments of the subject's body and the position of the targets were measured with an OPTOTRAK 3020 system (Northern Digital), which measures the three-dimensional position of infrared-light-emitting-diodes (ireds) with a resolution better than 0.2 mm within a range of about 1.5 m^3 (see Chapter 2). The positions of ireds were measured with a sampling frequency of 100Hz.

Ireds were placed on the subject's shoulder (*acromion*) and elbow (*epicondylus lateralis*). The position of the tip of the index finger was measured by means of an ired attached on a thimble on the index finger. This thimble also contained a visible red led that provided the subject with visual feedback of finger position in the FINGER and FRAME conditions. During the experiment the subjects wore a helmet with six ireds, which were configured such that the positions of at least three of them were visible for the OPTOTRAK system at all possible head orientations. This was necessary to calculate 3-D head location and orientation at all times.

At the beginning of the experiment, we asked subjects to orient their head such, that all ireds on the helmet were visible to the OPTOTRAK camera. We then held an ired at both of the subject's closed eyes and measured the position of the two eyes relative to the ireds on the helmet. With this calibration, we could derive the position of the eyes in space at any time during the experiment from the orientation and location of the helmet in space, even when the subject was facing away from the OPTOTRAK system. We made sure, that the orientation of the helmet on the subject's head did not change throughout the experiment.

Binocular eye orientation was measured using the scleral search coil technique (Collewijn et al. 1975) in a large magnetic field system (Remmel Labs). This system consists of a cubic frame of welded aluminum of 3 x 3 x 3 m^3, which produced three orthogonal magnetic fields at frequencies of 48, 60, and 80 kHz. Subjects were tested as close as possible to the center of the large magnetic field system.

During each trial subjects performed a step, and therefore their position relative to the large magnetic field varied. In order to correct for changes in the eye-coil signals due to small inhomogeneities of the magnetic field within the range of the step, we performed two calibrations of the eye coil signals: one at the location where subjects stood before the step, and one approximately at the location were they arrived after the step. During the calibration procedures subjects fixated a series of red leds attached to a board at a distance of 75 cm in front of the subject, which resulted in a calibration range from about –40˚ to +40˚ in both elevation and azimuth (for the full calibration procedure: see Chapter 2). For each eye, the two-dimensional calibration errors -defined as twice the standard deviation of the data relative to the calibration fit- were typically about 0.5˚ in azimuth and 1˚ in elevation on average; resolution was less than 0.04º. The errors in 3-D fixation position within the target range tested here were on average about 0.6˚ and 1.1˚ in azimuth and elevation, respectively, and 3 cm in radial distance from the cyclopean eye. Coil signals were sampled at 500 Hz. In offline analyses, the coil signals were resampled at 100 Hz (same sample frequency as the OPTOTRAK system) by cubic spline interpolation.

Data analysis

We define *pointing position* as the position of the ired on the tip of the index finger at the end of the pointing movement towards the target. We distinguish between two types of pointing errors: the *constant error*, which is the distance between the led position of a target and the average of all pointing positions towards that target, and the *variable error*, which reflects the distribution of the pointing positions towards a target relative to the average pointing position to that target. The distribution of the pointing positions for target i is described by the 3-D covariance matrix S_i.

$$S_i = \frac{\sum_{j=1}^{n} \pi_j^i \left(\pi_j^i\right)^T}{n-1} \qquad (3.1)$$

Where n is the number of trials to target i and $\pi_j^i = p_j^i - \bar{p}^i$ is the deviation of the finger position in trial j to target i relative to the mean pointing position $\bar{p}^i$ to target i. The three orthogonal eigenvectors of the covariance matrix S_i describe the main axes of the orientations of the variable error. The corresponding eigenvalues of the matrix give the size of the variable error in the directions of the eigenvectors. These eigenvalues of the covariance matrix S_i can be scaled to compute the limits that contain 95% of the data (see McIntyre et al. 1997). If one or two pointing positions deviated more than 3 SD from the ellipsoid fitted to the pointing positions, we left out these pointing positions and derived the covariance matrix again. Due to

this rejection procedure, less than 3% of the data was not incorporated in further analyses.

We tested whether variability in the pointing position was correlated to variability in the step. When the covariance between pointing position and the step was significant, we tested to what extent the variability in pointing positions could be explained by the variability in the step size, by fitting a linear regression, minimizing the quadratic error $\sum_{i,j}\left(\varepsilon_j^i\right)^2$ in:

$$\pi_j^i = \tau \cdot \sigma_j^i + \varepsilon_j^i \qquad (3,2)$$

where $\sigma_j^i = s_j^i - \bar{s}^i$ is the deviation of the step in trial j relative to the mean step $\bar{s}^i$ for pointing to target i. Since, by the above definitions, π_j^i and σ_j^i have mean values equal to zero, ε_j^i represents Gaussian noise with mean value zero. The weight τ corresponds to the slope of the linear regression. In the analysis to investigate any relation between gaze and pointing except for a mutual correlation by step size, the step's contribution ($\tau \cdot \sigma_j^i$) was subtracted from the pointing position data p_j^i. By doing so we corrected the pointing positions for any direct effect of the step's variability. The same was done to correct gaze for the influence of the step's variability, when gaze showed a significant covariance with the step. A χ^2-test demonstrated that second or higher order terms did not result in a significantly better description (taken into account the number of degrees of freedom and the uncertainty of the higher order fit parameters; see Results section).

Although subjects were rather consistent in the timing of their stepping, slight differences in onset, duration, and extent of the step were observed. For each trial, the velocity profile was fit by a normal distribution centered around the time of peak velocity as a bell-shaped approximation of the velocity profile. The onset and offset of the step were derived from this fit, as the moments in time, when the velocity exceeded a threshold of $e^{-(3.75)^2}$ times the peak velocity, which corresponds to positions at 3.75 SD of the normal distribution.

For an accurate estimate of the average trajectory of the binocular fixation position during the step, the gaze position data during the steps were resampled onto 300 samples between onset and offset of the step, using cubic spline interpolation. The average trajectory of fixation position in time is then derived from all time-resampled trajectories.

To calculate the covariance between pointing position and fixation position, we focused on the interval from the end of the step until the time when the index finger had reached the pointing position. In order to derive the average behavior of the fixation position during intervals that were different in length for different trials, we stretched the fixation data in each such interval onto 300 samples, as explained above. The covariance between fixation position and pointing position was then derived between the resampled fixation data and the corresponding pointing

position for that trial for each sample *i* (with *i* between 1 and 300). This procedure revealed the changes in the covariance between fixation and pointing during the delay period when the subject has completed the step until the index finger has reached the pointing position.

RESULTS

Pointing results

In this study, we investigated pointing movements towards remembered visual targets after an intervening self-initiated step. This task requires memorizing the target position and updating of target position relative to the subject after the step. In this section, we will first focus on the errors in pointing and fixation after a step and their relation to the size and direction of the step. Then we will discuss the relation between pointing position and fixation during and after the step.

Figure 3.2 shows a top view of the main results for subject JV for pointing after a step for three different feedback conditions (DARK, FINGER and FRAME, in Figures 3.2A, B and C, respectively). All pointing positions lie to the left and slightly in front of the targets, relative to the subject. The constant pointing errors in Figure 3.2 are on average about 10 cm, 11 cm and 7 cm for the DARK, FINGER and FRAME condition, respectively (range 6 to 13 cm). The results for this subject are typical for all subjects: For all subjects and all conditions, constant pointing errors ranged from 2 to 18 cm. Averaged over all subjects, the constant errors were not significantly different in the DARK and FINGER condition: 10 cm (SD= 3.5 cm) and 10 cm (SD= 3.4 cm), respectively ($t= 0.6$, $p>0.10$). In the presence of the illuminated frame (FRAME condition) the average constant error was significantly smaller than in the DARK and FINGER condition (7 cm (SD= 3.1 cm), $t= 2.7$; $p<0.05$ for both).

The variability of the pointing responses -as indicated by the ellipsoids- is large for pointing after stepping in complete darkness (DARK and FINGER conditions, Figure 3.2A and B) compared to that in the FRAME condition (Figure 3.2C). Averaged over all subjects, the variable errors in the FRAME condition -measured as the volume of the 95% confidence ellipse- were more than twice as small as the variable errors in the DARK and FINGER condition. These differences were significant ($p<0.01$). Variable errors were not significantly different in the DARK and FINGER condition ($p>0.10$).

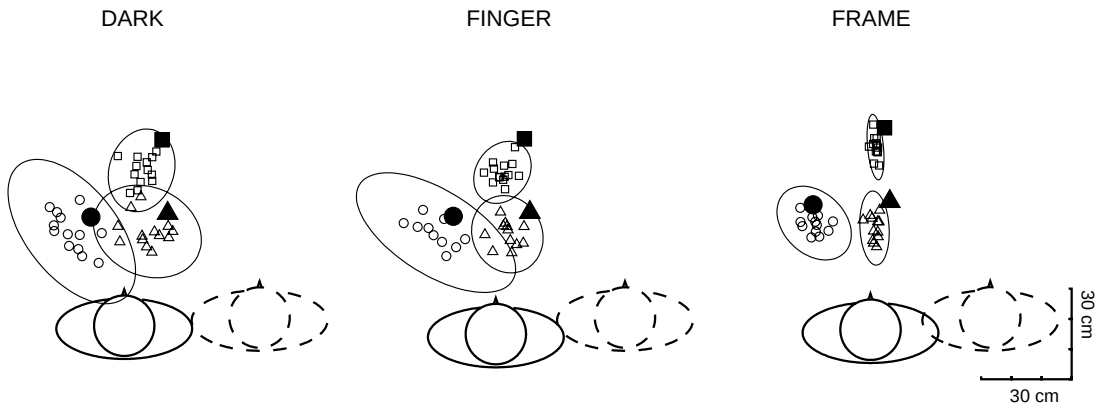

FIGURE 3.2: Top view of the pointing positions for subject JV in the FINGER condition (A), DARK condition (B) and FRAME condition (C). Target positions are indicated with large, black symbols: a triangle (target 1), a dot (target 2) and a square (target 3). The pointing positions are indicated with the small open symbols corresponding to the target. Ellipses show the 95% confidence distribution of the pointing positions. A drawing of a fictive subject indicates the overage position of the subject before the step (dashed lines) and after the step (solid lines).

During the step to the left, the subject in Figure 3.2 (JV) tended to step slightly backwards by about 5 cm. Some subjects systematically stepped slightly backwards, whereas others stepped slightly in forward direction. The size of the forward/backward component of the step was on average about 10% or less of the size of the sideward component (maximum 5.7 cm). The variability in step size appeared to be highly useful in our analyses to determine the relation between step size, fixation position, and pointing position. If subjects incorporate the step perfectly in the pointing movement to the remembered target, pointing position would be on the target, irrespective of variability in the step. However, for pointing after a step in a dark environment (DARK and FINGER conditions), the variability in pointing appeared often to be significantly correlated with the variability of the step ($p<0.05$), in the forward or sideward direction, or in both. Figure 3.3 shows an example of regressions for subject JV in the FINGER condition (same data as shown in Figure 3.2), for targets 1, 2 and 3 (left, middle and right column) in sideward and forward direction separately (top rows and bottom rows, respectively). This figure shows that for this subject, the pointing variability revealed a significant covariance in the sideward or forward direction for each target: Targets 1 and 3 show a significant covariance for the forward direction, whereas target 2 shows a significant covariance for the sideward direction ($p<0.05$).

The covariance between step-size and pointing position was positive for almost all subjects in all conditions. A Wilcoxon-Signed Rank test showed that the covariance across subjects was significantly larger than zero ($p<0.05$) for each condition. However, although significantly positive across all subjects and conditions, the covariance was not always significant because of the scatter in the data (see e.g. Figure 3.3). A Rank-Sum test (Krauth, 1988) revealed that more

subjects showed a significant covariance for targets 1 and 2, than for target 3 ($p<0.05$, see also Table 3.1). Averaged over all cases, where the covariance was significant, the mean covariance was 0.69 (SD= 0.18), 0.60 (SD= 0.23) and 0.64 (SD= 0.25) for the FINGER, DARK and FRAME conditions, respectively. These values were not significantly different for the three conditions.

	DARK	*FINGER*	*FRAME*
target 1	3	4	3
target 2	5	6	2
target 3	1	3	0

TABLE 3.1: Number of subjects that showed a significant covariance between the variability of pointing and stepping. Subjects are counted if the covariance was significant either in forward direction, in sideward direction or in both. In each condition, six subjects participated.

When a significant correlation was present, the slope of the linear regression of variability in pointing as a function of the variability in step was usually larger than 0.4, and not significantly different for the forward and sideward direction or for different targets. The average slope for all subjects and all targets was 0.60 (SD= 0.23, range 0.32 to 1.19) in the DARK condition, and 0.69 (SD= 0.18, range 0.40 to 0.95) in the FINGER condition. In the FRAME condition, the subjects accounted almost correctly for the step size in pointing. As a consequence, the covariance between the variability of pointing and step variability was low (below 0.4) and usually not significant in the FRAME condition ($p>0.1$).

The *Goodness of Fit* of the significant linear regression showed that about 23% of the sideward pointing variability was explained by the variability in the step, whereas in the forward direction, the variability in the step explained about 35% of the pointing variability. This indicates that about 65% of the variability is not explained by the step. This remaining variability has to be attributed to noise or to other inputs such as possibly the variability in gaze.

We used a χ^2-test to evaluate whether a second-order fit of pointing variability as a function of step variability gave a significantly better fit compared to the linear regression. This test demonstrated that including a second or higher order term did not result in a significantly better description (taken into account the number of degrees of freedom and the uncertainty of the higher order fit parameters). Thus a linear regression was sufficient.

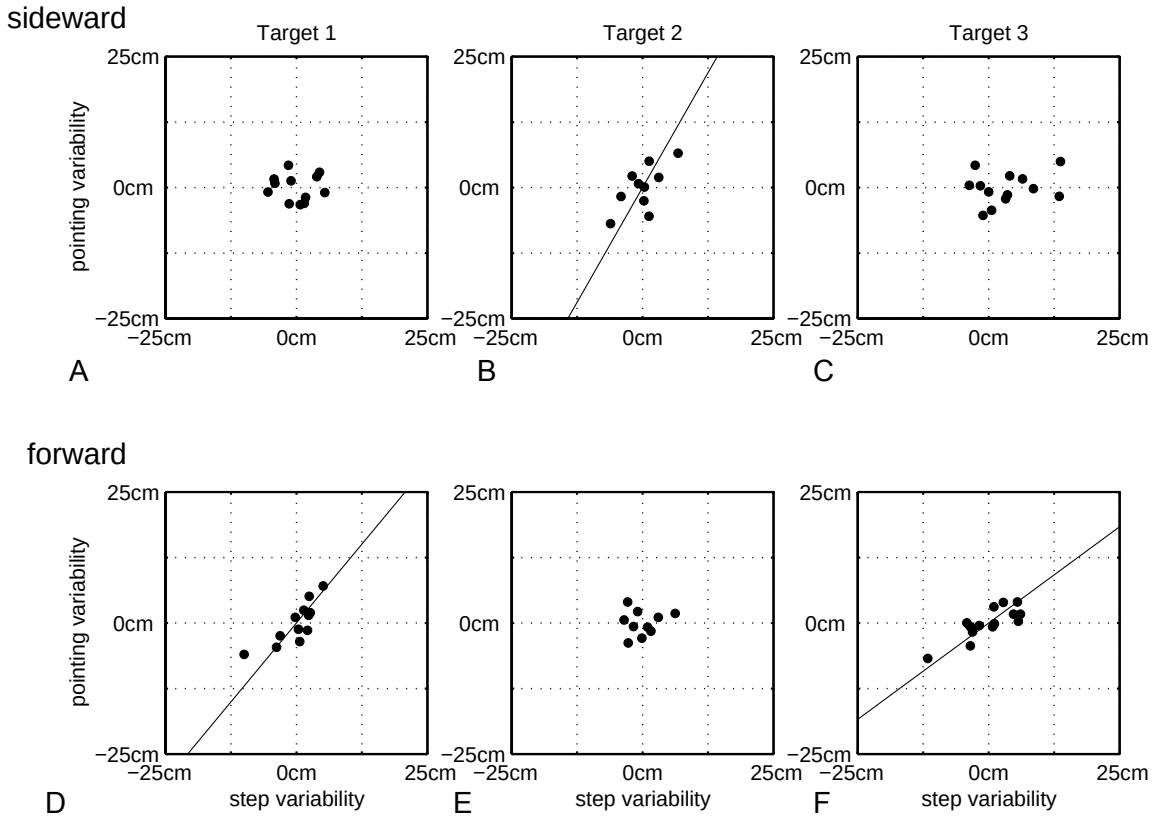

FIGURE 3.3: Example of the relation between the variability in pointing and the variability of the step, for subject JV (same data as in Figure 3.2) in the FINGER condition, for targets 1 (left column), 2 (middle column) and 3 (right column), respectively. Regression plots are shown for the variability in the step and pointing for sideward direction (top rows) and forward direction (bottom rows) separately. A regression fit is only displayed, when the relation between pointing and the step is significant ($p<0.05$).

Gaze during the step

Several studies have reported that gaze direction might affect pointing accuracy (Henriques et al. 1998, Medendorp and Crawford 2002a, Admiraal et al. 2003). Therefore, we investigated gaze during and after the step in order to see whether errors in pointing could be related to errors in fixation. We will first show the average trajectory of fixation for one typical subject. Since the exact timing of the onset and end of the steps relative to disappearance of the target varied, we resampled the fixation data from step onset until step offset before averaging over trials (see Methods).

Figure 3.4 shows the average trajectory of fixation, starting at target offset until the end of the step for subject MA in the DARK, FINGER and FRAME conditions in Figures 3.4A, B and C, respectively. At the end of target presentation, fixation is on target (filled symbol) for all conditions. During the step, however, fixation does

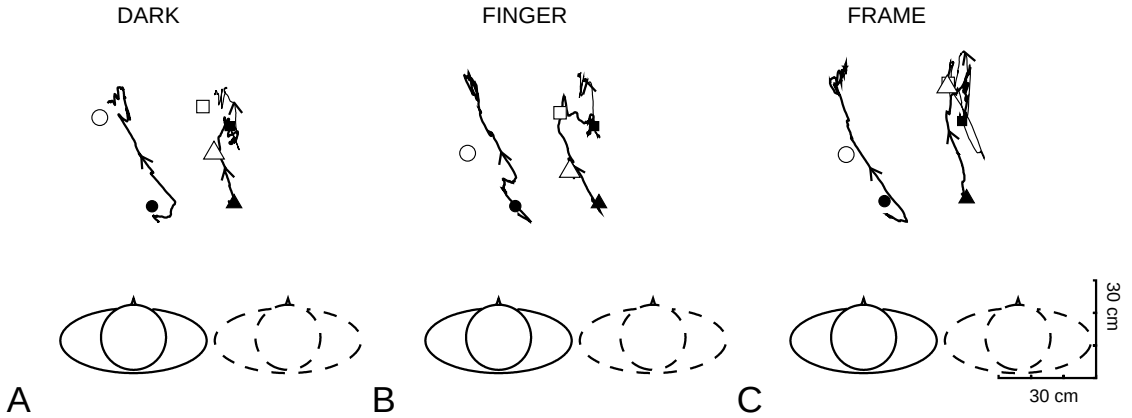

FIGURE 3.4: Top view of the average trajectories of fixation from step onset to step offset for subject MA in the FINGER condition (A), DARK condition (B) and FRAME condition (C). Target positions are indicated with filled dots. Arrows indicate the evolution of the gaze trajectories in time. Open symbols indicate gaze position at the time of pointing (about 1s after step offset): a triangle for target 1, a dot for target 2 and a square target 3. For clarity, the trajectory for target 3 is indicated by a thin line, whereas the trajectories for targets 1 and 2 are indicated by a thick line.

not remain on target but drifts away, mainly in radial direction relative to the subject as indicated by the arrows. At the end of the step, fixation is at a position behind the target, and to the left of the target.

Remarkably, the presence of a visual background during the step in the FRAME condition does not prevent gaze from drifting during the step, as is the case for the DARK and FINGER condition. Deviations of fixation position from the target at the end of the step are similar in the FRAME condition and the DARK and FINGER conditions (compare the ends of the traces in Figure 3.4C with those in Figures 3.4A and B).

The open symbols in Figure 3.4 indicate the fixation position at the end of the pointing movement when the index finger has reached the pointing position. Fixation while pointing (open symbols) is closer to the target than fixation at the end of the step in the FINGER and FRAME conditions, indicating that fixation has returned from the far fixation position at the end of the step to a distance closer to the subject at the time of pointing. At the end of the step, the distance between fixation and target position is 32 cm (SD= 7 cm), 33 cm (SD= 7 cm) and 35 cm (SD= 8 cm) for the DARK, FINGER, and FRAME condition, respectively, averaged over all subjects. The distance becomes 23 cm (SD= 7 cm), 14 cm (SD= 4 cm) and 18 cm (SD= 4 cm) at the time of pointing. In the DARK condition –when the finger is not visible during pointing- fixation position remains far from the target relative to the subject, close to the position of fixation at the end of the step (compare the open symbols and the ends of the trajectories in Figure 3.4A).

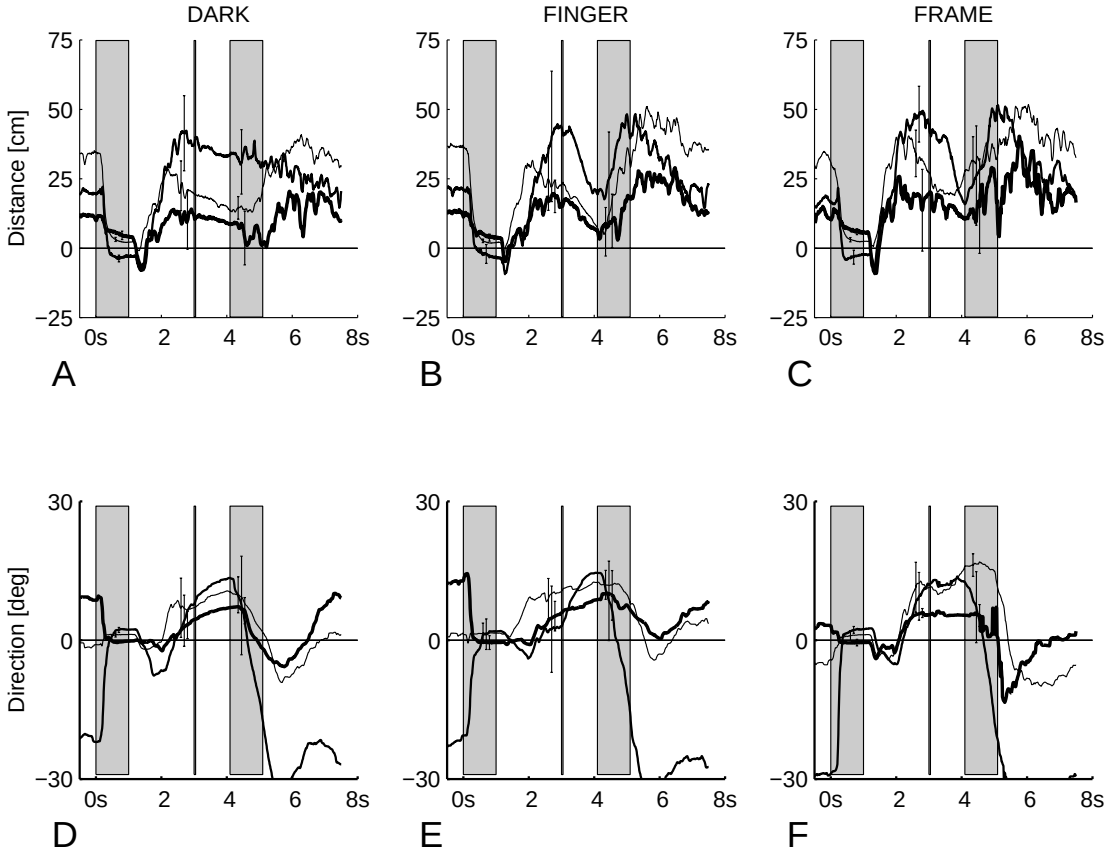

FIGURE 3.5: Difference between average fixation relative to perfect fixation as a function of time for target 1 (thin line), target 2 (normal line) and target 3 (bold line). Standard deviations are indicated by an error bar at the time when the target is fixated (t= 0.5 s), just before the cue to start the movement (t= 2.5 s) and when the subject points to the target (t= 4.5 s). Vertical gray bars represent the interval of target presentation (0.0 s < t < 1.0 s) and the interval of pointing (4.1 s < t < 5.1 s). The vertical line at t= 3 s indicates the presentation of the auditory tone that marked the end of the delay period.

Figure 3.4 only shows the spatial trajectories of fixation position during the step, but it does not give detailed temporal information about the changes in binocular fixation position during and after the step. The temporal aspects of the fixation position are displayed in Figure 3.5, where we compare the measured gaze direction and fixation distance with the gaze direction and fixation distance that are required to keep fixation on the target. Since the required gaze direction and fixation distance depend on the size and direction of the step, and thus varies slightly between trials, we have plotted the measured fixation position in terms of its deviation from the required fixation position, i.e. the error in gaze direction and fixation distance. These deviations are averaged over all trials and displayed for the same subject as in Figure 3.4.

The difference between the direction and distance of measured and ideal fixation are very similar for all targets. The difference is close to zero just before target offset (t= 1 s) and increases until the time of the auditory cue to start pointing. The

error for distance decreases for all targets for the FINGER and FRAME condition, but less so for the DARK condition. Errors in direction increase until the time of the auditory cue to start pointing, and remain more or less constant until pointing has been completed.

Comparison of fixation and pointing

For a good comparison of the fixation position of the eyes and the pointing position, Figure 3.6 shows a top view of the fixation positions directly after the step (top panels) and at the time of pointing (bottom panels) along with the corresponding pointing distributions (represented by ellipses) for the same subject as shown in Figure 3.2.

Fixation at the end of the step is too far behind and to the left of the target, when viewed from the subject. For subject JV, the deviation of fixation position from the target position at the end of the step is about the same in the DARK and FINGER conditions: averaged over all subjects the directional errors relative to the cyclopean eye are 10º (SD= 11º) and 12º (SD= 8º) to the left for the DARK and FINGER condition, respectively. On the other hand, fixation errors in distance relative to the cyclopean eye are larger in the FRAME condition than in the DARK and FINGER conditions: on average (over all subjects) 31 cm (SD= 17 cm) in the FRAME condition and 13 cm (SD= 11 cm) and 5 cm (SD= 15 cm) in the DARK and FINGER condition, respectively.

The top panels in Figure 3.6 (panels A to C) clearly show that the distributions of the pointing positions (indicated by ellipsoids) do not correspond to the distributions of fixation positions at the end of the step. However, in the period between the end of the step and the pointing movement gaze moves in the direction of the pointing position (compare data in top and bottom panels for corresponding conditions). Comparison of Figures 3.6A and D shows that in the DARK condition, fixation position remains more or less at the same location taken at the end of the step and is not affected by the pointing movement. However, in the conditions where subjects have feedback of their finger position during pointing (FINGER and FRAME conditions), fixation position at the time of pointing is clearly different from fixation position at the end of the step. In the FINGER condition, fixation positions at the time of pointing lie close to the distribution of pointing positions (see Figure 3.6E), which is easily understood, since the tip of the finger is visible in this condition. In the FRAME condition (Figure 3.6F), fixation returns only partly towards the pointing position.

The mean constant errors for pointing and fixation for all subjects are shown in Figure 3.7. The top two panels in this figure show the constant errors in fixation position at two moments in time during the trial: Top and middle panels show fixation errors directly at the end of the step and at the end of the pointing movement, respectively. The lower panels display the constant errors in pointing.

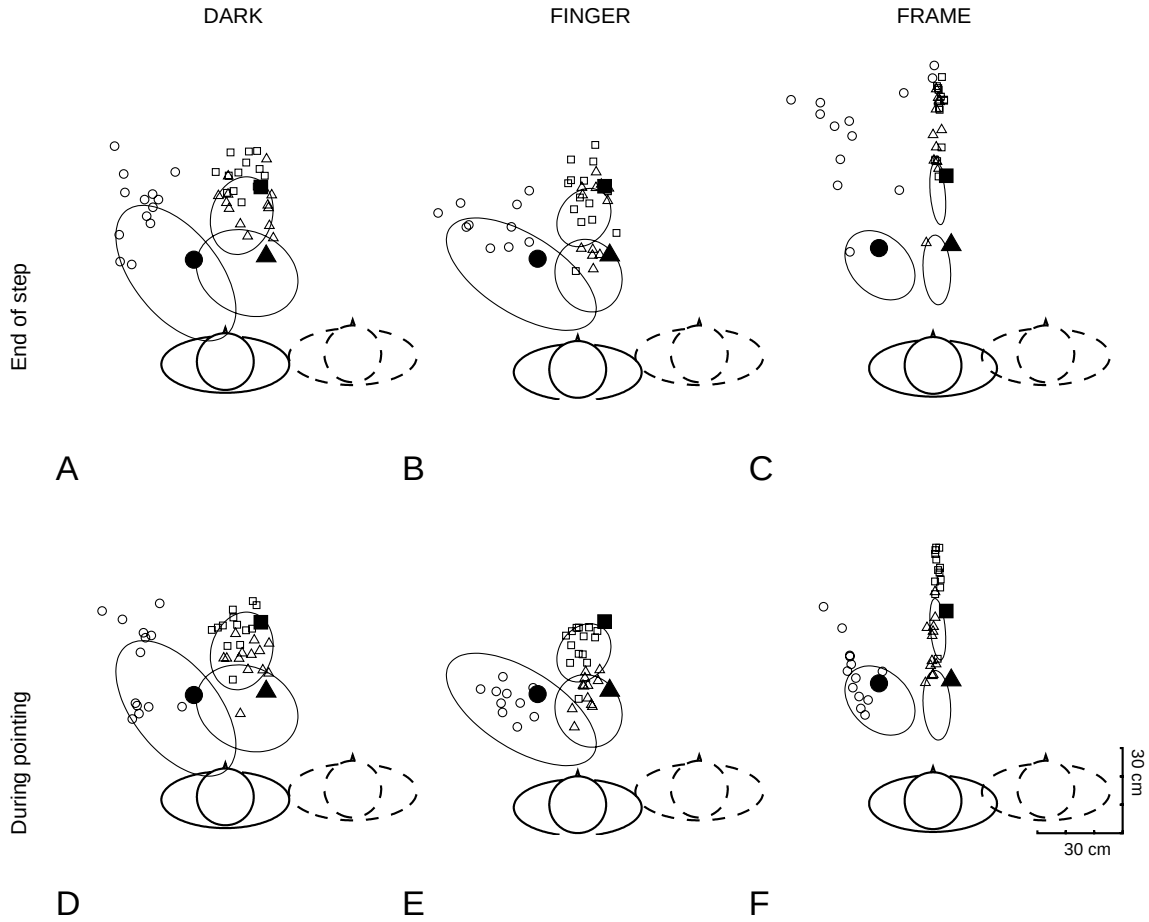

FIGURE 3.6: Top view of fixation positions at the end of the step (A-C) and at the time of pointing (D-F) for subject JV in the DARK condition (left column), FINGER condition (middle column) and FRAME condition (right column). Target positions are indicated by filled symbols: a triangle (target 1), a dot (target 2) and a square (target 3). The gaze positions at the time of pointing are indicated by small open symbols corresponding to the target symbol. Ellipses show the 95% confidence distribution of the corresponding pointing positions.

At the end of the step, errors in binocular fixation position are relatively large and mainly in radial direction relative to the subject's cyclopean eye (Figures 3.7A-C). Mean distance errors are (averaged over all subjects) 10 cm (SD= 4.5 cm) and 13 cm (SD= 4 cm) in the DARK and FINGER conditions, respectively, and somewhat larger in the FRAME condition (21 cm (SD= 5.5 cm)). In all feedback conditions, directional fixation errors at the end of the step are largest for target 1 (mean over all subjects 9^o; SD= 2^o) and smaller for targets 2 and 3 (mean 5^o; SD= 2^o). At the time of pointing, the distribution of the fixation errors in the DARK and FINGER condition clearly depends on the target position: for the most distant target (target 3) fixation distance is underestimated by 4 cm (SD= 2 cm) and 5 cm (SD= 2.5 cm) (averaged over all subjects) for the DARK and FINGER condition, respectively, whereas the fixation distance towards the two proximal targets (targets 1 and 2) is overestimated, by 7 cm (SD= 3 cm) for target 1 and by 14 cm (SD= 3.5

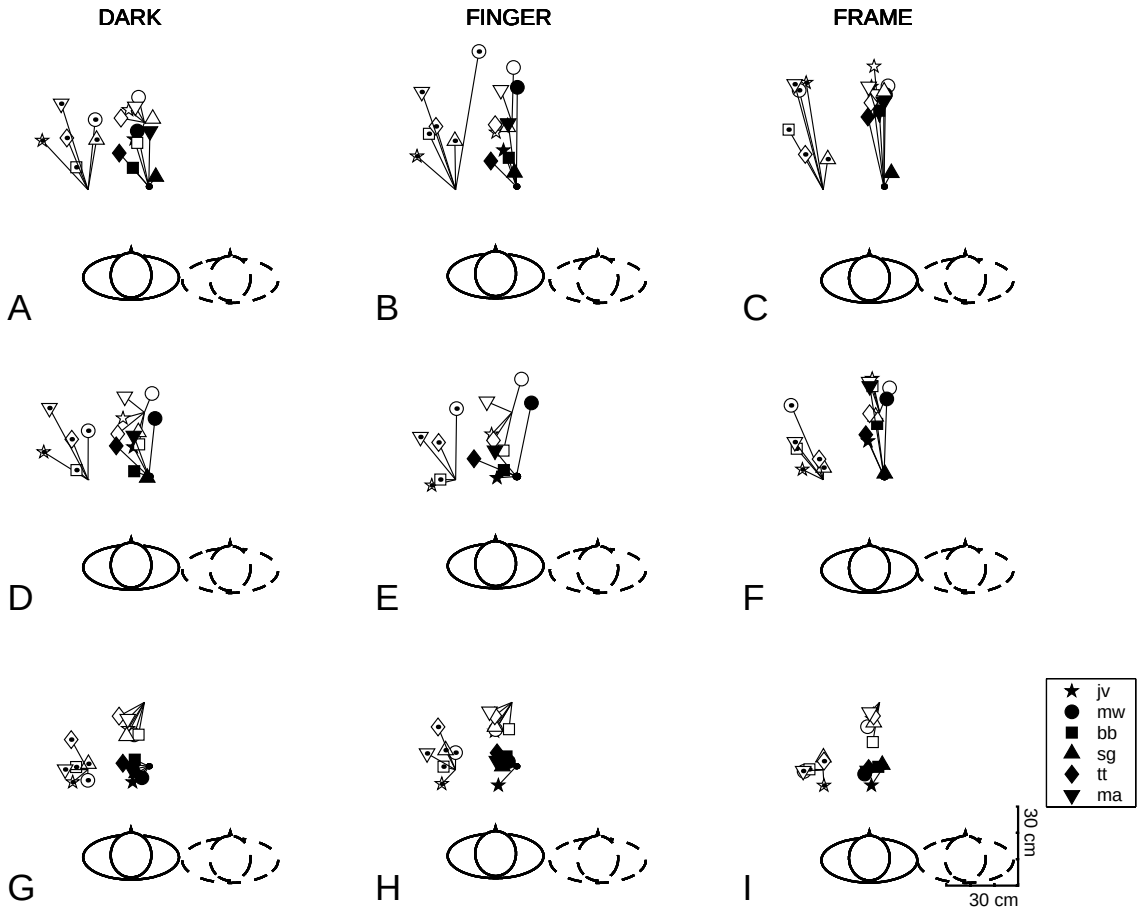

FIGURE 3.7: Overview of the constant errors of gaze relative to the target position directly after the step (A-C), and at the time of pointing (D-F). Constant pointing errors are shown in panels G-I. Different symbols refer to data from different subjects (see inset). Symbol fillings correspond to the target (filled for target 1, dot for target 2, open symbol for target 3). The location of the targets is indicated by a small black dot. The constant errors are displayed for the DARK condition (left column), the FINGER condition (middle column) and the FRAME condition (right column), separately.

cm) for target 2 (see Figures 3.7D-E). In the FRAME condition, fixation errors are significantly smaller during pointing than at the end of the step ($p<0.05$). However, gaze direction is always too far to the left and fixation distance is too large for all targets (on average over all subjects 17 cm (SD= 2 cm), 13 cm (SD= 2 cm) and 6 cm while pointing to targets 1, 2 and 3, respectively, compared to 24 cm (SD= 5 cm), 27 cm (SD= 6 cm) and 10 cm (SD= 3 cm) at the end of the step).

For an easy comparison between fixation and pointing, the lower panels in Figure 3.7 show the constant pointing errors for the three feedback conditions for all subjects. The figure shows that pointing errors are on average much smaller than errors in fixation during pointing. In particular, the higher accuracy in pointing in the FRAME condition is not accompanied by a higher accuracy in fixation.

The relation between pointing and fixation

In order to remove the effect of the step on the relation between pointing position and fixation position, we corrected the fixation position directly after the step for the influence of the variability of the step by fitting a linear relation, like we did for the pointing position. Similar to the pointing positions, fixation variability sometimes correlates significantly to the variability in the step (see Table 3.2). However, this is less often the case than for the covariance between the variability of pointing position and step variability (compare data in Table 3.1 and 3.2).

	DARK	FINGER	FRAME
target 1	2	3	0
target 2	4	4	1
target 3	1	2	1

TABLE 3.2: Number of subjects that showed a significant covariance between the variability in fixation at the end of the step and stepping. Subjects are counted if the covariance was significant either in forward direction, in sideward direction or in both. In each condition, six subjects participated.

Similarly as for pointing position, the variability in step size affects the fixation position directly after the step by different amounts for the three targets: target 2 often shows a significant covariance of fixation and step in most subjects, most often in the DARK and FINGER condition. In the FRAME condition, a significant effect of the variability of the step on fixation variability is found for two subjects only and for each of them for a different target (targets 2 and 3, see Table 3.2). In all conditions the covariance is positive, and for those that were significant the average linear regression has a slope of about 0.80.

In order to test whether there is a correlation between pointing positions and fixation other than due to a mutual dependence on the step, we first corrected fixation position and pointing position for the variability related to the step, when the covariance between step variability and pointing or fixation variability was significant. When the covariance was not significant, no correction was made.

In the following we will consider the covariance between pointing position and fixation position for distance and direction separately, in the time interval between the end of the step until the end of the pointing movement. The pointing position is defined as the position of the fingertip at the end of pointing and, therefore, does not change in time (see Methods). Changes in the covariance during the time interval are therefore the result of changes in fixation. The duration of the time interval varies for different trials, with an average duration of 900 ms (SD= 350 ms). In order to compare fixation and pointing during intervals of different length, we divided the time interval between step offset and the end of the pointing movement for each trial in 300 equidistant time intervals (see Methods), and we interpolated the corresponding gaze-in-time data to match the new time scale.

For each of the resulting 300 samples, we calculated the covariance between fixation position and pointing position. Figure 3.8 shows the resulting covariance as a function of time, for the DARK, FINGER and FRAME condition (left, middle and right panels, respectively). The covariance between fixation and pointing for distance (R) and direction (φ) are displayed separately, in the top and bottom panels, respectively. The horizontal axes correspond to the time interval between the end of the step and the time when the index finger reached the pointing position. The minimum value of the correlation coefficient that indicates a significant relation between fixation and pointing ($p<0.05$) is marked by a horizontal gray bar. The number of correct trials differed slightly between subjects and conditions. The minimum value of the correlation coefficient that indicates significance is therefore also slightly different per subject. In each condition, the width of the horizontal bar indicates the range of minimum values for the subjects displayed in the panel.

In the FINGER condition, only two subjects showed a significant covariance between the radial distance of pointing and fixation at the time just after completion of the step. By the time the finger has reached the pointing position, a significant covariance was found for four subjects (Figure 3.8B). Two subjects never showed a significant covariance between radial distance of fixation and pointing in the FINGER condition. In the DARK and FRAME conditions, the average covariance in radial distance per subject was slightly (but not significantly) lower than in the FINGER condition. For two subjects, the covariance did never reach significance. These subjects were not the same as the subjects that did not show a significant covariance in the FINGER condition.

The largest covariance was found for the directional components of fixation position and pointing position (Figures 3.8D, E and F). The bottom panels clearly show a highly significant ($p<0.01$) covariance directly after completion of the step. This covariance tends to increase to larger values by the time of pointing. The covariance for the directional component found in the FINGER condition (panel D) is significantly higher ($p<0.05$) than in the other conditions (panels E and F), which may not be very surprising since in this condition, subjects tend to redirect gaze towards the (visible) index finger. In the FRAME condition, in which feedback of the index finger is also available, subjects do not show such a clear change of gaze towards the index finger (see e.g. Figure 3.6).

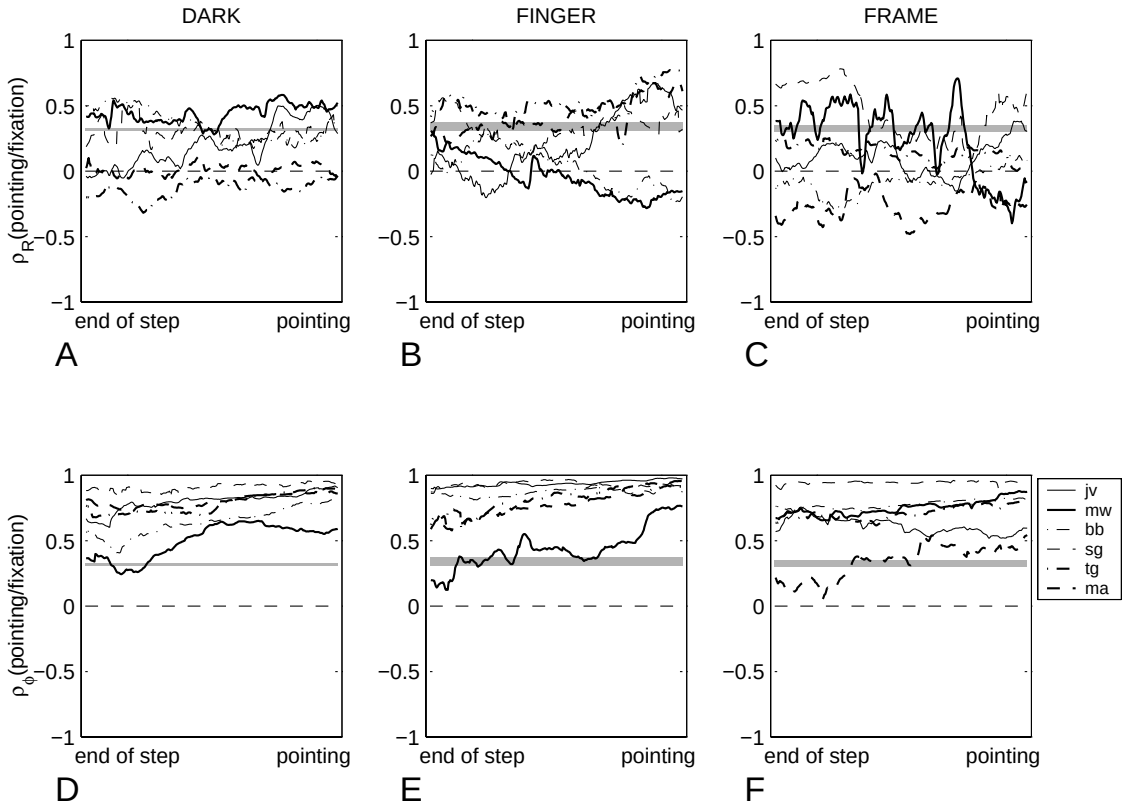

FIGURE 3.8: Covariance between pointing and gaze after correction for a mutual correspondence to step size as a function of time from the end of the step to the end of the pointing movement for distance (panels A, B, and C) and direction (panels D, E and F) relative to the cyclopean eye, for all subjects separately. The number of trials differs slightly between subjects (overall range: 26 to 40 trials) and consequently so does the 95% confidence value. In each panel, the gray horizontal bars cover the 95% confidence values for all subjects within the condition. The covariance is displayed for the DARK condition (left columns), the FINGER condition (middle column) and the FRAME condition (right column), separately. Different labeling of the lines refers to the covariance traces of different subjects (see caption).

DISCUSSION

In this study we have investigated the performance of binocular fixation and pointing towards remembered visual targets in 3-D space after a self-initiated step. The presence or absence of visual feedback of the environment appeared to have a large effect on the constant and variable errors of pointing. Similarly, fixation position differed quite considerably from the target position after the step depending on the visual feedback condition. These errors in pointing and gaze are compatible with the notion that subjects underestimate the size of the step, as suggested earlier by Medendorp et al. (1999). Moreover, although the variability in pointing and fixation was corrected for any mutual correlation to the variability in the step, the remaining variability in the final position for the pointing movement is to a large

extent related to the variability of fixation. The covariance between the latter two signals increases in the delay period after the step, but is larger for direction than for distance.

We will first discuss the effects of the step on the accuracy of pointing and fixation during the step. After that, we will discuss the relation between fixation and pointing after a step and its implication in terms of frames of reference.

Influence of the step on pointing

Several studies have shown that subjects make considerable constant pointing errors towards remembered visual targets without a step (e.g. Soechting and Flanders 1989; McIntyre et al. 1997; Admiraal et al. 2003) and after a step (Medendorp et al. 1999; Flanders et al. 1999; Daghestani et al. 1999). Our results show that the size of the constant pointing errors after a step depends on the amount of visual feedback: visual feedback of the index finger alone (FINGER condition) does not significantly decrease the constant pointing errors relative to that in the DARK condition, but vision of the environment (FRAME condition) does. A comparison of the constant errors for pointing without and with a step shows that the errors are considerably larger for pointing movements after a step (compare e.g. errors in Figures 3.2 and 3.7 in this chapter with those in Figure 2.3). In agreement with previous authors (Medendorp et al. 1999; Flanders et al. 1999; Daghestani et al. 1999), we found that constant pointing errors were mainly in the direction of the step. If subjects would incorporate the step size perfectly, pointing would be on target irrespective of step size. However, if subjects incorporate the step only for about 80% of the true step size in the pointing response, as suggested by Medendorp et al. (1999), subjects will make systematic errors. The constant errors that we found in this study are about 10 to 20% of the step size, which corresponds quite well to the estimate of accounting for about 80% of the true step size by Medendorp and colleagues.

Gaze during the step

The fixation position after the step shows a large constant error in radial direction relative to the subject (see Figure 3.7). This radial component of the constant error in fixation is due to a drift of gaze in radial direction after target offset, which has been described before for subjects who did not make a step while fixating at a remembered visual target (see Chapter 2). However, in the present study, which included a step, the fixation position after the step also has a large sideward component. In the following, we will discuss possible explanations for these sideward fixation errors. A first explanation may be, that the radial drift in gaze during the step introduces a sideward error at the end of the step. This is illustrated schematically in Figure 3.9. For equal time intervals during the step we have plotted the vector of a constant radial drift component relative to the subject's position. We have assumed a bell-shaped velocity profile for the step, and for each

of the two targets in Figure 3.9 the simulated drift velocity was chosen such, that simulated fixation ends at the same distance behind the target as the measured trajectory of fixation. Obviously, the trajectory of fixation depends on the target position relative to the subject before and after the step, and so will the final fixation position at the end of the step.

In Figure 3.9 we also included two of the typical trajectories for fixation during the step from Figure 3.4. For the target on the right (target 1) the simulated trajectory seems to end closely to the end of the measured trajectory. The curvature of the measured trajectory, however, is very different from that of the simulated trajectory. The simulated trajectory for the leftward target (target 2) clearly shows a much larger excursion than the measured trajectory and its end point lies too far to the left of the measured position.

The scheme in Figure 3.9 with a constant drift velocity in radial direction is obviously oversimplified. Presumably, the drift velocity of gaze is not constant and may not start immediately at the onset of the step. Moreover, gaze may not drift indefinitely, but may continue until a particular distance at about 80 cm from the subject (*dark vergence*, see e.g. Heuer and Owens 1989). Incorporating each of these aspects will reduce the amount of drift and thereby will reduce the drift component in the direction of the step. However, neither of these modifications can provide a good fit to the measured drift trajectories for all targets. This can be illustrated by the trajectories in Figure 3.9: The first part of the measured trajectory for target 1 requires the simulated gaze drift to be largest at the beginning of the step, whereas the measured trajectory of target 2 is best described with a gaze drift that is largest halfway through the step. These results are typical for all subjects and illustrate that a radial drift in gaze alone can not explain the constant error in fixation position at the end of the step.

Another explanation for the constant error in fixation position in sideward direction could be an inadequate translational vestibuloocular reflex (tVOR) in the dark. Previous studies have studied the tVOR in subjects while making active movements in hip and trunk, or during walking and running (Medendorp et al. 2002b; Crane and Demer 1997). In these studies, the adequacy of the tVOR was evaluated in terms of its *sensitivity*, defined as the ratio between the velocity of the gaze response and translational eye velocity. For a perfect tVOR for head movements perpendicular to the target direction, the sensitivity is equal to the inverse of target distance (see Medendorp et al. 2002b). The sensitivity of the tVOR in the dark was found to be too small to keep fixation at the (world-fixed) remembered target position. However, when the target was visible, any errors between ideal and measured gaze were almost negligible (Crane and Demer 1997; Medendorp et al. 2002b; Gielen et al. 2003). This may explain why the constant errors in the direction of the step are much smaller in the FRAME condition, which provides more visual feedback to stabilize gaze.

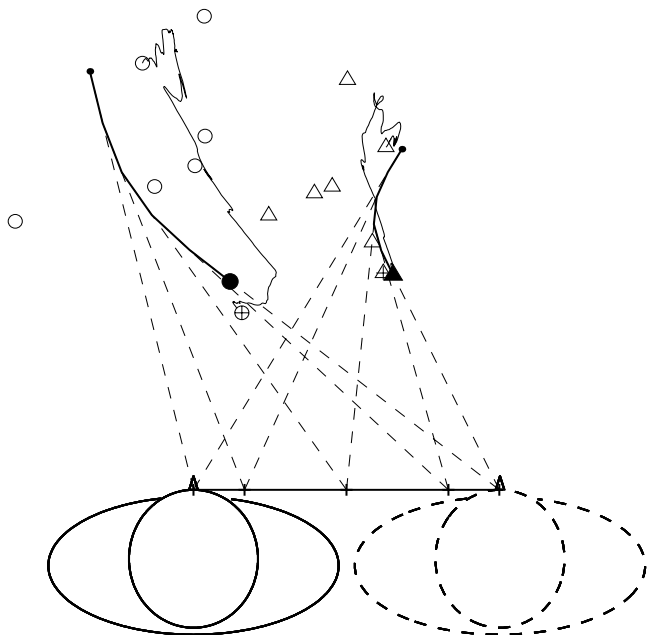

FIGURE 3.9: Simulated trajectories of gaze during the step for a constant radial drift in gaze (bold trajectories), and the measured trajectories taken from Figure 3.3A (thin trajectories). The simulated trajectory is constructed at 5 equidistant time intervals during the step, which result in equally sized drift-segments, indicated by dots along the simulated trajectory. The simulated trajectory starts at the target (thick black dot). The end of the simulated trajectory is chosen such that the forward component of the simulated end point corresponds to the forward component of the end point of the measured gaze drift (open circle). The cyclopean eye position (which serves as the origin of the radial drift) translates with a bell-shaped velocity profile, which results in 4 translational segments corresponding to equal time intervals but of different length along the line from the cyclopean eye position before the step to its position after the step. Dashed lines indicate the direction of the radial drift, which changes according to the position of the cyclopean eye during the step.

Crane and Demer (1997) compared the stability of fixation on a visible target during self-initiated head translations and during walking and running. They found that the ocular response to natural head movements such as the sway during walking and running was adequate to stabilize fixation. During the -more artificial- self-initiated translations resulting from active movements in hip and trunk, the VOR gain corresponded closely to the rotational component of the movement, but did not correctly take into account the translation of the head. When the target was extinguished (remembered target) the standard deviation of fixation position in horizontal direction is at most about 2º during walking and running. For the active head translations, the variability of fixation in horizontal direction had a standard deviation of about 4º.

Can the results of Crane and Demer (1997) and Medendorp and colleagues (2002b) explain the present results? If we consider the step -which typically had a duration of about 1 s- as half of a periodic back-and-forth movement of 0.5 Hz -as

studied by Crane and Demer (1997) and Medendorp et al. (2002b)- we predict that the sideward gaze error due to insufficient sensitivity of the tVOR for a remembered target situated at about 35 cm from the eyes (target 1) would be about 3º at most (see Figure 5 in Medendorp et al. 2002b). For targets 2 and 3 -at distances of on average about 50 and 60 cm, respectively- the sideward errors should be even smaller (since the deficiency in sensitivity increases with decreasing target distance). However, the observed sideward gaze errors in the present study are much larger than this (10º, 5º and 5º, for targets 1, 2 and 3, respectively, see Figure 3.7 in the present study). Therefore, the constant gaze errors along the step direction can not be fully explained by deficiencies in tVOR.

Since neither the gaze drift, not the tVOR could explain the sideward component of the constant gaze errors during and at the end of the step, we speculate that the constant errors also depend on underestimation of the step size (see Medendorp et al. 1999), possibly related to errors in the use of proprioceptive signals and efference copies, in line with suggestions by Medendorp et al. (2002b) to explain the differences between gaze control for passive and active head movements while fixating a visual or a remembered visual target.

Relation between gaze and pointing

Previous studies have shown that variable errors in pointing to remembered targets are related to the variability in gaze at the time of pointing even without a step (e.g. Bock (1986); Enright (1995); Henriques et al. 1998; Van Donkelaar and Staub 2000; Medendorp and Crawford 2002a; Admiraal et al. 2003). In the present study, which included a step, the relation between variability in fixation position and pointing may be more difficult to detect, because of the mutual dependence on the step. Figure 3.10 schematically illustrates how the step-dependent constant error in pointing (or fixation), as described above, may lead to a covariance between the step and pointing (or fixation). The figure shows an example of two steps, of 50 cm and 45 cm, respectively (black arrows). If only 80% of the step is accounted for, as argued by Medendorp et al. (1999), the pointing movement will be based on the erroneously perceived location of the subject's shoulder after the step (white arrows) and the (remembered) target position. If we translate the vector from the position where the subject believes the shoulder is due to the underestimation of the step to the actual position of the shoulder, the pointing movement ends at an incorrect pointing position (squares). Consequently, this explains why the variability in pointing positions is related to the variability in the step. The same argument may explain why underestimation of the step causes similar errors in binocular fixation. The influence of the step on the variability of pointing and fixation could be estimated from the linear relation between the step on the one hand and pointing and gaze on the other hand. This linear relation was used to correct the variable errors for any direct influence of the step.

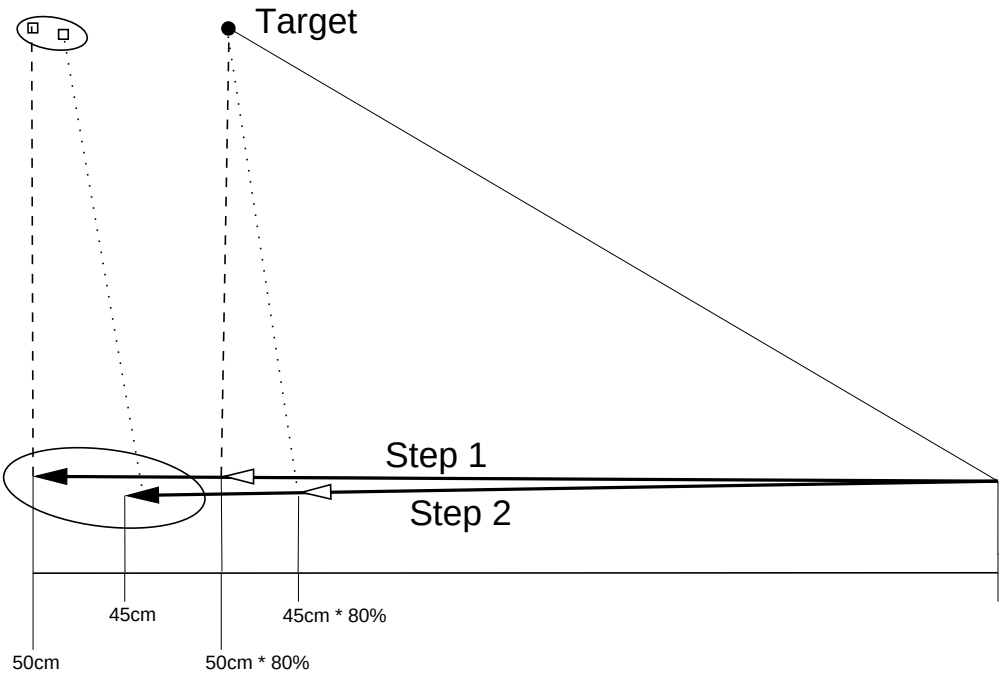

FIGURE 3.10: Schematic illustration of how underestimation of the step size may lead to a covariance between the pointing positions (white squares) and the step. Two steps (black arrows) of different size and direction are underestimated, such that only 80% of the step is accounted for (white arrows). The planned pointing movement corresponds to the vector from the perceived end point of the step (tip of the white arrow) towards the target (dashed lines), but originates from the actual position (tip of the black arrow). Two ellipses represent the estimated distributions of the step end points and the distribution of the corresponding pointing positions.

After eliminating the influence of the step from the variable error of pointing and fixation, neither pointing nor fixation is correlated to the step. Yet, the variability in fixation and pointing appeared to be significantly correlated: In all visual feedback conditions, the fixation position directly after the step covaries with its concomitant pointing position. Moreover, the covariance between fixation position and pointing increases gradually in the period between the end of the step and the time of pointing, towards a maximum at the time when the pointing position is reached.

One explanation for the covariance might be a common command signal that drives gaze and pointing towards the same target position. Variability in the common command signal will inevitably lead to a covariance between fixation and pointing. Undoubtedly, such a common input signal will be there, since both pointing and gaze are directed towards the visually perceived initial target position. If the covariance between fixation position and pointing were due only to such a common command signal, one would expect the gradual drift in fixation in the delay period to diminish the covariance between pointing and fixation. This is obviously not the case, as is shown in Figure 3.8, which shows that the covariance increases, rather than decreases in time. Thus, a common input related to the remembered visual target cannot explain the increase in the covariance between fixation and pointing during the delay period.

Therefore, we hypothesize that fixation position affects the pointing movement, which is in agreement with previous studies, which demonstrated an effect of gaze on pointing accuracy (see e.g. Pouget et al. 2002; Medendorp and Crawford 2002a; Admiraal et al. 2003). When fixation position at the time of pointing is used to define the pointing target, the gradual drift in fixation during the delay period towards the time of pointing results in an increasing covariance during this period, which is indeed what we found.

In a previous study, Flanders et al. (1999) measured the orientation of the head in a pointing task that included a forward step. They reported that errors in pointing were geometrically related to the errors in head orientation during pointing. In the present study, we not only measured head orientation but also the orientation of the two eyes throughout the trial. This allowed us to compare pointing and fixation both in direction and in distance. We found that the pointing position is related to the gaze direction, in agreement with Medendorp and Crawford (2002a), but we also found a strong relation to fixation distance. Therefore, we conclude that pointing depends on the binocular fixation position.

Table 3.1 shows that the variability of pointing was more often correlated to the variability of the step for near targets (targets 1 and 2) than for the far target (target 3). This may be surprising since the suggestion, that only 80% of the step size is incorporated in pointing, would predict similar errors for far and near targets, and therefore, would predict a similar correlation between pointing and step for all targets. A possible explanation for this apparent discrepancy may be the following: The data in Figures 3.2 and 3.6 show that both the constant error in the direction of the step as well as the variable error in the direction of the step is about the same for targets 1 and 3, both for pointing (Figure 3.2) and for gaze (Figure 3.6). The main difference in pointing positions and gaze for targets 1 and 3 is in radial distance: the drift in gaze in radial direction during the step is smaller for target 3 than it is for target 1. Presumably, this is due to the fact that gaze in darkness tends to drift to a distance of about 80 cm (*dark vergence*, see Heuer and Owens 1989), and target 3 lies close to this preferred distance. As a consequence, gaze drift is almost absent for target 3 and the effect of the step on gaze may be relatively small. This might have led to a smaller effect of the step on pointing position and therefore, to a smaller covariance between step size and pointing position.

Frame of reference

The improvement of pointing performance towards remembered targets in the presence of a (visual) environment led previous authors to question in what frame of reference the CNS plans goal directed movements and how the CNS copes with ego-motion (Medendorp et al. 1999; Pozzo et al. 1998; Marteniuk et al. 2000; Pigeon et al. 2003). Since the present study is the first to measure pointing movements along with 3-D gaze during a step, the finding that binocular fixation is involved in the planning of an arm movement after a step provides new insight in this discussion.

Medendorp et al. (1999) addressed the question what coordinate frame could best be used to describe the pointing errors after a step. They tested a Cartesian model for errors in x-y direction in the horizontal plane and another model, which relates errors to spherical coordinates of the pointing position relative to the shoulder. The cross coupling between the x and y-components (sideward and forward direction, respectively) in the description was not significantly different from zero, whereas there was a significant coupling between the r and φ components (for distance and azimuth, respectively) in the spherical description. This led these authors to the conclusion that the data were best described in Cartesian coordinates. The analysis by Medendorp et al. (1999) required a broad range of step sizes and target positions. Since we tested only a small range of step sizes in the present study, the analysis by Medendorp et al. applied to our data could not discriminate between the two hypotheses.

Some other recent studies (Pozzo and colleagues 1998) asked subjects to pick up an object from the floor, or focused on reaching an object from a table while walking past it (Marteniuk et al. 2000). Both studies found that the planning of the reach included all segments of the body involved, and that the trajectories of the hand or wrist in space were remarkably straight, indicating a movement planning in terms of the trajectory in allocentric coordinates. Pigeon et al. (2003) limited the movements of the whole body to a passive rotation around the vertical axis, while the trajectory of the wrist was evaluated during a reach. With different rotational velocities subjects used different configurations of the arm during the pointing movement. The trajectory of the wrist in space, however, was preserved, and a description in terms of allocentric coordinates was smoother and corresponded to a more bell-shaped velocity profile than a description in egocentric coordinates. Therefore, these authors conclude that turn-and-reach movements are controlled in an allocentric frame of reference.

In the present study, we showed that the underestimation of the step is less pronounced in the pointing responses when the environment is visible (FRAME condition), than after stepping in the dark (FINGER and DARK conditions). One explanation could be that the visual environment serves to store the target position in an allocentric frame of reference instead of an internal frame of reference, which is the only one available in the FINGER and DARK conditions. After the step, the remembered position relative to the visual environment can be used to derive the target position relative to the new position of the subject. By doing so, the CNS no longer needs to rely solely on the vestibular, efferent and proprioceptive signals related to the ego-motion, which may be less accurate than vision of the continuously lit visual environment. However, since vision is most accurate in direction relative to the cyclopean eye and less so in distance, the improvement due to such a strategy will mainly result in an improvement in pointing direction in the FRAME condition relative to the FINGER and DARK condition, and less so in distance (see Van Beers et al. 2002). The data shown in Figures 3.2 and 3.6 clearly support this interpretation.

Another explanation for the smaller underestimation of the step in the FRAME condition, which does not exclude the explanation suggested in the previous paragraph, may be that vision of the environment during the step helps to improve the perception of the displacement. Such an effect may be reflected in a more correct location of 3-D fixation and pointing. We found that the visual frame causes significantly smaller errors in pointing, but did not reduce errors in fixation. The directional errors in the FRAME condition were not significantly different from those in the FINGER and DARK conditions. However, binocular gaze errors in distance are larger in the FRAME condition than in the FINGER and DARK conditions, due to a large drift towards the visual frame. Based on this finding, we suggest that the visual environment was sufficient to remember the target relative to the visual frame and that fixation on the target position was less important in the FRAME condition, than in the FINGER and DARK condition.

From the present study, it is difficult to come to a final conclusion concerning the frame of reference used to represent the target position in the various visual conditions. Moreover, many authors have indicated that the effects of more complex processes, such as the use of an alternative frame of reference for the storage of remembered target positions (McIntyre et al. 1998), the storage of relative sizes or positions of target objects (Hu et al. 1999; Hu and Goodale 2000; Carrozzo et al. 2002) become evident only after a delay of about two seconds. In our study, the interval between the offset of the target, and the onset of the pointing movement lasted just about two seconds, in which subjects also performed the step. Therefore it is well possible that the present results reflect a combination of strategies, which makes it impossible to distinguish between separate strategies.

CHAPTER 4

THREE-DIMENSIONAL HEAD AND UPPER ARM ORIENTATIONS DURING KINEMATICALLY REDUNDANT MOVEMENTS AND AT REST

INTRODUCTION

A pointing direction of the fully extended arm can be obtained in many different orientations of the upper arm with the rotation of the upper arm along its long axis as a redundant degree of freedom. In other words, straight-arm pointing determines only two of the three rotational degrees of freedom of the shoulder. Despite this kinematic redundancy, several studies have reported consistent and reproducible three-dimensional (3-D) upper arm orientations during straight-arm pointing movements (e.g. Straumann et al. 1991; Theeuwen et al. 1993; Medendorp et al. 2000). Similarly, the three rotational degrees of freedom of the head exceed the number necessary to specify the head's facing direction. Yet, various studies have shown that 3-D head orientation is uniquely determined by two-dimensional (2-D) facing direction (Glenn and Vilis 1992; Radau et al. 1994; Medendorp et al. 1999). These findings reflect a reduction of the number of rotational degrees of freedom, an observation known as *Donders' law*.

Donders' law is expressed by the fact that the rotation vectors, which describe the orientation of the upper arm or head as a rotation relative to some reference orientation, are constrained to a 2-D surface (Glenn and Vilis 1992; Hore et al. 1992; Miller et al. 1992). A strict interpretation of Donders' law requires that this surface, which appears to be curved for the upper arm and the head, should equally well describe orientations during movements and orientations at rest (i.e. orientations before and after a movement). Although this has been implicitly assumed by many studies (e.g. Straumann et al. 1991; Miller et al. 1992; Theeuwen et al. 1993), the literature presents some contradictory observations on this issue. Hore et al. (1992) tested orientations of the hand during movement and at rest and did not find any differences. However, Crawford et al. (1999) reported that head

Adapted from: M.A. Admiraal, W.P. Medendorp, C.C.A.M. Gielen,
Exp. Brain Res. 142: 181-192, 2002.

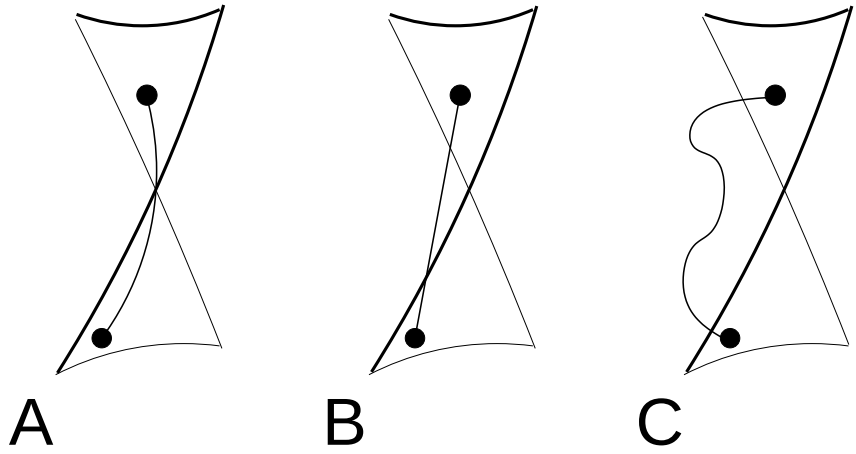

FIGURE 4.1: Implications for movement strategies in rotation vector space. The 2-D surface is the same in each panel. Solid dots indicate the initial and final positions. The orientation of the axes that span the rotation vector space are indicated in panel A. The origin of the axes coincides with the center of the 2-D surface, but is shifted for the sake of clarity. A) Moving along the 2-D surface. When orientations during movement obey Donders' law, the angular rotation axis cannot be a fixed rotation axis, but changes in time. B) Fixed-axis rotation between two orientations that obey Donders' law. The movement path in rotation vector space is shorter than in panel A. C) Moving along a variable axis. When Donders' law is violated during movement with angular rotation vectors, which are not fixed, many different trajectories from begin to end orientation are possible.

movements of monkeys made transient, but dramatic departures from the 2-D surface taking the shortest path between two eccentric fixation points on the surface. Similar observations were found in humans for fast back-and-forth head movements (Tweed and Vilis 1992).

Until now, a systematic analysis of the validity of Donders' law during upper arm or head *movements* has not been done. Elaborating on previous literature, which agrees on the observation that orientations at rest can be described by a 2-D surface, the present study specifically examines whether orientations during movements are constrained to the same 2-D surface.

The notion that orientations at rest can be described by a 2-D surface is compatible with other studies, which have suggested that the final arm orientation after a reaching movement is planned in advance and is used as a control variable by the central nervous system (CNS) (see e.g. Flanders et al. 1992; Rosenbaum et al. 1995; Gréa et al. 2000). In this context, the effect of movement velocity could be important. The presumption of this study, i.e. the validity of Donders' law for head and upper arm orientations at rest, implies that movement velocity will not affect the orientations at the end of the movement, which is in agreement with the results of Nishikawa et al. (1999). However, during the movement the effect of movement velocity on the adopted orientations remains to be seen. Low velocity movements can be regarded as a sequence of orientations at rest, corresponding to a trajectory along the surface. If movement velocity increases, trajectory control might be less tight, and deviations from the surface might occur. If this holds true, then various

trajectories can be hypothesized to move the arm or head from the initial to the final orientation, as shown in Figure 4.1.

When Donders' law applies at all times, irrespective of movement velocity, then all orientations during a movement are constrained to the same curved surface, which describes the orientations at rest (Figure 4.1A). This requires a non-fixed rotation axis in the shoulder or head and implies that the motor program to move the arm along a complex trajectory in the curved 2-D surface should be rather complicated. The second hypothesis is that the motor program brings the arm or head with a single, fixed-axis rotation from the initial to the final orientation, as shown in Figure 4.1B (see also Crawford et al. 1999). In that case orientations during movement lie on a straight line between the rotation vectors that specify initial and final orientation, independent of movement velocity. Such a movement clearly violates Donders' law, since in this case the orientations during the movement do not coincide with the curved surface describing orientations at rest. As to the third hypothesis, illustrated in Figure 4.1C, the CNS only specifies initial and final orientations but does not take into account the complex biomechanical properties of the extended arm or the head, thus avoiding complicated computations associated with multi-joint movements. In such a strategy, movement velocity might influence the orientations during the movement. The first two hypotheses (Figures 4.1,A and B) imply that orientation during a movement is carefully controlled by the CNS throughout the movement, whereas the latter (Figure 4.1C) does not necessarily require a strict control of orientations during a movement.

Summarizing, the aim of this study is to investigate whether orientations of the upper arm and head are the same at rest and during movement for equal pointing and facing directions, respectively, and how any differences might be influenced by movement velocity. The answer to this question provides new data for comparison with predictions from various models in the literature about motor control.

METHODS

This study investigated 3D orientations of the upper arm and head in two separate experiments. The experiments were approved by the ethics committee of the University Medical Center. Five adult subjects (aged 26-47 years) participated in the experiments; all gave their informed consent. None of the subjects had any known history of neurological or musculo-skeletal disorders. Two subjects (SG and PM) were familiar with the purpose of the experiments. The results of these subjects were not different from those of the other subjects. All subjects were right-handed and pointing movements were made with the right arm.

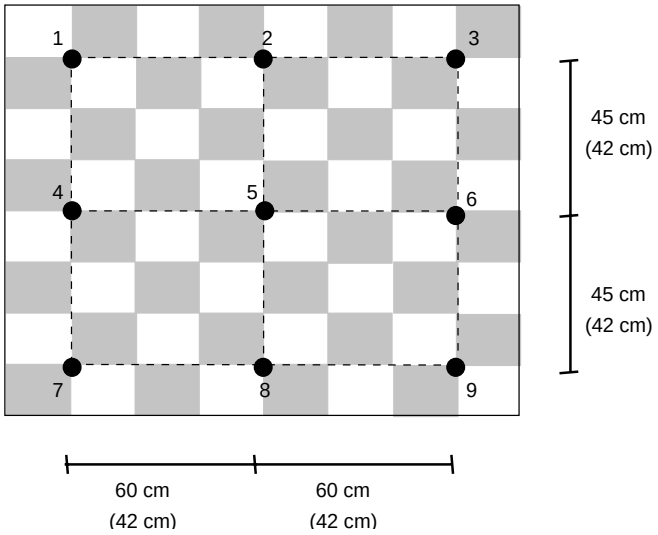

FIGURE 4.2: Schematic overview of the nine targets on a checkerboard background. Movement paths included in the evaluation are indicated by dotted lines. Distance between targets is indicated for the arm (for the head in parentheses).

Experimental setup

The subject sat with the trunk fixated to the chair such that the shoulder and head were free to rotate in all directions. In both the arm and the head experiment, the subject was positioned such that the central target (target 5 in Figure 4.2) was near the center of the mechanical range of the upper arm or head, respectively.

Visual stimuli generated by a personal computer were projected by a LCD projector (Philips Proscreen 4750) on a translucent screen. For the arm movement experiment, the screen was placed at a distance of 90 cm from the subject's shoulder. For the head movement experiment, the distance between the screen and the subject's eyes was 80 cm. The visual scene covered an area of 120 cm x 96 cm, which consisted of a checkerboard pattern with 8 x 8 alternating black and yellow rectangles (15 x 12 cm each) and a bright yellow, circular target with a diameter of 1.5 cm that appeared on top of the checkerboard pattern. Targets could appear at nine locations, situated on a rectangular or square grid, for the arm and head, respectively (see Figure 4.2). Zero-elevation and zero-azimuth were defined as the elevation and azimuth when the subject was pointing or facing straight ahead. With these definitions, the workspace of the shoulder ranged from 0º to +67º in azimuth, and from -26.5º to +26.5º in elevation. The workspace for the head ranged from -25º to +25º for both azimuth and elevation.

The position and orientation of the upper arm and head were measured with an OPTOTRAK 3020 system (Northern Digital, Ontario, Canada), which measures the 3-D position of infrared-light-emitting-diodes (ireds) with a resolution better than 0.2 mm within a range of about 1.5 m^3. The OPTOTRAK system was mounted on

the ceiling above the subject at a distance of approximately 2.5 m behind the seated subject, tilted downward at an angle of 30º relative to the ceiling. In both experiments, positions of ireds were measured with a sampling frequency of 100 Hz.

To measure the orientation of the upper arm, a cross with ireds on each of the four tips was attached to the upper arm, about 2 cm proximal to the elbow. The length of each arm of the cross was 2.5 cm. The position of the cross was adjusted such that the OPTOTRAK system could always measure the position of at least three ireds during all movements. We were able to determine orientations for the upper arm with accuracy better than 0.3º in all directions.

To determine head orientations, subjects were wearing a helmet with four ireds mounted on top and two ireds on the back (see Medendorp et al. 1998). The weight of the helmet, which was firmly fixed to the head, was less than 0.25 kg. At all times during the experiment, at least three ireds were visible for the OPTOTRAK. Head orientations could be determined with an accuracy better than 0.2º in all directions (see Medendorp et al. 1998; Veldpaus et al. 1988).

Experimental protocols

Arm. At the start of each sequence of movements, subjects pointed to the central target to define a reference orientation for the arm. Next, the subjects had to point toward new targets that appeared in quasi-random order at the nine target positions at 2-second intervals. Six combinations of start and end targets occurred more frequently than others (target pairs: 1-3, 4-6, 7-9, 1-7, 2-8 and 3-9, see Figure 4.2). These target pairs resulted in either vertical or horizontal movements at different azimuth or elevation angles. Since movements were made in both directions, 12 different movements were analyzed. Each pair of targets occurred at least 32 times during the complete set of movements, 16 times for each movement direction. In order to prevent fatigue, subjects were tested in 16 blocks with 20 movements each. Each block lasted about 40 s and was followed by a brief rest period. Subjects were instructed to point with the fully extended arm from target to target with a single aiming movement.

Instruction for movement velocity, indicated with 'normal', 'low' or 'high', was given at the beginning of each block of 20 movements, which resulted in a range of velocities from about 50 to 200 °/s. Movements that were not completed within the 2-s interval of target presentation, and movements that were initiated in a wrong direction, were discarded from further analysis.

Head. Subjects were instructed to point their nose toward the targets that appeared at an interval of 2 s. As with the arm, a wide range of movement velocities was tested, ranging from about 100 to 300 °/s. All subjects made 320 head movements, divided into 16 blocks with 20 movements each. Movements were discarded from further analysis, when a new target appeared before the movement to the previous target was completed. The same target pairs as described for the arm

were used for the head measurements: the six pairs of initial and final positions all occurred at least 32 times; 16 times for each movement direction.

Data analysis

Ired data initially were represented in a coordinate system related to the OPTOTRAK system. For evaluation purposes, the data were transformed into a right-handed coordinate system, with the x-axis defined along the pointing or facing direction of the reference position, the z-axis vertically pointing upwards and the y-axis perpendicular to both.

The orientation of the upper arm or head was described by a rotation vector, which rotates a particular reference position into the current position. This rotation vector is defined as $\vec{r} = \tan(\theta/2) \cdot \vec{n}$, where $\vec{n}$ represents the direction of the rotation axis in 3D, and θ the angle of the rotation around this axis (see Haustein 1989).

Beginning and end of a movement were determined on the basis of an angular velocity criterion (threshold: 10 °/s). This threshold enabled us to investigate almost the complete range of orientations along the movement trajectory. Accordingly, static orientations are defined as those orientations of the upper arm or head corresponding to angular velocities below 10 °/s. Next, we fitted a second-order function to the static rotation vector data, given by:

$$r_x = a + br_y + cr_z + dr_y^2 + er_y r_z + fr_z^2 \qquad (4.1)$$

where r_x, r_y and r_z represent the torsional, vertical and horizontal components of the rotation vector $\vec{r}$, respectively. This description represents a 2-D surface in a 3-D rotation vector space. The scatter of the data relative to the fitted surface is described by the standard deviation of the distances in torsional direction of the rotation vectors towards the fitted surface (see Glenn and Vilis 1992; Hore et al. 1992; Theeuwen et al. 1993; Medendorp et al. 1999).

Evaluating deviations from the surface

Since we were interested in the spatial aspects (i.e. orientation) of the upper arm and head during a movement rather than in the temporal aspects, each trajectory was spatially resampled onto 250 equidistant sample points. Consequently, the (constant) distance between two sample points depended on the total length of the trajectory.

We evaluated the 3-D trajectory of orientations of the head and upper arm during a movement, and compared it to a trajectory along the surface, referred to as *predicted trajectory*. Since many different trajectories are available to move from the starting position to the final position along a curved surface, one trajectory over the surface had to be selected. We compared the measured trajectory with the

trajectory over the surface described by the projection of this measured trajectory on the curved surface in torsional direction. This trajectory represents positions with the same amounts of elevation and azimuth as the measured orientations, but possibly with a different amount of torsion. Should the measured trajectory lie in the surface, then the measured trajectory and the predicted trajectory fully coincide.

As a measure of the correspondence of torsion of the trajectories as a function of azimuth and elevation for movements with the same start and end position, we calculated the correlation coefficient between the trajectory -spatially resampled- in rotation vector space for a movement and the mean of the trajectories of the other movements with the same start and end position. We performed this calculation for the five fastest movements for each subject and each pair of targets. For each of these five movements, we also calculated the correlation coefficient between the trajectory and the predicted trajectory along the surface. When movements reveal systematic deviations of torsion relative to the predicted trajectory, the correlation of a movement trajectory with the mean of the other trajectories should be larger than the correlation with the predicted trajectory. We compared the mean correlation coefficient between the trajectories relative to each other with the mean correlation coefficient for the trajectories with the predicted trajectory. Differences in mean correlation coefficients were evaluated by means of a t-test.

We used a different analysis to test the effect of movement velocity on the orientations during movements. Orientations during movements sometimes appeared to have a small constant bias in torsional direction, corresponding to the torsional bias at the onset of the movement. For a good comparison of the measured trajectories for different movement velocities, we have shifted each measured trajectory in torsional direction such that the initial and final orientations lie as close as possible to the fitted surface. This shift was small, typically 1 to 3º. This procedure was applied only for the data used to study the effects of velocity and velocity-dependent deviations (Figures 4.7 and 4.8). Deviations from the surface were calculated as the distance between the shifted measured trajectory and the predicted trajectory. Since all trajectories were spatially resampled into 250 equidistant points, this corresponds to a summation of the distances of all 250 measured data points relative to the predicted data in the 2-D surface. In order to test whether movement velocity influences the amount of deviation relative to the surface, we calculated the correlation coefficient between peak velocity and deviation from the surface, for each pair of targets.

RESULTS

In this study we tested whether orientations of the upper arm and the head are the same during movement and during fixation at corresponding targets. Since the results for the head and upper arm reveal several similarities, they will be discussed simultaneously.

Figure 4.3 shows, for subject SG, the rotation vectors representing the orientations of the upper arm in the arm experiment. The upper panels show the rotation vectors representing the static orientations, i.e. orientations with angular velocities below 10 º/s (see Methods). A 2-D surface was fitted to the data sets using Equation 4.1. Figure 4.3A provides a frontal view on the static data and the 2-D surface. Figure 4.3B provides a side view on the same surface in 3-D space, such that the scatter of the data relative to the curved surface can be observed as clearly as possible. For the upper arm orientations depicted in Figure 4.3A-B, the standard deviation of the data relative to the surface is 3.1º. For all subjects, the standard deviation varied between 3.1 and 4.6º (mean= 3.8º; SD= 0.6º). Figure 4.3 shows that the best fitting surface to the arm data is not a flat plane, but a surface with a curvature and a twist (coefficients d, e and f in Equation 4.1). For all subjects the surfaces are slightly curved and twisted, although considerable inter-subject variability occurs in the amount of curvature and twist. For all subjects, the mean twist coefficient (coefficient e in Equation 4.1) was -0.03 (SD= 0.12, range= -0.20 to 0.11). The values of the coefficients d and f, which indicate the curvature of the surface, are of the same magnitude as that of the twist coefficient e (mean values of –0.01 (SD= 0.18) and 0.15 (SD= 0.19) for coefficients d and f, respectively).

Figure 4.3C shows the same data as those of Figures 4.3A and B, complemented by the rotation vectors for orientations during movements that were made at self-paced velocities. For the sake of clarity we plotted one of every three sampled data points during the movement, since showing all data points would create a dense cluster of points, obscuring any differences between rotation vectors for the arm at rest and during movement. At first glance, the scatter of the movement data relative to the surface does not appear to differ much from that of the data at rest relative to the same surface. A quantitative analysis reveals that for this subject the scatter is slightly smaller for the static data than for the movement data (3.1º vs. 3.9º). This was found for all subjects (mean 3.8º (SD= 0.6º) vs. 4.2º (SD= 0.5º) for static and movement data, respectively). A t-test revealed that this difference in scatter between the data at rest and the movement data was significant ($t=3.42$, $p<0.05$).

A more detailed analysis demonstrates that the scatter of the rotation vectors for arm movement data relative to the surface does not reflect just random noise but, instead, reveals stereotyped differences. For example, in Figure 4.3D the four solid

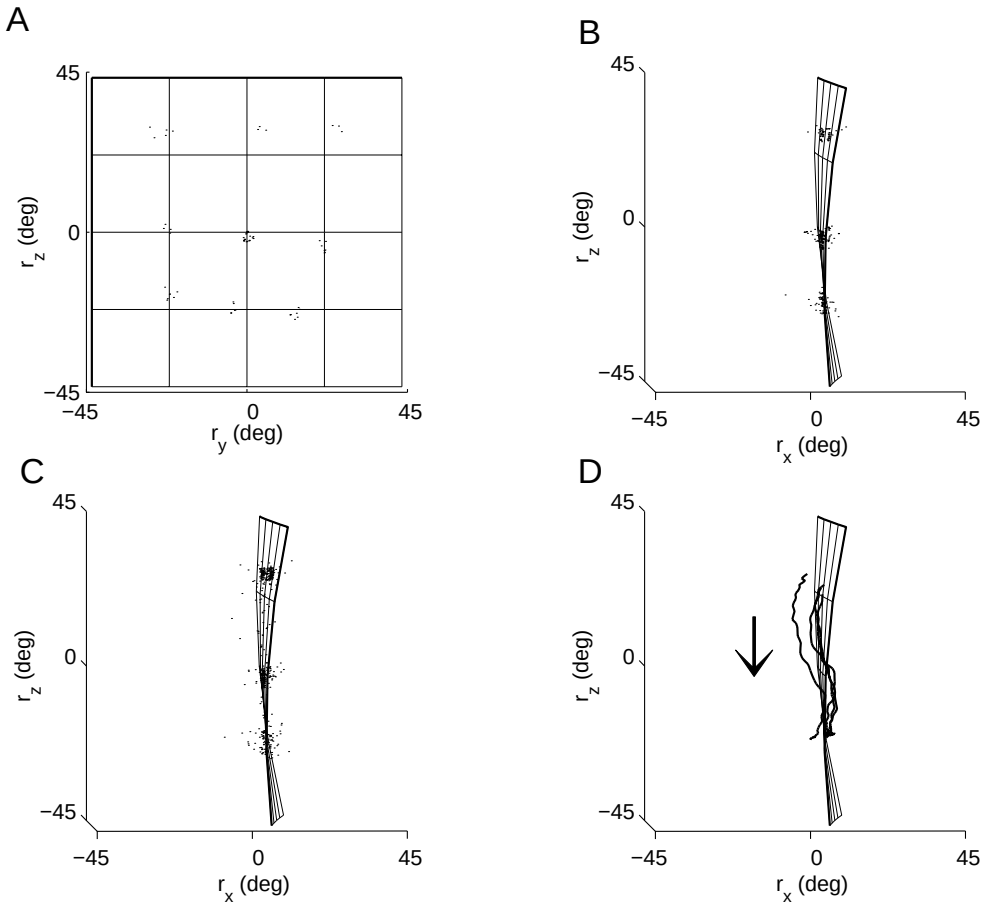

FIGURE 4.3: Rotation vectors and 2-D surface for the static (A-B) and movement (C-D) orientations of the arm. Panel A shows the projections on the plane of the horizontal and vertical rotational components. Dots indicate the rotation vectors of the all orientations reached with a velocity < 10 º/s. The nine clusters in panel A correspond to pointing to the nine targets. Panel B shows a quasi 3-D view on the two dimensional surface fitted to the static data. The dots in panel C represent rotation vectors of orientations both at rest and during movements with self-paced velocity. One out of every three measured orientations is shown. The four lines in panel D represent data of arm orientations for four movements from target 1 to target 3.

lines show data of four horizontal arm movements from target 1 (upper-left) to target 3 (upper-right, see Figure 4.2). Apart from a more or less constant offset of a few degrees in torsional (r_x) direction, the four trajectories have a very similarshape, with the r_x component (a measure for torsion of the upper arm) initially decreasing from a value close to the surface, then increasing to larger values (corresponding to maximal excursions relative to the surface of 4 to 9º) before finally returning again to a smaller value with a torsion close to the fitted surface.

The rotation vectors in Figure 4.4 represent the orientations of the head, for the same subject as in Figure 4.3 (subject SG). The upper panels show the rotation vectors representing the static orientations, i.e. orientations with angular velocities

below 10º/s; the rotation vectors in the lower panels represent orientations with angular velocities higher than 10º/s.

Figure 4.4A shows a frontal view on the rotation vectors for head orientations at rest. Comparison of the static data for facing (Figure 4.4A) and for pointing (Figure 4.3A) reveals that there is more scatter in facing direction (Figure 4.4A) than in pointing direction (Figure 4.3A) for each of the targets.

Figure 4.4B presents the same data as Figure 4.4A in side view, in order to show the shape of the surface as clearly as possible. The surface fitted to the head orientations is mainly characterized by a twist coefficient (coefficient *e* in Eq. 1, see e.g. Medendorp et al. 1999; Ceylan et al. 2000). Although the amount of twist varies between subjects (mean twist coefficient= -0.62, SD= 0.23, and range= -0.35 to -0.88), the twist coefficient is very prominent for all subjects. The shape of the surface for the head is therefore very similar for all subjects. The large twist coefficient indicates that the shape of the surface fitted to the head data differs from the shape of the surface fitted to the arm data, which has a much smaller twist coefficient.

The standard deviation of the head data relative to the surface for subject SG in Figures 4.4A, B is 1.8º, which is clearly smaller than the standard deviation relative to the surface fitted to the arm data (3.1º) for the same subject shown in Figures 4.3A, B. For all subjects, the mean scatter of the head data relative to the surface was 2.6º (SD= 0.5º, range= 1.8º to 3.2º). The standard deviation relative to the surface is significantly smaller for head data than for arm data with mean values of 2.6 and 3.8º, respectively ($F(1,8)=11.8$, $p<0.025$).

Figure 4.4C shows the same static data for the head as shown in Figures 4.4A, B, complemented with the rotation vectors for head orientations during the movements that were made at self-paced velocities. For all subjects, the scatter of the rotation vectors of the orientations during movement relative to the surface was larger than that of the static data (for the subject SG: 2.3º vs. 1.8º). A t-test showed that this difference in scatter was significant ($t=5.36$, $p<0.05$).

As with the arm data, a more detailed analysis of the head data demonstrates that the scatter of the rotation vectors relative to the surface reveals stereotyped differences. Figure 4.4D shows four head trajectories from target 9 to target 7 (lower-right and lower-left, respectively, see Figure 4.2). All four trajectories are very similar. The rotation vectors follow a more or less straight trajectory from the starting orientation close to the surface and, in the final phase of the movement, bend towards the end orientation close to the surface. The trajectories in Figure 4.4D deviate from the surface with maximal excursions of 2 to 4º.

The data in Figures 4.3D and 4.4D illustrate that trajectories of rotation vectors for movements with the same initial and final orientation tend to deviate from the

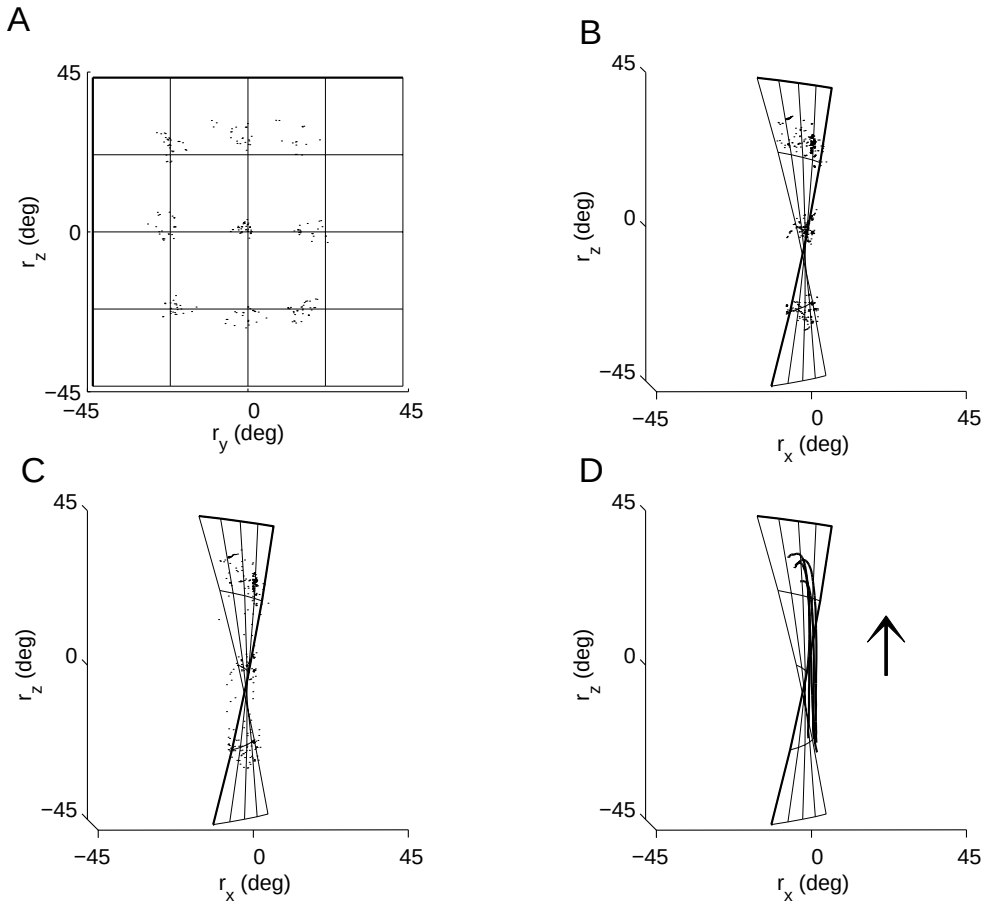

FIGURE 4.4: Rotation vectors and 2-D surface for the static (A-B) and movement (C-D) orientations of the head. Panel A shows the projections on the plane of the horizontal and vertical rotational components. Dots indicate the rotation vectors of the all orientations reached with a velocity < 10 º/s. The nine clusters in panel A correspond to facing the nine targets. Panel B shows a quasi 3-D view on the two dimensional surface fitted to the static data. In panel C, dots represent rotation vectors of orientations both at rest and during movements with self-paced velocity. One out of every three measured orientations is shown. The four lines in panel D represent data of head orientations for five movements from target 1 to target 3.

curved surface fitted to the static rotation vectors in a consistent, reproducible way. Although the orientations at the beginning and end of a movement reveal a random scatter relative to the fitted surface, the orientations during a movement reveal consistent and reproducible deviations relative to the surface. The fact that the trajectories of rotation vectors revealed consistent deviations from the surface was found for many target pairs, although the shape of the deviations was different for movements between different target pairs. This is illustrated in more detail in Figures 4.5 and 4.7 for the arm and in Figure 4.6 for the head.

Figure 4.5 shows a further analysis of the trajectories of rotation vectors during high-velocity arm movements (see Methods) for three target pairs (columns) for three subjects (rows). Figures 4.5A-C show 2-D projections in the r_x-r_z plane of

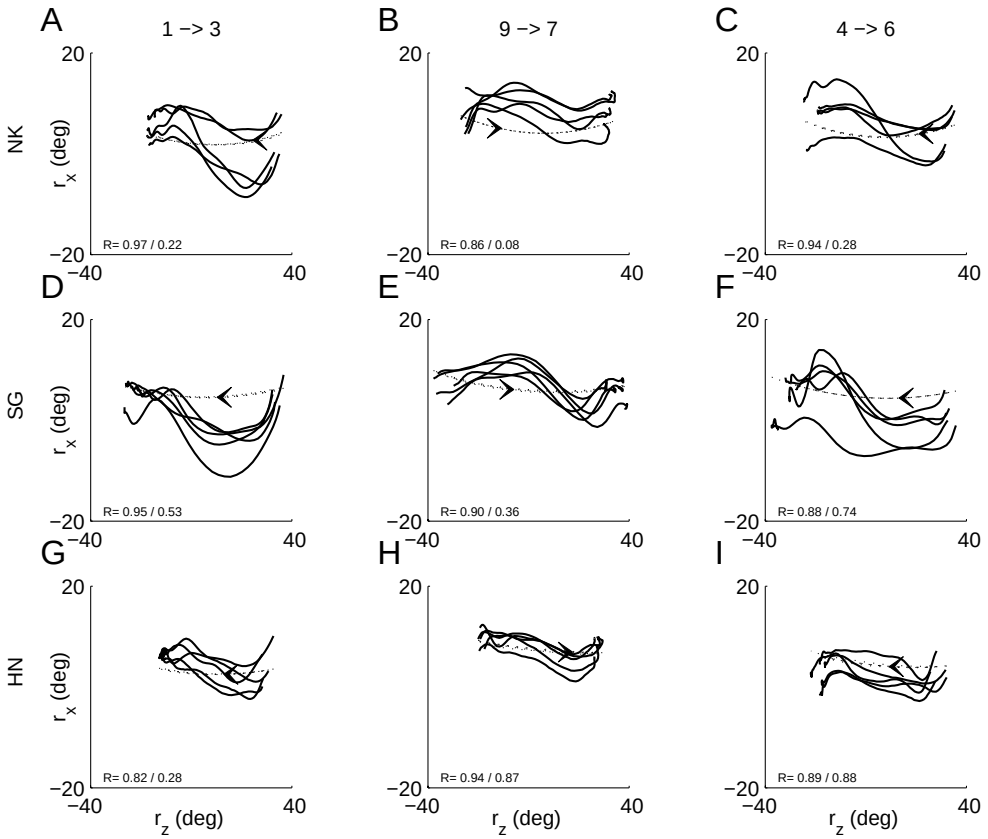

FIGURE 4.5: Arm movement trajectories for three pairs of begin and end targets, for three subjects. Thick lines represent the five trajectories with a high velocity for movements from target 1 to 3 (panels A, D and G), from target 9 to 7 (panels B, E and H) and for movements from target 4 to 6 (panels C, F and I). Trajectories are displayed for: subject NK (A-C), subject SG (D-F) and subject HN (G-I). The dotted lines indicate the projection of the trajectory in the 2-D surface. Arrows indicate the direction along the trajectory in time. In each panel, the mean of the correlation coefficients between each of the trajectories and the mean of the four other trajectories (r_{mean}) as well as the mean of the correlation coefficients between the trajectories and the predicted trajectories along the surface ($r_{surface}$) is indicated in the lower left corner: $r_{mean} / r_{surface}$.

rotation vectors obtained from subject NK. Movement paths displayed in Figure 4.5A represent rotation vectors of five movements from target 1 to target 3. To illustrate the differences between the movement data and the static data in the curved surface, dotted lines represent the projection of these movement trajectories on the curved surface (see Methods). Since the projections of the different movements almost fully overlap, the five dotted lines can hardly be distinguished. Apart from a more or less constant offset relative to the surface, the trajectories of rotation vectors for the arm are very similar.

Comparison of trajectories between the same pair of targets for different subjects reveals clear similarities between the trajectories. For example, Figures 4.5A, D and G show rotation vectors for movements from target 1 to target 3 for subjects NK, SG and HN, respectively. Trajectories start with a positive r_z

component and move towards a negative r_z component (movement direction is indicated by an arrow). For the movement from target 1 to target 3 all subjects showed an initial decrease in torsion (r_x component) larger than that predicted by the surface and, thus, the trajectories deviate from the surface. This decrease is followed by an increase in torsion and a final decrease in torsion leads the trajectory back to the surface. Similar observations can be made for movements from target 9 to target 7 (Figures 4.5B, E and H) and for movements from target 4 to target 6 (Figures 4.5C, F and I).

Figure 4.6 shows the rotation vectors for head movements between three pairs of targets for three subjects. Just as for the arm, trajectories between the same target pairs are very similar, apart from a small offset relative to the surface. Figures 4.6A, D and G show rotation vectors for movements from target 7 to target 9 for subjects NK, SG and HN, respectively. All subjects show trajectories that start near the surface and then follow a rather straight path with a slightly decreasing torsional (r_x) component. Movement along the surface would require a very different trajectory with an increasing torsional component, as indicated by the dotted lines that represent the torsional projections of the trajectories on the surface. At the end of the movement, the torsional component increases, returning to values corresponding to that of the surface. The trajectories displayed in Figures 4.6A, D and G correspond to the time interval in which movement velocity exceeds the 10 º/s threshold. Therefore, by the end of the displayed trajectory, the surface may not have been reached. Figures 4.6B, E and H show rotation vectors for movements between targets 9 and 7 for the three subjects NK, SG and HN, respectively. Here, clearly all movement paths start and end near the surface, but during the movement the paths tend to have a more positive torsion relative to the projection on the surface. Finally, Figures 4.6C, F and I show data for movements starting at target 6 and ending at target 4. Again, movements start with an increase in torsion, and end with a decrease, thus returning to the surface. For all subjects, similar deviations from the surface seem to occur for head movements between the same target pairs.

In order to quantify the similarity between the trajectories, we compared the trajectories of the five fastest movements for each pair of targets, for each subject. For each of these five movements, we compared the trajectory with the mean of the four other trajectories, by computing the correlation coefficient. This was done both for the arm movements as well as for the head movements. We also computed the correlation coefficient between the trajectory and the predicted trajectory along the surface. Finally, for each pair of targets and for each subject, we determined the mean correlation coefficient for the comparison with the other trajectories and the mean correlation for the comparison with the predicted trajectory along the surface (see Methods). This resulted in two sets of 60 correlation coefficients (12 pairs of targets for 5 subjects). In Figures 4.5 and 4.6, the values of the mean correlation coefficients are indicated for each of the movements displayed.

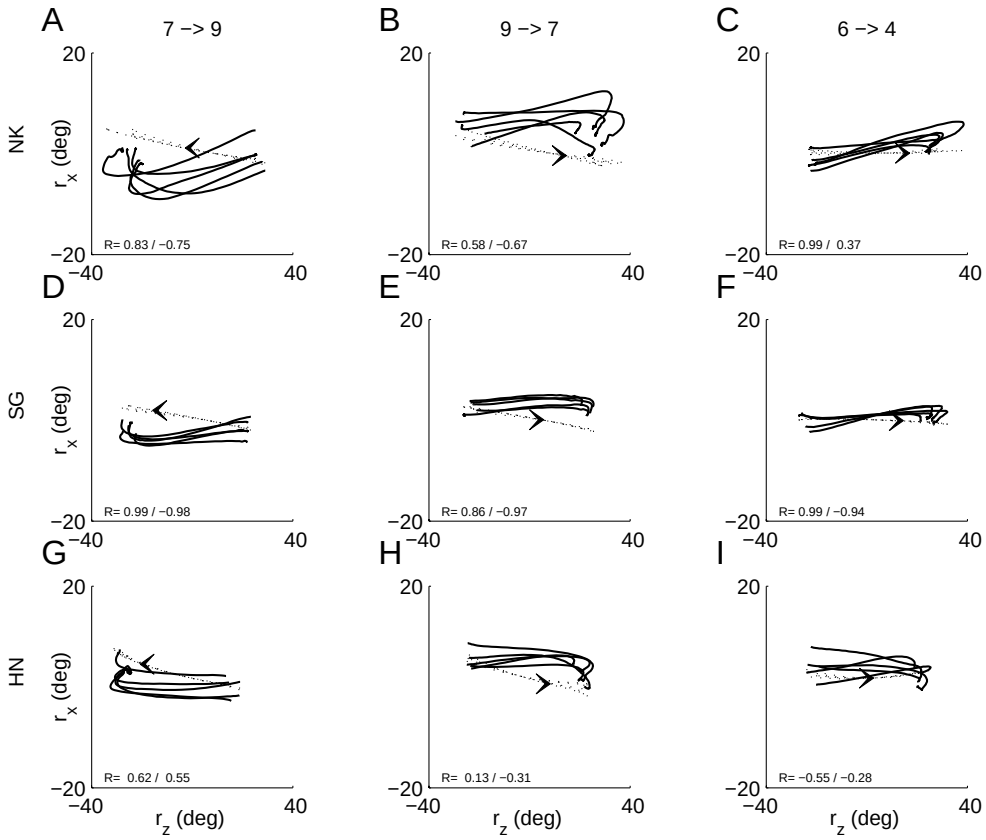

FIGURE 4.6: Head movement trajectories for three pairs of begin and end targets, for three subjects. Thick lines represent five trajectories with a high velocity for movements from target 7 to 9 (panels A, D and G), from target 9 to 7 (panels B, E and H) and for movements from target 6 to 4 (panels C, F and I). Trajectories are displayed for: subject NK (A-C), subject SG (D-F) and subject HN (G-I). The dotted lines indicate the projection if the trajectory in the 2-D surface. Arrows indicate the direction along the trajectory in time. The mean of the correlation coefficients between each of the trajectories and the mean of the four other trajectories (r_{mean}) as well as the mean of the correlation coefficients between the trajectories and the predicted trajectories along the surface ($r_{surface}$) is indicated in the lower left corner of each panel: $r_{mean} / r_{surface}$.

For 25 out of 60 correlation coefficients for arm movements, the correlation with the other trajectories was significantly higher than that with the predicted trajectory. None of the correlation coefficients with the predicted trajectory was significantly higher than that with the other trajectories.

A similar approach was followed for the trajectories of head movements. For 14 out of 60 coefficients, the correlation with the mean of the other trajectories was significantly higher than that with the predicted trajectories. The correlation coefficient between the trajectories and the predicted trajectories was never significantly higher than that with the mean of the other trajectories. These results

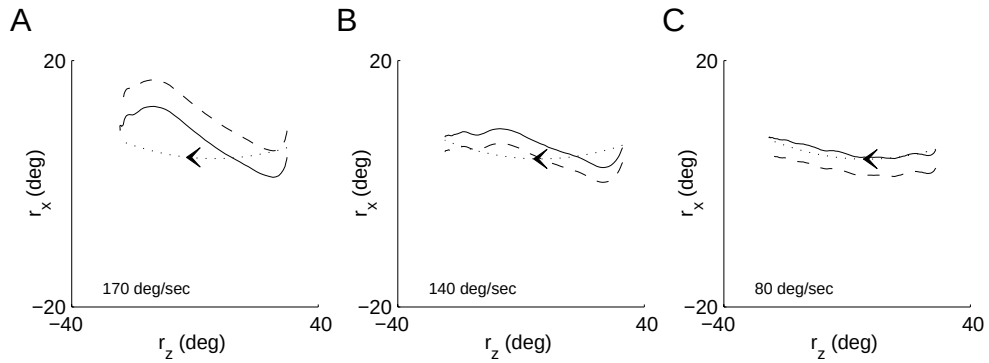

FIGURE 4.7: Example of the effect of velocity on the deviation from the surface during movements of the arm. Dashed lines represent the original trajectories from target 7 to 9 for subject NK. Thick lines represent trajectories that are shifted towards the surface in torsional direction (see Methods). Panels A, B and C show trajectories with peak velocities 170, 140 and 80 deg/s respectively. The dotted line represents the projection of the trajectories on surface. Arrows indicate the direction along the path in time.

demonstrate that trajectories during a movement are often very similar. They are closer to each other than to the predicted trajectory in the 2-D surface with rotation vectors for the arm or head at rest.

In order to investigate the effect of movement velocity on the trajectory of rotation vectors during the movement, Figure 4.7 shows three trajectories obtained from subject NK, for arm movements from target 7 to target 9, for three different movement velocities. Figures 4.7A, B and C show movements with a peak velocity of 170, 140 and 80º/sec, respectively. In order to focus on the shape of the trajectories during the movements, we corrected for the constant torsional offset as much as possible by shifting the trajectories towards the surface such, that the distance of the rotation vectors at the beginning and end of the movement towards the fitted surface is minimal (see Methods). After the shift, all trajectories start and end near each other.

Comparison of the trajectories in the three panels shows that for these movements the amount of deviation from the surface increases with increasing movement velocity. This was a frequently observed tendency, which will be elaborated in more detail below. Furthermore, the scatter relative to the surface varied, depending on the velocity of the movement. When only orientations at 'high' velocities were taken into account, the scatter relative to the surface was larger than when orientations at low velocities were included.

For a quantitative evaluation of the effect of velocity on the amount of deviation, we expressed the amount of deviation in terms of the distance towards the surface integrated along the spatially resampled movement path (see Methods). Figure 4.8 shows this measure of deviation as a function of peak angular velocity

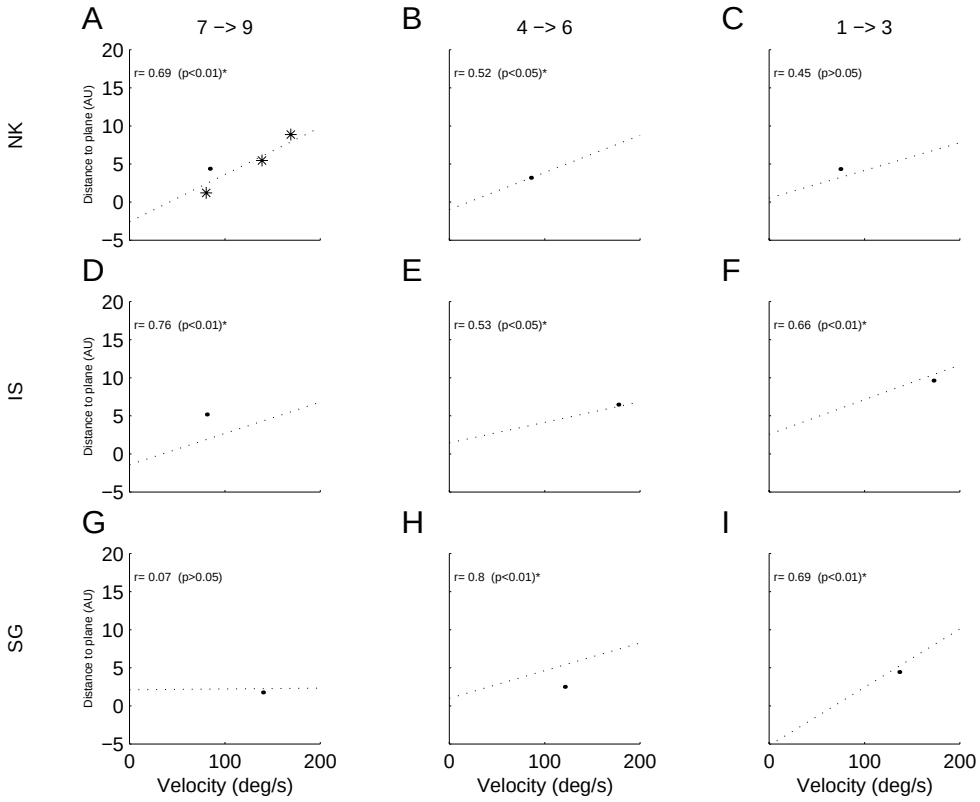

FIGURE 4.8: Velocity dependent deviations from the surface for the arm, for three pairs of begin and end targets, for three subjects. Dotted line represents the best linear fit to the data. The corresponding correlation coefficient and its significance is displayed in each panel. Panel A shows data from subject NK, for movement from target 7 to target 9. An asterisk (*) indicates the data for the trajectories from Figure 4.7. Panels B and C show data from subject NK for movements from target 4 to 6 and from target 1 to 3, respectively. Panels D-F show data for subject IS and panels G-I show data for subject SG.

for the upper arm. Figure 4.8A shows all movements from target 7 to target 9, for subject NK. The data in Figure 4.8A that correspond to the trajectories displayed in Figure 4.7 are marked by an asterisk. Figure 4.8A clearly shows a positive correlation (r=0.69) between peak angular velocity and the amount of deviation from the surface for these arm movements. This correlation is highly significant ($p<0.005$). An analysis of all data (12 target pairs for 5 subjects) revealed similar positive and significant ($p<0.05$) correlations for 31 of the 60 sets of arm movements. Twelve of these sets of movements showed even higher correlations, ranging from 0.68 to 0.87 ($p<0.005$). Figures 4.8B and C show movements for the same subject, between targets 4 and 6 and targets 1 and 3, respectively. The middle rows (Figures 4.8D-F) show the same data for movements for subject IS and the bottom panels (Figures 4.8G-I) show the data for subject SG. An asterisk indicates the correlation coefficients for the data in Figure 4.8 that are significant at a 5 % significance level.

For head movements, we found that the correlation between peak angular velocity and the amount of deviation from the surface was less obvious than it was

for arm movements. Further analysis of the head movements revealed that only 10 of 60 sets of movements had significant correlation coefficients ($p<0.05$) between peak angular velocity and the amount of deviation from the surface. Although a frequency of 10 out of 60 movement sets is well above chance level, it is significantly smaller than that for the arm. For the head movements with a significant correlation, the dependence of the amount of deviation on peak angular velocity was about four times smaller than that for arm movements. Moreover, for head movements, both positive and negative correlations were found. This means that increasing the angular velocity leads to larger deviations for movements between some target pairs, but to smaller deviations for movements between other target pairs.

DISCUSSION

In this study we tested whether arm and head orientations are the same during movement and at rest for identical pointing directions. Corroborating previous findings (Glenn and Vilis 1992; Hore et al. 1992; Miller et al. 1992; Theeuwen et al. 1993; Crawford et al. 1999; Medendorp et al. 1999, 2000) we found that the rotation vectors representing orientations of the upper arm and head during movements are close to a curved surface representing arm or head orientations at rest, respectively. A detailed analysis revealed that the differences between the dynamic and static orientations were often systematic and reproducible for each target pair. This result implies a violation of Donders' law for head and upper arm movements and suggests a rejection of the movement strategy illustrated in Figure 4.1A. For arm movements, the movement trajectories clearly do not correspond to fixed-axis rotations (see Figure 4.5), which rejects the fixed-axis rotation strategy as illustrated in Figure 4.1B. Orientations of the head during the first part of the movement follow straight trajectories in rotation vector space, which could be interpreted as evidence for a fixed-axis rotation strategy (see also Tweed and Vilis 1992; Crawford et al. 1999). The curved path at the end of the movement should then be interpreted as a corrective movement to bring the orientations back to the 2-D surface. However, a strict interpretation of these results also rejects the strategy as illustrated in Figure 4.1B for the head. The broad repertoire of alternatives, which belongs to the movement strategy of Figure 4.1C, will be discussed later in the Section "Implications for models on motor control".

Furthermore, the differences between arm orientations during movement and at rest often become larger for higher peak velocities. A similar result was found by Nishikawa et al. (1999), who evaluated the arm plane angle (a parameter related to upper arm torsion) and reported a 'dynamic overshoot' in the change of the arm plane angle for the fastest movements in their study. For head movements, the correlation between peak velocity and difference between orientations during movement and at rest was less clear; the number of significant correlations was smaller, and moreover, both negative and positive correlations were found.

Our conclusion, that the orientation of the head and arm during movements is different from that at rest, may seem contradictory to previous observations, which did not report any differences between orientations of the arm and head during movements and at rest (Glenn and Vilis 1992; Hore et al. 1992; Miller et al. 1992; Theeuwen et al. 1993; Medendorp et al. 1999). However, this apparent contradiction can be resolved easily. Our data are similar to that in the previously mentioned studies. Based on the fact that the scatter relative to the surface was almost the same in both conditions, these studies concluded that Donders' law was obeyed in static and dynamic conditions. In agreement with these studies the present study showed that the size of the scatter is roughly the same in static and dynamic conditions. The slightly larger scatter in the dynamic condition in this study may be related to the higher movement velocity relative to that used in previous studies, which only tested self-paced velocity movements (e.g. Hore et al. 1992; Miller et al. 1992; Theeuwen et al. 1993; Medendorp et al. 1999). However, in addition to the results of previous studies, the results in this study show that orientations of the head and upper arm do not scatter randomly during movements between a given target pair, but vary in a systematic and consistent way across and within subjects. These results imply a violation of Donders' law, which was not concluded by previous authors.

Furthermore, the controversy in the literature as to whether Donders' law is valid for static upper arm orientations (see Soechting et al. 1995; Gielen et al. 1997) may raise the question of whether the use of a 2-D surface, fitted to the orientations at rest, as a reference to evaluate orientations during movements is a valid procedure. The 2-D surface is a least-squares fit, which minimizes the variance of the data relative to the fitted surface. Consequently, it is the best description of the data at rest and can therefore be used as a reference. Figure 4.3C shows that orientations during a movement follow reproducible trajectories in rotation vector space and that these trajectories do not scatter randomly. Therefore, the conclusion that orientations during movement differ from orientations at rest is independent of the interpretation of the fitted 2-D surface and, consequently, is not affected by any controversy about the validity of Donders' law for orientations at rest.

Orientations during a movement were found to have a small torsional bias of 2 or 4 degrees at most, for the head or arm respectively, values which remain approximately constant throughout the movement (see Figures 4.5 and 4.6). In order to compare the shape of the trajectories of orientations during movements at different velocities, we had to correct for this bias (see Figure 4.7). Support for this procedure to correct for the torsional bias without affecting the shape of the trajectory is provided by Hore et al. (1992), who instructed subjects to start arm movements with a torsional offset and found that this offset remained constant throughout the movement.

Both for the arm and for the head the movement trajectories show reproducible deviations from the surface that describes orientations at rest. Although the shapes of these deviations are very similar for different movement velocities, the amplitudes of the deviations differ, depending on movement velocity. For half of the target pairs, the observation that differences between orientations during movement and at rest become larger for higher peak velocities was significant. For head movements, the effect of peak velocity on the difference between orientation during movement and at rest was significant for a much smaller proportion (about 16%) of the movements. The correlation was relatively small and not as clear as for the arm; for some targets, peak velocity and head movements revealed a negative correlation whereas for other targets, a positive correlation was found. At this moment, we cannot provide a satisfying explanation for the different effect of peak velocity on the orientations during movements for the arm and for the head.

Implications for models on motor control

Previous studies on arm and head movements have mainly focused on the orientation of the arm or head at the end of a movement. In the present study, we focused on the orientations during movement and compared them with orientations at rest. One of the main results of this study is that dynamic orientations of the upper arm and head differ from static orientations for the same pointing or facing direction. This raises the question of whether differences between static and dynamic orientations are the result of a neural strategy or whether these deviations are just small artifacts due to inaccuracies in motor programming by the CNS. This issue will be addressed in the following sections.

Models for arm movements

As explained in the Introduction, there is abundant evidence that final orientation after a reaching movement is planned in advance and that it is used by the CNS in motor programming. This is in agreement with the observation that orientations at the beginning and end of movements are well described by a 2-D surface and with the observation that orientations at the end of a movement do not depend on movement velocity (Nishikawa et al. 1999).

The extended arm can be modeled as a solid cylinder with the same inertia for movements in elevation and azimuth. If movements of such a cylinder are constrained by an efficiency criterion (such as predicted, for example, by the minimum work hypothesis (Soechting et al. 1995) or by minimum torque change (Uno et al. 1989)), rotations in the shoulder should be fixed-axis angular rotations with the smallest possible rotation angle. Fixed-axis rotations bring the arm to the final position by a straight trajectory in rotation vector space (similar to Figure 4.1B), which obviously is not the case (see curved trajectories of rotation vectors during movements in Figures 4.3, 4.4, 4.5 and 4.6).

Flash (1987) proposed that the paths of the end effector for multi-joint arm movements are the result of a virtual trajectory of equilibrium points. The observed path might differ from the virtual path because of the complex biomechanical properties of the arm. If so, these differences will be more prominent for higher movement velocities. The result that deviations of arm orientations during movements relative to orientations at rest are larger for higher movement velocities could therefore be considered compatible with this model. However, we will argue that the biomechanical properties of the arm (e.g. inertia) and gravitation cannot explain the shape of the deviations from the surface observed in this study. Our analyses demonstrate that the differences between orientations of the arm in static conditions and during movements are mainly in torsional direction. The inertia of the fully extended arm is the same for movements in elevation and azimuth. Therefore, the torsional component of the spatial paths of the upper arm should not be different from that of the virtual path for horizontal and vertical movements. Taking the effect of gravity into account might lead to deviations of the vertical component of movement paths relative to the virtual path, but does not effect the torsional component of the arm.

Another explanation for the differences in orientations at rest and during movement may arise from the neuromuscular properties of the arm. Muscles in the shoulder produce accelerations in a mixture of directions. Activation of the pectoralis major muscle, for example, produces both abduction and endorotation of the upper arm. Activation of a muscle to accelerate the arm in a specific direction will thus simultaneously introduce accelerations in unintended directions. Activation of other muscles is then needed to cancel these byproducts.

Ghez and Gordon (1987) reported that during isometric impulses and steps of flexor force in the elbow, flexor and extensor muscles are successively activated. They concluded that the neural commands to opposing muscles acting at a joint must be adapted to constraints imposed by the properties of the neuromuscular plant. Such co-activation could be triggered by reflexes. Gielen et al. (1988) have shown that long latency stretch reflexes (50-75 ms) incorporate coordinated responses from various muscles, but that short-latency reflexes do not. It is well known (Lacquaniti and Soechting 1986; Soechting and Lacquaniti 1988) that latencies of mono-synaptic reflexes are different for various muscles in the human arm. These differences in latency have been attributed to differences in conduction time along nerve fibers from motoneurons in the spinal cord to the muscle. These differences will have a small effect on the precise coordination of movements in 3-D for low movement velocities. For fast movements, however, the effect of differences in activation time for co-activated muscles on the movement trajectories will become more prominent. This might explain the correlation between peak velocity on the one hand and the difference between orientations during movement and those at rest on the other hand.

Models for head movements

Tweed (1997) postulated a model for eye-head saccades in 3-D, which assumes that orientations of the head are determined by a system (Donders' operator) that specifies head orientations according to Donders' law, followed by a system (so-called head-pulse generator) that generates the proper motor commands to move the head towards the final orientation (see also Medendorp et al. 1999). Deviations during movement could be due to the fact that Donders' operator is located before the pulse-generator. From this point of view, the fact that the first and major part of the trajectory for head movements reported in this study is a more or less straight path in rotation vector space might indicate that the head-pulse generator induces a fixed-axis rotation for the head, followed by a correction movement, which brings the end of the trajectory back to the surface that characterizes the static data.

If arm movements are described by a similar model, the equivalent of the head-pulse generator for the arm might in a similar way be located after Donders' generator, which may lead to violations from Donders' law during movement. This is compatible with previously proposed models for arm movements that postulate internal models that mimic the input/output characteristics, or their inverses, of the motor apparatus to move the limb from the starting to the (predefined) final orientation (see Kawato 1999). According to this line of thought, the trajectories would be the result of a deliberate planning by the CNS, instead of a distortion of some planned trajectory.

For each pair of targets the very reproducible trajectories can have different torsional offsets of at most 2 or 4º, for the head and arm respectively, which remain approximately constant throughout the movement. This suggests that the arm or head constraints are not implemented at the level of position commands but presumably at the level of velocity commands or maybe at some higher level such as acceleration (Ceylan et al. 2000; Medendorp et al. 2000). These so-called non-holonomic constraints do not restrict the allowable positions of the system, but only the permitted velocities in certain positions. Moreover, while velocity-level control can account for the fact that head and arm depart from their static Donders' surface during movements, position-level control would force one to conclude that the Donders' operator is outside of the motor feedback loop.

In order to discriminate between the various models, more detailed studies on postures during movements are necessary. This study provides a first step towards these studies by presenting a new framework to analyze orientations during movements in great detail.

CHAPTER 5

MODELING KINEMATICS AND DYNAMICS OF HUMAN ARM MOVEMENTS

INTRODUCTION

The human arm is a multi-articulate limb with relatively many degrees of freedom, which provides a large flexibility. This flexibility also allows that a particular simple motor task can be executed using various postures. In this context it is surprising that several studies have shown that the kinematics of arm postures is quite consistent and reproducible within and across subjects (see e.g. Soechting et al., 1995). Beside postural flexibility at the end point of a movement, the many degrees of freedom of the arm also allow many different movement trajectories, which all bring the hand from the initial position to a given end position. Yet, the path of the index finger during a reaching movement has been reported to be consistent from trial to trial both within subjects and across subjects (Georgopoulos et al. 1981; Soechting and Lacquaniti 1981).

The fact that movement kinematics and dynamical movement trajectories are consistent within and between subjects has raised the question to what extent movement kinematics and movement dynamics are related. One possibility might be that movements are planned at a kinematic level (e.g. in joint coordinates or in extrinsic coordinates) and that, once such a plan exists, the forces to produce the desired movement trajectory are generated. This class of models is usually referred to as “posture based” models. One particular model from this type is Donders' law, which was originally proposed for eye movements. It states that torsion of the eye is uniquely determined for each gaze direction (Donders 1848; Tweed and Vilis 1987). Later studies have reported that Donders' law is also obeyed for head and arm movements (Straumann et al. 1991; Hore et al. 1992; Miller et al. 1992). However, more detailed analyses (see Soechting et al. 1995; Gielen et al. 1997) revealed small but systematic deviations from the unique torsion for pointing directions, which are inconsistent with Donders’ law. Another type of posture-based predictions follow from the equilibrium trajectory hypothesis (Hogan 1985, Flash

Adapted from: M.A. Admiraal, J.M.A.M. Kusters, C.C.A.M. Gielen,
accepted for Motor Control, 2004.

1987), which states that the trajectories are achieved by gradually shifting the hand equilibrium positions between the beginning and end point of movements.

Another possibility might be that movement trajectories are the result of some optimization process or may be due to some dynamical constraints and that kinematics are a result of movement dynamics. An example from this class of models is the minimum work model (Soechting et al. 1995). Soechting and his colleagues suggested that the deviations of Donders' law could be explained by assuming that movements are made based on the criterion of minimization of work. This implies that the final posture of a movement is the result of minimizing the amount of work that must be done to transport the arm from the starting posture towards a target. The minimum work hypothesis is an alternative for sequential planning of kinematics and dynamics. According to the minimum work hypothesis, the dynamics and kinematics follow tightly connected from the optimization criterion given the movement time and the initial and final position of the movement. The same is true for other optimization models, which have been proposed to explain the reproducible nature of movement trajectories, like the minimum torque-change model (Uno et al. 1989), the minimum commanded-torque-change model (Nakano et al. 1999), the minimum variance model (Harris and Wolpert 1998), and the stochastic optimal control model proposed by Todorov and Jordan (2002).

Obviously, the models mentioned above cannot all be correct. In this context it is remarkable to notice that a quantitative comparison between the performances of each of these models for movements in 3-D space has not been performed yet. Such a comparison would be important for several reasons. First, a comparison could discriminate between viable models and models which have to be rejected. Second, a quantitative comparison could reveal whether a single model can provide a good fit to the data or whether the central nervous system might use multiple criteria, with each criterion suitable for one or a small set of contexts (see e.g. Haruno et al. 1999; Haruno et al. 2001). In that case it might be that a model gives a good performance for a particular set of movements or movement instructions, but fails for another. Given the different optimization criteria of the various models (e.g. minimum-work, minimum-torque-change) it might well be that the performance of the models depends on the context and instruction to the subject, as was proposed by Todorov and Jordan (2002).

The aim of this study was to investigate arm movements to distant targets with the fully extended arm (pointing movements) and movements between various targets in 3-D space at various distances relative to the subject, requiring flexion/extension of the elbow (reaching movements). Subjects were instructed to make arm movements towards randomly presented targets. In order to investigate whether the central nervous system might use multiple criteria, with each criterion suitable for one or a small set of contexts (see e.g. Haruno et al. 1999; Haruno et al. 2001), subjects were tested at three different movement velocities: 1) without any

instruction regarding velocity, where movement velocity was freely chosen by the subject, and with the instruction, 2) to "move as accurately as possible" or 3) to "move fast". The aim of these experiments was not to generate a new unique set of data, since many studies have collected similar data. Rather these data were collected to serve as a reference to test the predictions by the minimum work model and the minimum torque-change model. As will be explained later, the predictions of arm postures by the minimum-commanded-torque-change model and the minimum-variance model for the fully extended arm (including torsion along the long axis of the arm) are similar to the predictions by the minimum-work model for many initial and final targets. The predictions by these movements were compared to the null-hypothesis of a unique posture for each target position (Donders' law). We have not tested the equilibrium point (EP) hypothesis, since the EP-hypothesis has many versions: it can be formulated at the single-muscle level, at a single-joint level, and at a single-effector level. Therefore, the EP hypothesis, as it stands now, cannot make unambiguous general predictions with respect to arm postures.

METHODS

Fifteen adult human subjects (aged 21- 49 years) participated in the experiments. None of them had any known sensory, perceptual, or motor disorders. All subjects gave informed consent to participate in the experiments and none of the subjects was familiar with the purpose of this study. All subjects were right-handed and all movements were made with the right arm. Two experiments were performed, and subjects participated either in the POINTING experiment (six subjects) or the REACHING experiment (nine subjects). The experimental protocols were approved by the medical ethical committee of the University of Nijmegen and all subjects gave informed consent before the experiment.

Experimental setup

Visual stimuli were generated by a personal computer and were projected by a LCD projector (Philips Proscreen 4750) on a translucent screen. The visual scene projected on the translucent screen covered an area of 120 cm x 96 cm, corresponding to a maximum visual range for the subject of 62 x 51 deg in the POINTING experiment, and 74 x 62 deg in the REACHING experiment. In the POINTING experiment, the computer generated a video image of a checkerboard pattern with 8 x 8 alternating black and yellow rectangles (15 cm x 12 cm each) on the projection screen. On top of this background, the pointing targets (yellow spheres with a diameter of 1.5 cm) were projected. In the REACHING experiment, the computer generated a video image of a virtual 3-D scene on a plane parallel to the projection screen. The video image consisted of 2 images of the scene, one in green representing the projection of the 3-D scene as viewed by the left eye, and one in red representing the projection of the 3-D scene as viewed by the right eye.

The subject was wearing a pair of goggles with a red filter (Kodak Wratten nr. 25) for the right eye and a green filter (Kodak Wratten nr. 58) for the left eye, providing the subject with stereovision. Targets for the reaching movements were small yellow spheres (diameter 1.5 cm), which appeared in front of a checkerboard background, which consisted of 8 x 8 alternating black and yellow rectangles (15 cm x 12 cm each). The images for the left and the right eye were generated in the proper perspective relative to the observer such that the checkerboard background appeared at a distance of about 10 cm in front of the projection screen as seen by the observer.

The participants sat on a chair, which had a straight and high back support. The position and height of the chair could be adjusted such that the subject's right shoulder was in front of the center of the visual scene. In the POINTING task, the subject's body was rotated 45 degrees relative to the projection screen, whereas in the REACHING task the subject was positioned straight in front of the projection screen (see Figure 5.1). Subjects were fixated to the chair by seat belts, which allowed all rotations in the shoulder, but kept their trunk and shoulder in a fixed position in space throughout the experiment. This was verified by measuring the position of the shoulder , as is described below.

The position and orientation of the upper arm were also measured with an OPTOTRAK-system (Northern Digital), which is capable of measuring the positions of infrared light emitting diodes (ireds) with a resolution better than 0.2 mm within a range of 1.5 m^3. The OPTOTRAK system was mounted on the ceiling above the subject at a distance of approximately 2.5 m behind the seated subject, tilted downward at an angle of 30 degrees relative to the ceiling. The movements were sampled at a rate of 100 Hz.

A cross with ireds on each of the four tips was attached to the upper arm just proximal to the elbow joint and at the forearm, just proximal relative to the wrist joint. The lengths of the arms of the crosses were 6 and 12 cm for the crosses on the forearm and upper arm, respectively. Additional (single) ireds were attached to the shoulder (acromion), to the elbow (epicondyle lateralis) and to the tip of the index finger. Subjects were instructed to keep the index finger in full extension such that the forearm, hand and index finger were all aligned.

Experimental paradigms

Subjects were tested in two experiments. The first experiment (POINTING task) focused on pointing movements with the fully extended arm to targets displayed on the projection screen at a distance of 100 cm (range 54 degrees in both azimuth and elevation). In the second experiment (REACHING task) targets appeared in various directions and at various distances relative to the shoulder (range 60 deg in azimuth and 50 deg in elevation), requiring flexion of the arm (see Figure 5.1). By definition, a vertically downward orientation of the upper arm corresponds to an elevation angle (θ) of zero degrees. The azimuth angle (η) is positive when the

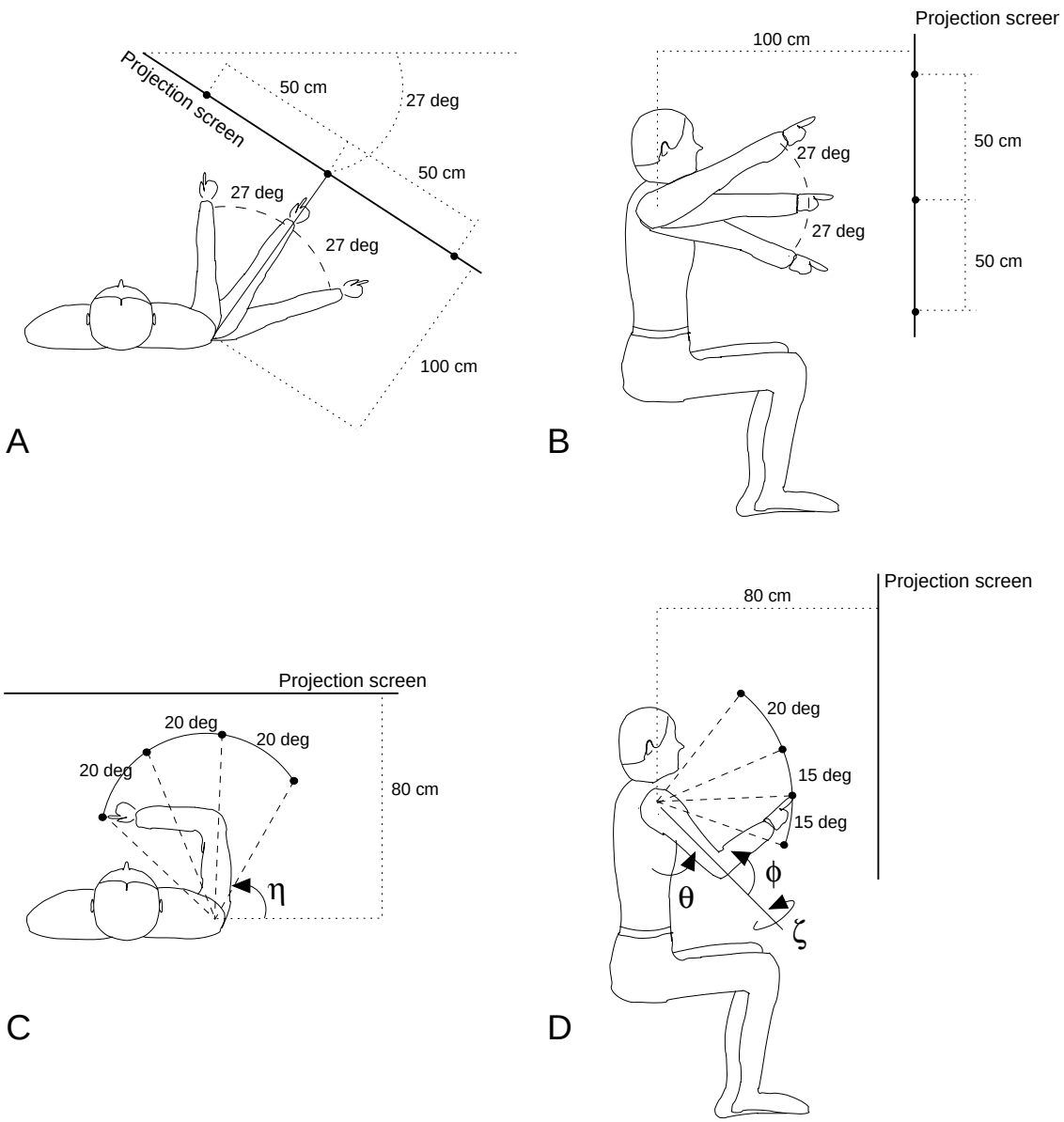

FIGURE 5.1: Top view and side view on the subject for the POINTING and REACHING experiment. Panels A and B represent a top view and side view, respectively of the experimental setup in the pointing experiment, panels C and D represent the top and side view of the experimental setup in the reaching experiment. The definition of rotation angles (η, θ, ζ and φ) used to define the arm's orientation in the reaching experiment is indicated by arrows in the two bottom panels.

upper arm is directed leftward, negative when it is oriented to the right, and zero for the straight-ahead direction. When the elbow is fully extended, the flexion angle (ϕ) is defined to be zero; flexing the elbow corresponds to positive flexion. Torsion (ζ) is defined as the rotation around the humeral axis of the upper arm. With zero degrees of torsion, the upper arm and forearm lie in a vertical plane for all flexion angles.

In both experiments, we tested arm movements in a task that sets all-but-one available degrees of freedom. In the POINTING task, this remaining degree of freedom corresponds to the torsion of the arm, whereas in the REACHING task, this remaining degree of freedom lies in the combination of angles θ, η and ζ. Setting one of these three angles defines the other two. Hence, the outcome of the analysis does not depend on which angle is evaluated. For consistency, we have chosen to evaluate the amount of torsion of the upper arm (ζ) both in the POINTING experiment, and in the REACHING experiment.

Pointing task

In the first experiment subjects sat with the right shoulder at a distance of 100 cm in front of the projection screen. Five bright yellow, spherical targets with a diameter of 1.5 cm were displayed on top of the checkerboard pattern on the projection screen. Four target positions were at the corners of a 100 cm by 100 cm square, numbered I to IV in clockwise direction, starting with the upper left target. The fifth target (V) was in the middle of the square, right in front of the right shoulder (see Figure 5.2A). When pointing to these four targets, the azimuth angles in the shoulder ranged from -27 to +27 degrees, and elevation angles ranged from -27 to +27 degrees. Subjects had to point to the targets with the fully extended arm.

At the start of each trial, subjects were instructed to point at target V for about 1 second, and then at target I. From there, the pointing movement moved either in clock-wise direction (order I-II-III-IV-I) for about 8 cycles, or in anti-clockwise direction (order I-IV-III-II-I) for 8 cycles. Subjects were instructed to make arm movements from one target to the next, while stopping at each target for a short period after each movement.

Each movement direction was tested with three instructions: In the first type of trials the instruction to the subject was to move from one target to the next with a self-paced, smooth movement (SELF-PACED). In the second type of trials the subject was instructed to move fast from one target to the next, but such that the movement stopped at each target before moving to the next target (FAST). In the third type of trials, subjects were instructed to move to each target with a single, smooth movement, but as accurately as possible (ACCURATE). Each type of instruction was repeated two times (FAST and ACCURATE) or four times (SELF-PACED) for both movement directions.

At the end of this series of experiments, subjects were asked to point at random in various directions with the fully extended arm. These postures were used to estimate the dependence of torsion of the upper arm on azimuth and elevation for various directions of azimuth and elevation. According to Donders' law, torsion should be uniquely determined for each direction of azimuth and elevation (see *Models for movement planning* section).

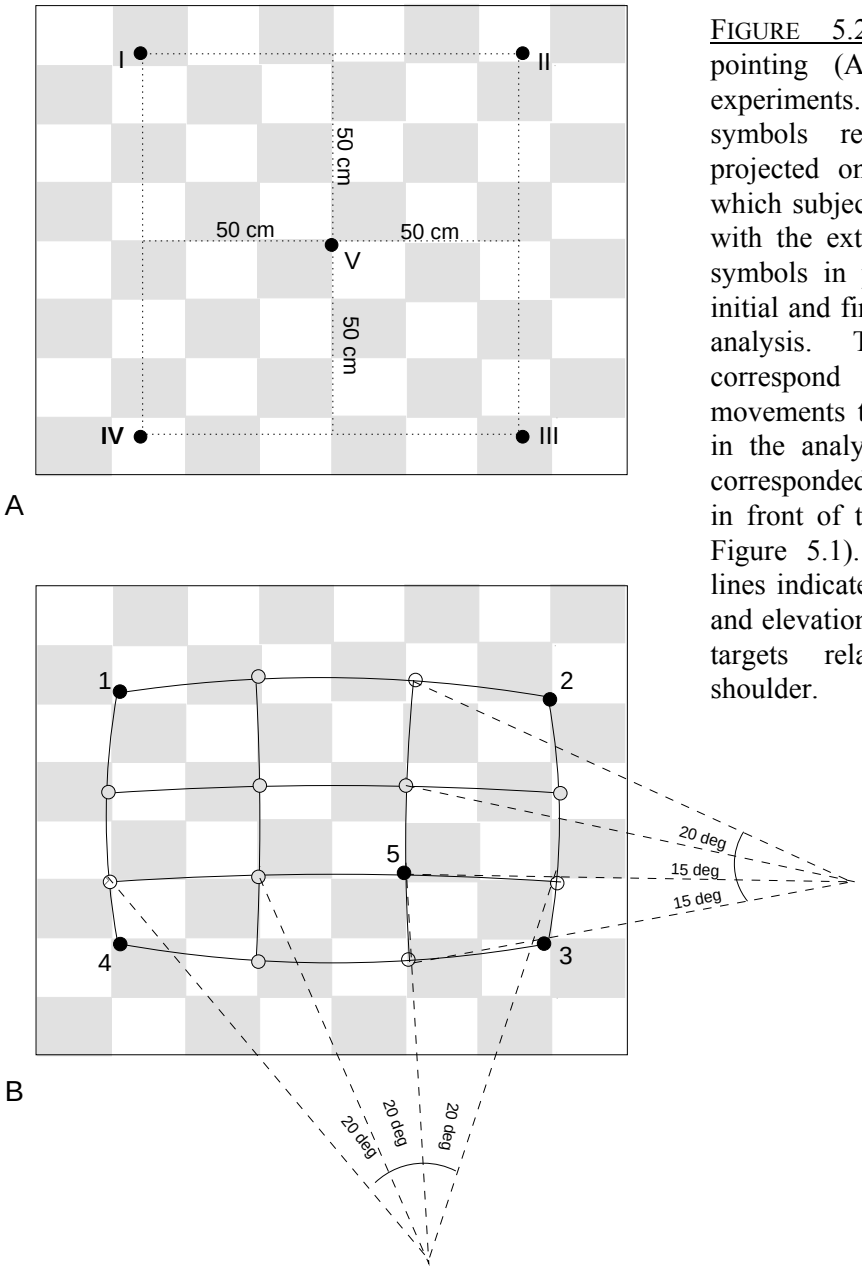

FIGURE 5.2: Targets for the pointing (A) and reaching (B) experiments. In panel A, the filled symbols represent the targets, projected on the screen, towards which subjects were asked to point with the extended arm. The filled symbols in panel B represent the initial and final targets used for the analysis. The open symbols correspond to targets for movements that were not included in the analysis. Targets V and 5 corresponded to a position straight in front of the right shoulder (see Figure 5.1). In panel B, dashed lines indicate the azimuth (bottom) and elevation (right) position of the targets relative to the right shoulder.

Reaching task

For the second experiment, the subject was placed with the shoulder at a distance of 80 cm from the screen (see Figures 5.1C and D). In this experiment we tested postures of the arm, when subjects reach to a virtual target within reaching distance in 3-D space. Subjects were asked to position the tip of the index finger at the virtual target position until it disappeared and a new target appeared. Subjects were instructed to maintain the current posture after each movement until they accurately localized the new target, before making a single aiming movement to the new target. When the new target was not found or not perceived accurately because

it appeared (partly) out of view behind the subject's arm, subjects were instructed not to make a movement, and wait for the next target to appear.

For each subject, we adjusted the target positions such that the targets appeared at equal distances relative to the shoulder corresponding to elbow flexion near 90 degrees when the subjects reached the target correctly. Targets appeared at one of sixteen locations on a grid, such that movements to neighboring targets required changes of 20 deg in azimuth and 20 or 15 deg in elevation relative to the shoulder (see bottom panels in Figure 5.1 and Figure 5.2B). The target remained at its location for two seconds. Targets appeared in a pseudo-random order, which was the same for all subjects. In the analysis we only selected movements starting or ending at one of the four targets at the corners of the grid (targets 1, 2, 3 and 4) and at a location straight ahead of the right shoulder (target 5). Using these 5 positions as begin and end targets for aiming movements gives 20 possible combinations. All subjects made at least 5 movements for each of these 20 target pairs.

Since we examined whether postures of the arm did depend on postures for previous targets, we tried to arrange the same initial posture at the beginning of each series of movements. According to Soechting et al. (1995) postures should be most reproducible, when the right arm was pointing to a target at the lower left side. Therefore, each pair of targets from the 20 combinations was preceded by target 4 (at the lower left target at -40 deg azimuth and -15 deg elevation).

To prevent fatigue, subjects were tested in ten blocks with 15 movements each. Between blocks subjects could pause as long as they needed.

Models for movement planning

Donders' law

Donders' law assumes that the Central Nervous System (CNS) uses a unique orientation of the upper arm for each position of the hand. The orientation of the upper arm during pointing is expressed in terms of a rotation axis and rotation angle, which rotates the upper arm from a reference position to the current position. This rotation vector is defined by

$$\vec{r} = \tan\left(\frac{\alpha}{2}\right) \vec{n} \qquad (5.1)$$

where $\vec{n}$ represents the unit vector of the rotation axis in 3D, and α is the angle of rotation along that axis (see e.g. Haustein 1989; Straumann et al. 1991). When the right position (the so-called *primary position*, see Haustein 1989) is taken as a reference position, the three orthogonal components of rotation vector $\vec{r}$ (r_u, r_v and r_w) represent the torsional component, elevation component and azimuth component, respectively. The relation between torsion angle (ζ) and the torsional

component r_u follows from the definition in Equation 5.1, where $\vec{r}$ equals r_u when $\vec{n}$ is along the humeral axis of the upper arm, and $\alpha = \zeta$.

Donders' law assumes that torsion is fully specified by azimuth and elevation of the upper arm while pointing. A polynomial fit was used to find the relation of the torsional component r_u as a function of r_v and r_w (see e.g. Gielen et al. 1997, Admiraal et al. 2002).

The minimum work model

The model for calculating minimum work was first presented by Soechting and colleagues (1995). In agreement with Soechting et al. we define a coordinate system to define target location and arm posture: the X-axis is in the lateral direction passing through the shoulders. The Y-axis is directed forward relative to the right shoulder, from which the Z-axis points upward. Since the subject's shoulder is strapped tightly to the chair, this XYZ-coordinate system is fixed in space. Pronation and supination of the forearm is left out of evaluation, since it does not affect the position of the index finger in space, because the wrist was kept straight throughout the experiments. Then, four joint angles are required to uniquely define the posture of the arm in this coordinate system - three angles that describe rotations at the shoulder joint and one that describes elbow flexion/extension (see Figure 5.1C and D).

The amount of work W that is necessary to move the arm from one point to another is given by:

$$W = \int \vec{T} \cdot d\vec{\Theta} \tag{5.2}$$

where $\vec{T}$ is the vector with torques in the shoulder and elbow and $\vec{\Theta}$ is the vector with joint angles in the shoulder and elbow. Ignoring gravitational forces, the amount of work done at time t is defined as the difference between kinetic energies at the position at time t and at the starting position. Since the arm starts from rest, its kinetic energy at the starting position is zero. Therefore, work at some time t can be written as:

$$W = \int \vec{T} \cdot \vec{\Omega} dt = \sum_{i=1,2} \left[\frac{1}{2} m_i \vec{v}_i^{\,T} \cdot \vec{v}_i + \frac{1}{2} \vec{\Omega}_i^{\,T} \cdot I_i \cdot \vec{\Omega}_i \right] \tag{5.3}$$

where parameter $i = 1,2$ refers to the two segments, forearm and upper arm, $\vec{\Omega}_i = d\vec{\Theta}_i / dt$ and m_i is the total mass of either the upper- or forearm, $\vec{v}_i$ is the speed of the arm's center of mass, and I_i is the inertia tensor of the arm.

When the rotations of the upper arm are described in an arm-centered coordinate system $[X', Y', Z']$, centered in the right shoulder instead of the earth-fixed Cartesian coordinates $[X, Y, Z]$, (see Soechting et al. 1995), the three separate components of the angular velocity vector of the upper arm read:

$$\begin{aligned}\Omega_{X'} &= \dot{\eta}\sin\varsigma\sin\theta + \dot{\theta}\cos\varsigma \\ \Omega_{Y'} &= \dot{\eta}\cos\varsigma\sin\theta - \dot{\theta}\sin\varsigma \\ \Omega_{Z'} &= \dot{\eta}\cos\theta + \dot{\varsigma}\end{aligned} \tag{5.4}$$

We assume that the upper arm and forearm can be considered as solid cylinders. Then their moments of inertia, computed about the center of mass, are the same for rotations in azimuth and elevation (I_{u1}, I_{f1} for the upper arm and forearm, respectively). Rotations around the humeral axis of the upper meet a much smaller moment of inertia (I_{u2}). As mentioned earlier, rotations around the forearm's long-axis are left out of evaluation.

The velocity of the arm's center of mass can be computed from the vector cross product between the angular velocity vector $\vec{\Omega}$ and the vector $\vec{r}$ connecting the shoulder to the arm's center of mass: $\vec{v} = \vec{\Omega} \times \vec{r}$.

After some algebra, one obtains for the work W,

$$\begin{aligned}W = \frac{1}{2}\Big[& I_1\left(\Omega_{X'}{}^2 + \Omega_{Y'}{}^2\right) + I_2\Omega_{Z'}{}^2 + \\ & + I_3\left(\left(\Omega_{x'} + \dot{\phi}\right)^2 + \left(\Omega_{Y'}\cos\phi + \Omega_{Z'}\sin\phi\right)^2\right) + I_4\left(\Omega_{Y'}\sin\phi - \Omega_{Z'}\cos\phi\right)^2 + \\ & + 2A\left(\left(\Omega_{X'}^2 + \Omega_{Y'}^2\right)\cos\phi + \Omega_{Z'}\Omega_{Y'}\sin\phi + \dot{\phi}\Omega_{X'}\cos\phi\right)\Big]\end{aligned} \tag{5.5}$$

See Appendix for the definitions of parameters I_1, I_2, I_3, I_4, and A. With the use of Equation 5.4, this can also be written as:

$$\begin{aligned}W = \frac{1}{2}\Big[& I_1\left(\dot{\eta}^2\sin^2\theta + \dot{\theta}^2\right) + I_2\left(\dot{\eta}\cos\theta + \dot{\varsigma}\right)^2 + \\ & + I_3\left(\Omega_{X'}^2 + \Omega_{Y'}^2\cos^2\phi + \Omega_{Z'}^2\sin^2\phi + \dot{\phi}^2 + 2\dot{\phi}\Omega_{X'} + 2\Omega_{X'}\Omega_{Y'}\cos\phi\sin\phi\right) + \\ & + I_4\left(\Omega_{Y'}^2\sin^2\phi + \Omega_{Z'}^2\cos^2\phi - 2\Omega_{Z'}\Omega_{Y'}\cos\phi\sin\phi\right) + \\ & + 2A\left(\left(\Omega_{X'}^2 + \Omega_{Y'}^2\right)\cos\phi + \Omega_{Z'}\Omega_{Y'}\sin\phi + \dot{\phi}\Omega_{X'}\cos\phi\right)\Big]\end{aligned} \tag{5.5a}$$

which is similar -but not equal- to the equation for the total amount of Work presented by Soechting et al. (1995). Compared to the equation presented by Soechting and colleagues, the above equation includes an extra term in the total work, which corresponds to:

$$\frac{A}{2}\left[\left(\Omega_{X'}^2 + \Omega_{Y'}^2\right)\cos\phi + \Omega_{Z'}\Omega_{Y'}\sin\phi + 2\dot{\phi}\Omega_{X'}\cos\phi\right] \tag{5.6}$$

Because we started from the same equations for the angular velocities as Soechting and colleagues, we expect this discrepancy to be a printing error in Soechting's equation. The appendix shows a more detailed derivation of our equation.

When we ignore the effect of gravity, the total work done during the movement is zero since the final velocity is zero. The positive work done to accelerate the arm is canceled by the negative work required to decelerate the arm at the end of the movement. Similar to Soechting et al. we assume that movement velocities are bell-shaped and that joint velocities in elbow and shoulder reach a peak value at the same time. The work will have a peak positive value at the time of peak velocity. Because of the bell-shaped velocity profiles, the peak value of kinetic energy is reached halfway during the movement. The work related to this peak value of kinetic energy is used as cost for the minimization of work.

The minimum torque-change model

All simulations of the minimum torque-change model, which have appeared in the literature so far, have been done for movements in a 2-D plane. In this paper we have used the minimum torque-change model of Uno et al. (1989) to describe arm movements in 3-D space. The cost function to be minimized (C_T) is the sum of squares of the rates of change in torque integrated over the duration of the entire movement (t_m):

$$C_T = \frac{1}{2}\int_{t=0}^{t_m}\sum_{i=1}^{N}\left(\frac{dT_i}{dt}\right)^2 dt \tag{5.7}$$

where T_i is the torque generated by the i-th actuator (joint) out of N joints evaluated. To calculate the torque, we used the Lagrange formalism:

$$L(\vec{q},\dot{\vec{q}},t) = K(\vec{q},\dot{\vec{q}},t) - V(\vec{q}) \tag{5.8}$$

with $\vec{K}$ the kinetic energy and $\vec{V}$ the potential energy. Like previous studies, we ignored gravity and set the potential energy $\vec{V}$ to zero. The torques follow from the Lagrange equation of motion:

$$\vec{T} = \frac{d}{dt}\left(\frac{\partial L}{\partial \dot{\vec{q}}}\right) - \frac{\partial L}{\partial \vec{q}} \tag{5.9}$$

The equation for the torques that result from the above equation is rather complex and will not be shown here.

Like Uno et al. (1989) we introduce a set of nonlinear differential equations to find the trajectory corresponding to minimum torque-change:

$$\frac{d\vec{\Xi}}{dt} = \vec{f}\left(\vec{\Xi}, \vec{u}\right)$$
$$\frac{d\vec{\psi}}{dt} = -\left(\frac{\partial \vec{f}}{\partial \vec{\Xi}}\right)^T \vec{\psi} \qquad (5.10)$$
$$\vec{u} = \begin{bmatrix} dT_\theta/dt \\ dT_\eta/dt \\ dT_\xi/dt \\ dT_\phi/dt \end{bmatrix}$$

where $\vec{\Xi}$ is a 3-N (in this case 12)-dimensional vector with the four joint angles (θ, η, ς and ϕ) as the first four components (same definitions as for the minimum-work model, see Figure 5.1), the first time-derivatives of the joint angles as the next four components ($\dot{\theta}$, $\dot{\eta}$, $\dot{\varsigma}$ and $\dot{\phi}$), and the torques in these joints as the last four components (T_θ, T_η, T_ς and T_ϕ). The vector $\vec{\psi}$ represents a Lagrange-multiplier vector with 3N components, of which the last N components are equal to the vector $\vec{u}$.

Equations 5.10 represent an autonomous nonlinear differential equation with respect to $\vec{\Xi}$ and $\vec{u}$ (see Uno et al. 1989). In this way, our optimization problem results in a boundary-value problem. This boundary-value problem can be solved in an iterative way, based on a Newton-like method.

The initial value of $\vec{\Xi}$ at time zero is specified (i.e. $\vec{\Xi}(t_0) = \vec{\Xi}_0$). However, the initial value of $\vec{\psi}$ is unknown, since the begin values for the torque-change are unknown. Therefore, when we assume a particular initial value of $\vec{\psi}(t_0)$ and solve the initial-value problem for the differential Equations 5.10, the final value $\vec{\Xi}(t_f)$ will not reach the target value $\vec{\Xi}_f$. Therefore, we define a residual error at t_f as:

$$\vec{E} = \vec{\Xi}_f - \vec{\Xi}(t_f) \qquad (5.11)$$

This error $\vec{E}$ is a function of the initial value $\vec{\psi}(t_0)$. The optimal trajectory, which obeys the constraints of minimum-torque change and which minimizes the error-function $\vec{E}(\vec{\psi})$, is found in the same way as described by Uno et al. (1989) based on a steepest gradient method of $\vec{E}(\vec{\psi}(t))$ with respect to the initial vector $\vec{\psi}(t_0)$ using a Newton-like iteration procedure.

Predictions for movement trajectories and orientations of the upper arm

When the fully extended arm is modeled as a solid cylinder, the inertia is the same for movements in elevation and azimuth. If movements of such a cylinder are constrained by an efficiency criterion such as predicted by the minimum work hypothesis (Soechting et al. 1995) or by minimum torque-change (Uno et al. 1989),

rotations of the fully extended arm in the shoulder should be single-axis rotations taking the shortest path from initial to final position. This implies that the direction of the angular velocity vector $\vec{\Omega}$ is in the direction of $\vec{r}_1 \times \vec{r}_2$, where $\vec{r}_1$ and $\vec{r}_2$ represent the positions of the index finger relative to the shoulder for initial and final target position, respectively, and where $\times$ denotes the vector product operator. Such shortest-path rotations correspond to movements along the geodete of a sphere in workspace.

The arguments above explain why the minimization models predict movements over the geodete of a sphere for pointing movements with the fully extended arm. However, it is well known that movements along a closed path by a concatenation of subsequent movements following the geodetes that connect the initial and final positions of the via-points, gives rise to an accumulation of torsion (see Tweed and Vilis 1987; Gielen 1993). This implies that the orientation of the upper arm should depend on the number of previous clock-wise or counter-clock-wise cycles. However, Donders' law predicts that orientation of the upper arm for a particular pointing direction is constant, irrespective of the number of previous clock-wise or counter-clock-wise cycles. In the pointing experiment we have tested these predictions by asking subjects to make clockwise or counterclockwise movements between the corners of a square (targets I, II, III and IV in Figure 5.2A).

The predicted torsion follows from straightforward application of differential geometry, which predicts that the accumulation of torsion after a cycle is equal to the integral of the Gaussian curvature over the area bounded by the trajectory of the cycle (see Stoker 1989):

$$\Delta\zeta = \oint \frac{1}{R^2} dA \tag{5.12}$$

For the Clockwise and Counter Clockwise movements in the POINTING experiment, the Gaussian curvature corresponds to R^{-2}, where R is the distance between the index finger and the shoulder. The accumulation of torsion would than amount about 49 degrees per cycle. An accumulation of torsion is in contradiction with Donders' law, which predicts a unique torsion for each target.

RESULTS

Pointing with the fully extended arm

In the first experiment, subjects were asked to point with the extended arm to targets presented at different elevation and azimuth positions at a distance of 100 cm from the subject's shoulder. Figure 5.3 shows the measured trajectories (dotted lines) of the index finger for subject HP for repeated movements between the corners of a square in Clockwise direction (panel A) and Counter Clockwise direction (panel B). For pointing with the fully extended arm, the minimum-torque and minimum-work model give the same predictions for the trajectory of the index finger, indicated by solid lines.. These predicted trajectories correspond to rotations in the shoulder about the shortest angle from begin to end target (see Methods). They lead to curved trajectories along the geodete on the surface of the sphere with the center at the shoulder and a radius equal to the length of the arm. The measured and predicted trajectories are shown in a 2-D projection on the frontal plane of targets I, II, III, IV, and V (see Figure 5.1).

In general, the measured and predicted trajectories are quite similar, except for the movements between targets I and II in Clockwise direction (Figure 5.3A), where the measured trajectories deviated systematically from the predicted trajectories. For other movements, e.g. between targets II and III and between targets III and IV in the Clockwise direction (Figure 5.3A) and between targets II and I in the opposite direction (Figure 5.3B), the measured trajectories deviated slightly from the predicted trajectories in some trials.

The apparent correspondence between the measured trajectories and the predicted trajectories of the index finger in space does not prove that the predictions by the minimization models are correct, since the data in Figure 5.3 do not provide information about torsion along the humeral axis of the arm. A consequence of the predictions by the minimization models is that rotations in the shoulder are rotations along the shortest path, which result into an accumulation of torsion in the upper arm for movements along a closed trajectory. The predicted accumulation in torsion is either positive (increase in torsion) for movements in Clockwise direction (I to II, II to III, III to IV and IV to I) or negative (decrease in torsion) for the Counter Clockwise movements (I to IV, IV to III, III to II, II to I). Thus, with each full cycle the amount of torsion at a target position will be larger/smaller than at the previous trespassing. This prediction is contradictory to Donders' law, which predicts a unique amount of torsion for each target position.

Figure 5.4 shows the measured change in torsion of the upper arm for the first six cycles for six subjects. Since changes in torsion are not significantly different for various targets, each data point shows the change of torsion of the upper arm

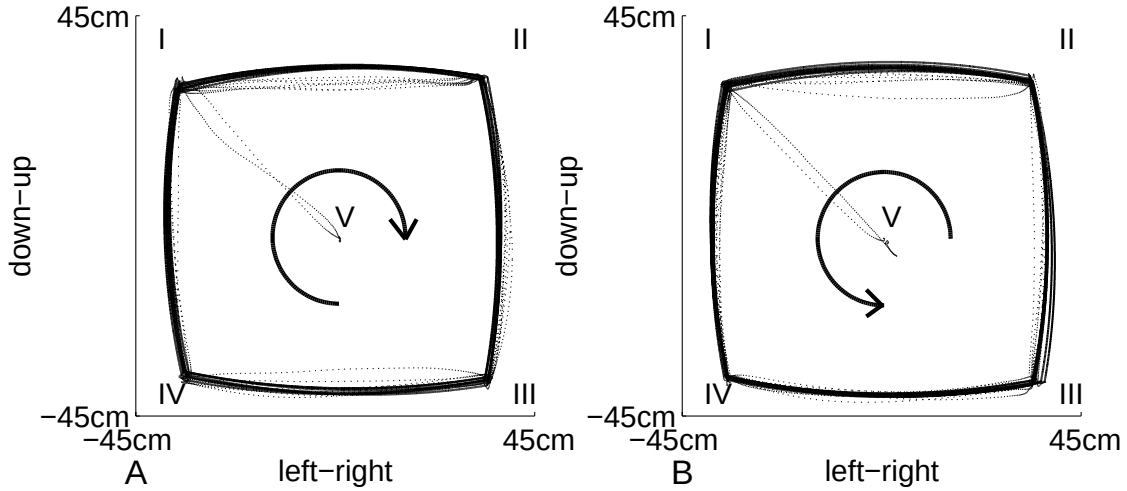

FIGURE 5.3: Projection on the frontal plane of the measured and predicted trajectories of the index finger between the corners of a square, in Clockwise direction (panel A) and Counter Clockwise direction (panel B). Data are shown for one subject (subject HP). Solid lines represent the trajectories corresponding to the predictions by the minimum-work and minimum torque-change model (the shortest path along the surface of a sphere, so called *geodetes*). Dotted lines represent the measured trajectories of the index finger. Positions I, II, III and IV indicate the endpoints of the movements, which lie on the corners of a square. Position V indicates the initial and final pointing direction.

averaged over all four targets for subsequent cycles relative to the torsion at the first passage through the target. The change in torsion is displayed separately for the Clockwise cycles (upper panels) and Counter Clockwise cycles (lower panels) for the SELF-PACED, ACCURATE and FAST movement conditions (left, middle and right panels, respectively).

Panels A and D show the measured torsion of the upper arm for SELF-PACED clockwise and counter-clockwise cyclic movements, respectively, for each cycle averaged over all targets. For the Clockwise cycles (top panels), the amount of torsion is significantly larger after the first cycle than at the beginning of the first cycle for all subjects ($p<0.05$). After the second cycle, torsion remains more or less constant: torsion in the third cycle is not significantly larger than in the second cycle. The standard deviation of torsion in the data is very similar for all subjects and for all cycles (range 1º to 7º; mean (SD)= 3º (1.5)).

The data in Figures 5.4A and B show that torsion typically increases for the first two cycles until it has accumulated to about 5 to 15 degrees. This result does not correspond to the predictions by the minimization models. As explained earlier, the minimum torque-change and minimum work models predict an accumulation of torsion for movements along a closed path, which would correspond to an accumulation of torsion after each cycle by 49 degrees for this experiment. Evidently, this is not case at all.

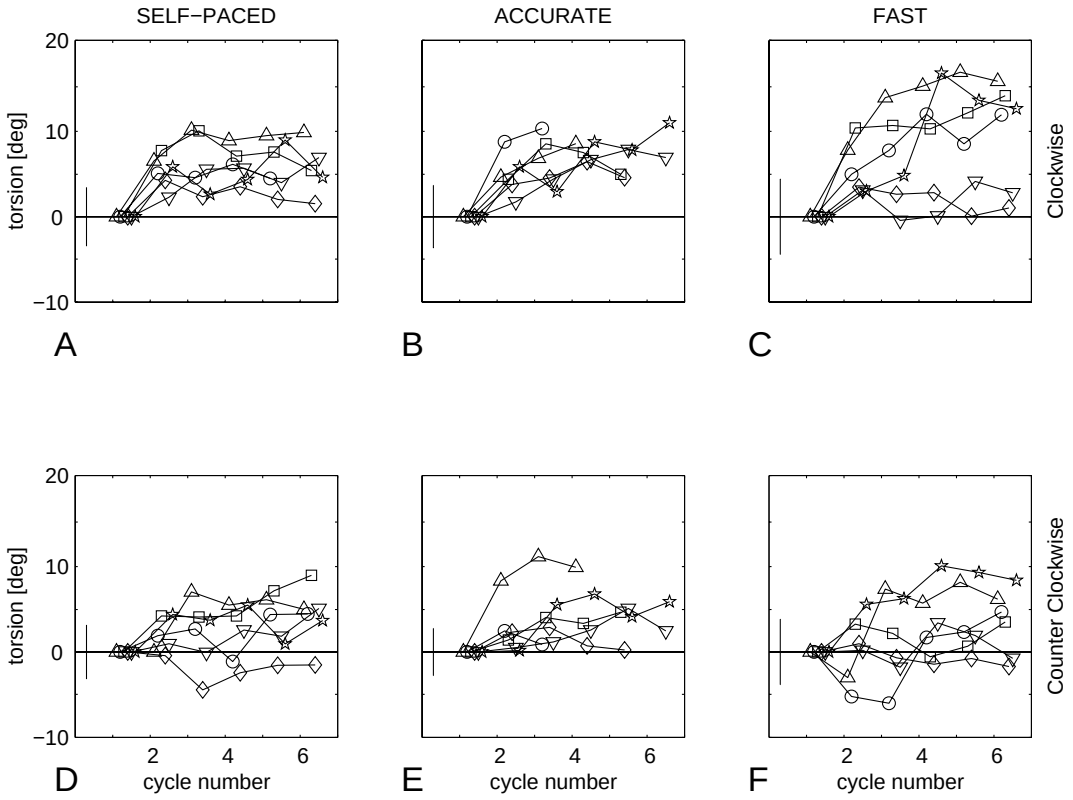

FIGURE 5.4: Changes in torsion, averaged over all four targets, for cyclic pointing movements relative to torsion at the first passage of the target. Upper (lower) panels show changes in torsion for Clockwise (Counter Clockwise) cycles for the SELF-PACED, ACCURATE and FAST conditions (left, middle and right panels, respectively). The data of the six subjects are indicated by different symbols. For different subjects and cycle numbers, the standard deviation is very similar (range 1º to 7º; mean (SD)= 3º (1.5)). Therefore, the mean standard deviation is shown in each panel by error-bars at the beginning of each axis, indicating the average standard deviation for data in all cycles for all subjects displayed in the panel.

Previous studies have shown that instruction to the subject affects torsion of the upper arm (see e.g. Medendorp et al. 2000). In order to investigate whether instruction to the subject might affect the accumulation of torsion in our study we tested subjects also with the instruction to move accurately or fast. The results are qualitatively similar to the SELF-PACED results in Clockwise and Counter Clockwise cycles. For all conditions except for the FAST Counter Clockwise condition, the amount of torsion for all subjects is significantly larger in the second cycle than in the first ($2.8 < t < 5.5$, $p<0.05$), but does not increase significantly anymore after the second cycle.

For the SELF-PACED and ACCURATE movements, the increase in torsion seems to be very similar between subjects (most obviously in the Clockwise cycles), whereas in the FAST movements the increase in torsion is less consistent between subjects. However, this effect of instruction was not significant (ANOVA, $p>0.1$).

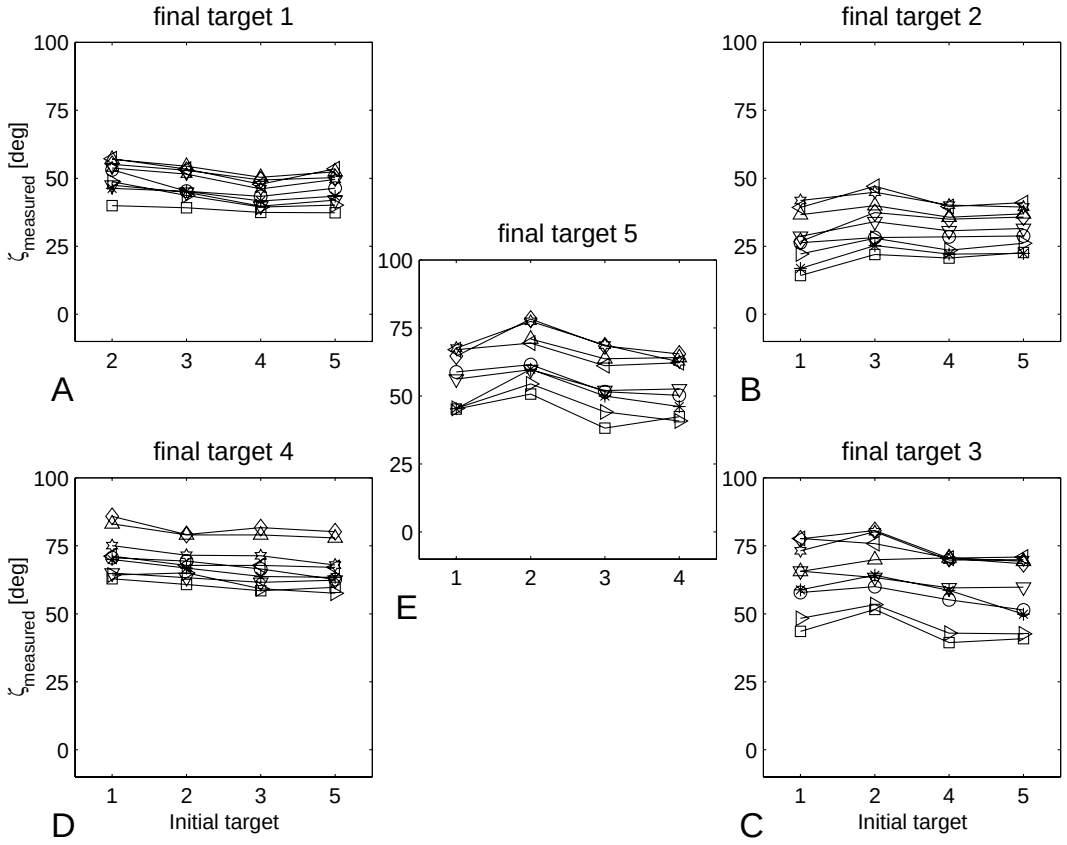

FIGURE 5.5: Humeral axis rotation angle as a function of initial position for postures of the upper arm at the end of movements toward targets 1,2,3,4, and 5. Each panel shows the amount of torsion during reaching for one of the five final targets as a function of the initial position of the movement. Different symbols refer to data from different subjects. Torsion of zero degrees corresponds to an orientation of the upper arm such that -when elevation is 90 degrees- the upper arm and forearm lie in a vertical plane, irrespective of elbow flexion.

Remarkably, changes in torsion are qualitatively the same in the Clockwise and Counter Clockwise direction, such that both tend to increase in the second cycle. This is surprising since the minimum work and minimum torque-change models predict accumulation of torsion in the opposite (i.e. negative) direction for Counter Clockwise movements.

Torsion of the upper arm during reaching movements

Figure 5.5 shows the amount of torsion of the upper arm (angle ζ) while reaching for targets 1 to 5 for movements starting from the other target positions. The results for each final position are displayed in separate panels arranged in a similar way as the target configuration (see Figure 5.2). Different symbols refer to data from different subjects. In agreement with previous studies (Soechting et al. 1995; Gielen et al. 1997), Figure 5.5 clearly shows that the amount of torsion at

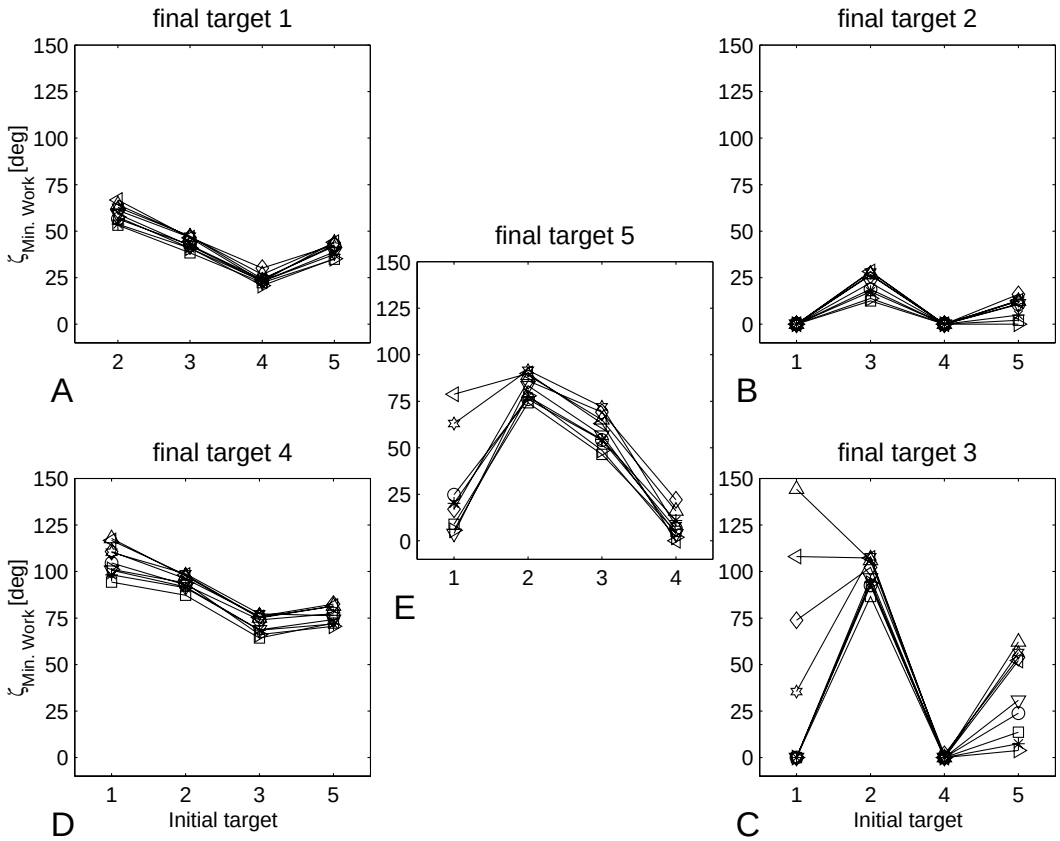

FIGURE 5.6: Prediction of the humeral axis rotation angle (ζ) by the minimum work model for movements to the five targets starting from different initial positions. For each subject, the mean posture at each begin position was used to predict the torsion at the end of the movement. Different symbols refer to predictions for different subjects.

the end of a movement depends on the initial position, and that these effects are very consistent across subjects. For each of the five possible end points, the deviation from the average torsion at the end position depends significantly on the initial position (ANOVA: $F(3,32)=58.9$, 20.2, 22.5, 30.6 and 43.0 for end points 1 to 5, respectively; $P<0.001$ for all endpoints).

Torsion of the upper arm was also simulated according to the minimum-work model. For each reaching movement, the input to the model was the measured posture at the initial position and the final target position in space. Figure 5.6 shows the predicted torsion angle ζ for five final targets as a function of the initial target at the beginning of the movement. The large variation between subjects in predicted torsion for movements from target 1 to final targets 5 and 3 (middle panel and lower right panel) is due to variation in initial posture at target 1 between the subjects. The dependence of predicted torsion of the upper arm on initial posture of the arm is qualitatively similar to that shown in Figure 5.5. However, quantitatively, the data are very different. The range of variation in torsion of the upper arm due to different initial postures is typically about ten degrees or less for each subject in the

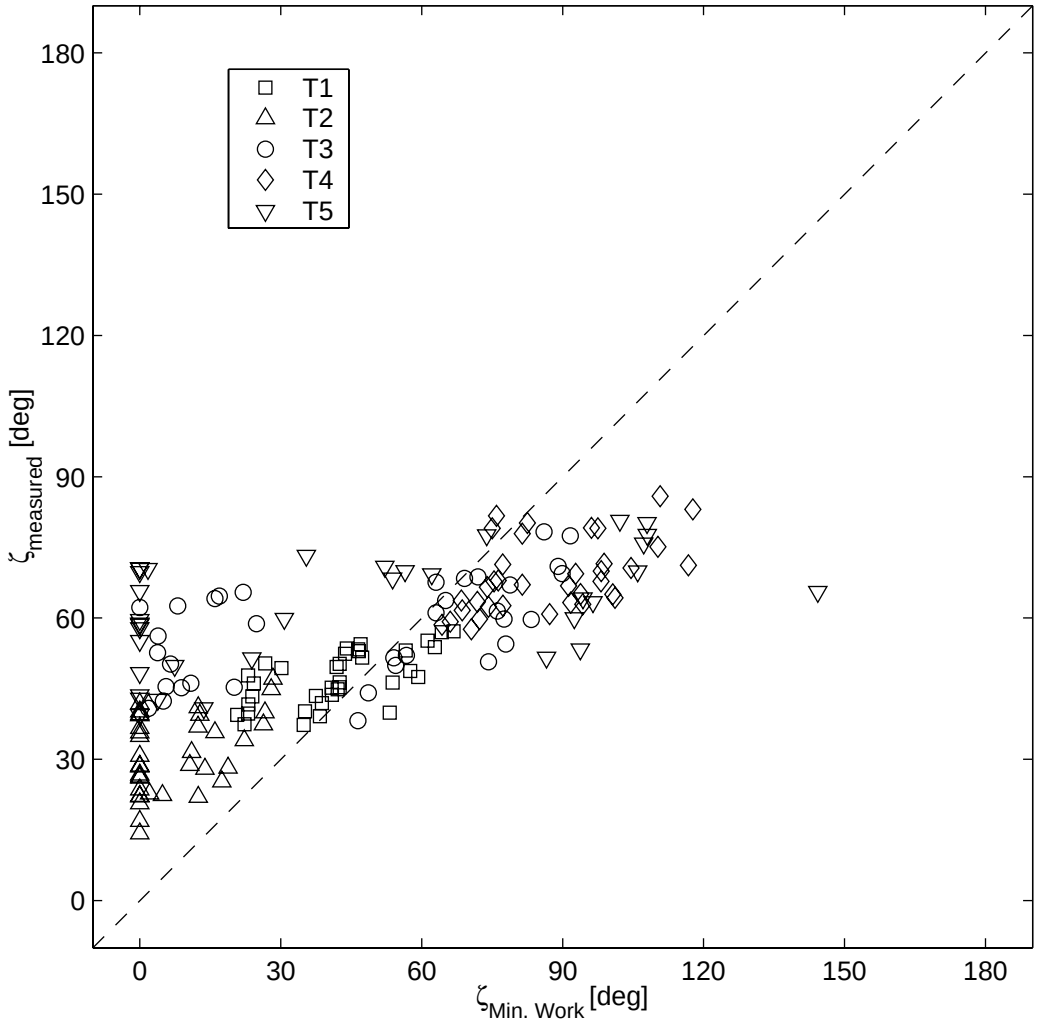

FIGURE 5.7: Measured torsion of the upper arm (vertical axis) versus the predicted torsion according to the minimum work model (horizontal axis) for all subjects. Different symbols refer to torsion at different final targets (see inset). For each subject, all end postures for a given pair of initial and final targets are averaged. Data in the figure correspond to the averages per target pair for each of the subjects individually.

real data, whereas it varies between 20 degrees (for final target 2, in Figure 5.6B) up to 100 degrees (for final target 3, in Figure 5.6E) for the minimum-work predictions.

In order to obtain a good overall comparison between the predictions by the minimum-work model and the measured data, we have plotted the measured torsion of the upper arm against simulated torsion (see Figure 5.7). For each subject we plotted 20 data points, corresponding to the averages of the repeated trials between the 20 possible pairs of initial and final targets. Different symbols correspond to the different endpoints of the movements.

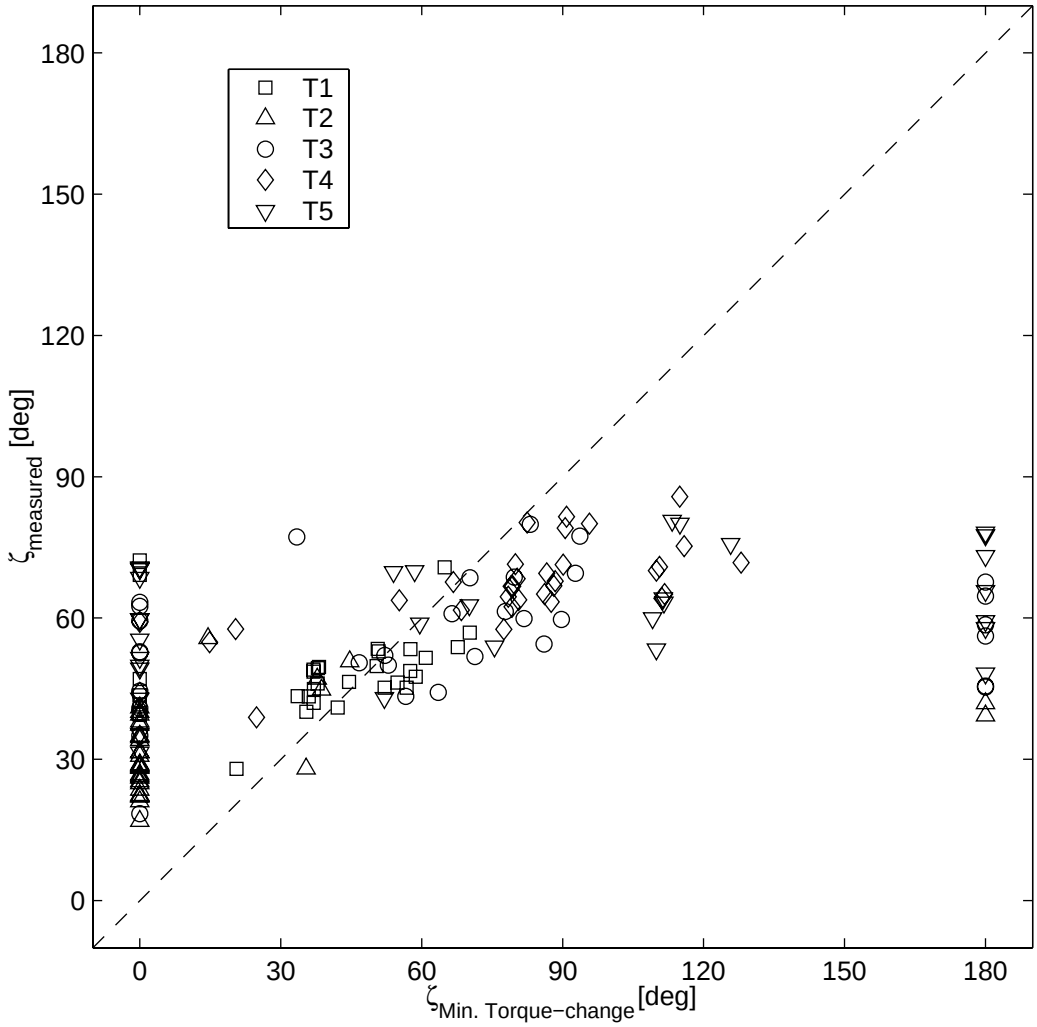

FIGURE 5.8: Measured torsion of the upper arm versus the predicted torsion according to the minimum torque-change model. Data are shown for all subjects. Different symbols correspond to torsion at different final targets. For each subject, the measured torsion is averaged over all movements between a pair of targets. The predicted amount of torsion is calculated based on the average initial postures of trials with the same initial and end targets.

If predicted and measured torsion were to be the same, the data would lie on the line of unity. Obviously, this is not the case. Figure 5.7 clearly shows that the measured and predicted data are correlated ($r=0.75$, $p<0.01$). The slope of a linear regression is about 0.3, which is significantly different from unity. The figure shows that for a large part of the data, the minimum-work model predicts a final torsion of 0 degrees. This is a consequence of the limits we choose for the minimization models, such that the predicted torsion would not exceed the (physical) range of torsion in the shoulder between 0 and 180 degrees.

The predicted torsion of the upper arm by the minimum-torque-change model for different target positions, starting from various begin positions, is shown in

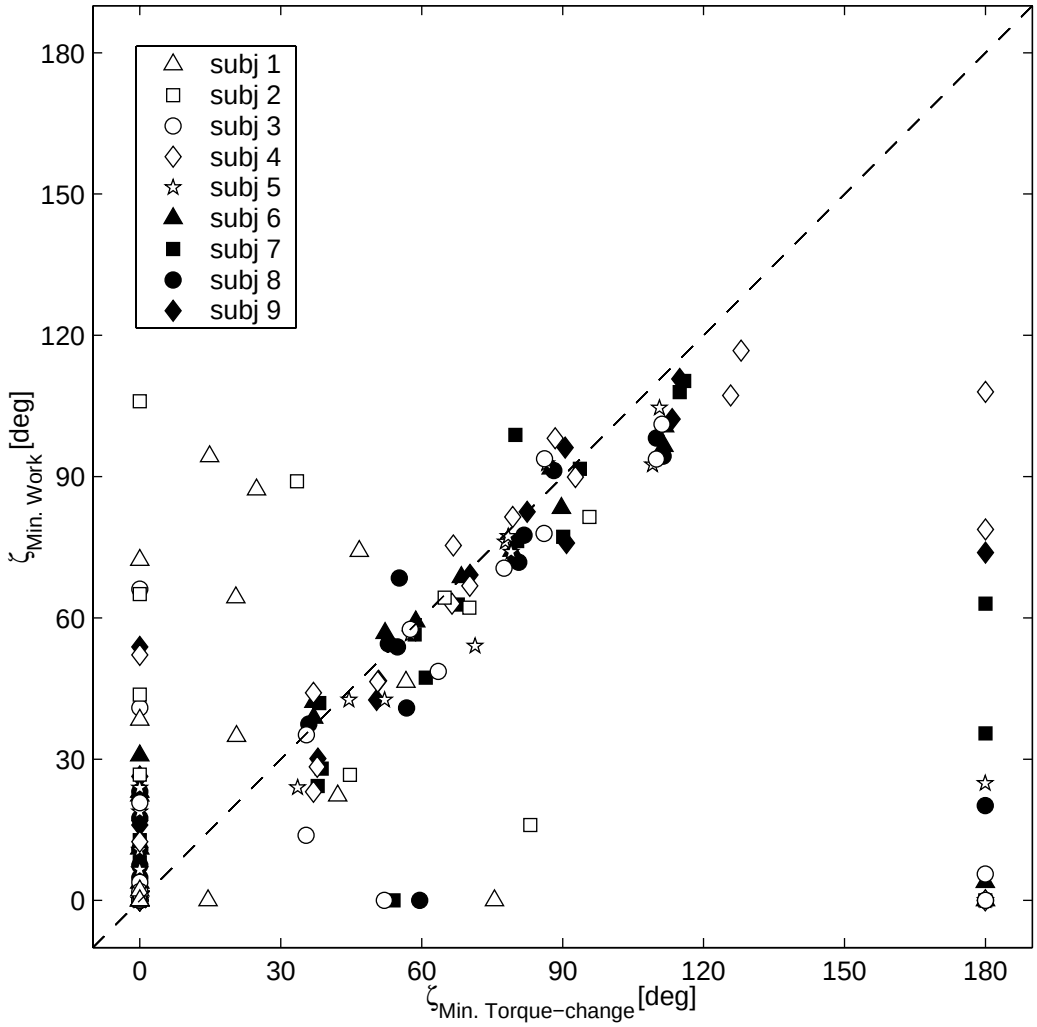

FIGURE 5.9: Predicted torsion of the upper arm according to the minimum torque-change model versus the predicted torsion according to the minimum work model. Different symbols refer to data from different subjects. For each subject, the measured torsion is averaged over all repeated trials between a pair of targets, such that each target pair is presented once for each subject.

Figure 5.8, where the predictions are plotted versus the measured torsion. For each subject we plotted the average of the measured torsion of the repeated trials for the 20 possible pairs of targets and the corresponding model predictions. Different symbols correspond to different endpoints of the movements.

Like for the minimum-work model, a large part of the predictions correspond to the limit values of 0 (minimum amount of torsion tested) and 180 degrees (maximum amount of torsion tested). The other data show a significant correlation with the measured data. The correlation coefficient between measured torsion and torsion predicted according to the minimal torque-change model was 0.72, which is significant on a 99% level. However, the slope of the linear regression fitted to the measured and predicted data in Figure 5.8 was 0.3, which is close to the slope of the

linear regression through the data for minimization of work in Figure 5.7, but significantly different from unity.

For many target pairs, the predictions by the two minimization models are similar. Figure 5.9 shows the relation between the predictions by the two models. For each subject we plotted the average of the predicted torsion for all 20 pairs of initial and final targets according to the minimum torque-change model versus the predicted torsion according to the minimum work model. Different symbols correspond to data from different subjects.

Figure 5.9 shows that for some target pairs, the minimum torque-change prediction reaches a limit value of 0 or 180 degrees in torsion, where the minimum work model does not. For the target pairs that did not result in a prediction near the extremes, the two models often agree ($r= 0.78$, $p<0.01$), and the slope of a linear regression through the relevant data in Figure 5.9 is 0.73.

DISCUSSION

This study concentrated on the question whether the kinematics of arm postures can be described by one of various models for human motor control, that have been proposed in the literature. Many different types of models have been proposed in the literature, but as far as we know, no study has been done to compare the performance of various models with experimental data on movements in 3-D space. We have compared the predictions by Donders' law and by the minimum work and minimum torque-change models with experimental data for a well-defined set of goal-directed movements. The first conclusion is that none of the models could give a good prediction for the data. The experimental data revealed significant and systematic deviations from the predicted postures.

For POINTING movements with the extended arm along a closed trajectory, torsion of the arm increased after the first cycles. This accumulation looks similar to results of Klein Breteler et al. (2003) who studied reaching movements that included elbow flexion through consecutive triple segments (triangles) to assess the validity of Donders' law for repetitive drawing movements. These authors reported that in most cases, the elevation of the elbow at the end of the first segment of the triangle increased after each cycle. The amount of increase of elbow elevation depended on the relative positions of the three targets that defined the corners of the triangles. The increase in torsion violates Donders' law, which requires that torsion for each pointing direction should be the same, irrespective of any previous movements. A change in torsion for these cyclic movements corresponds to the predictions of the minimum-work (Soechting et al. 1995) and minimum-torque-change model (Uno et al. 1989). However, the observed increase in torsion (typically a 5 to 15 degrees), which is quantitatively in agreement with variations in torsion for movements along a triangle (see Klein Breteler et al. 2003), was much smaller than that predicted by these models (about 49 degrees per cycle), and was

expected to be in opposite directions for Clockwise vs. Counter Clockwise cycles. The data revealed that changes in torsion where in the same direction for Clockwise vs. Counter Clockwise movement cycles. Moreover, the minimization models predict that torsion increases or decreases by the same amount after each cycle, which would result in an accumulation of torsion. A first glance on Figure 5.4 might suggest that torsion saturates after a few movement cycles. Any saturation, however, is unlikely to be the result of reaching the extremes of the physiological range of movement. The range of torsion of the upper arm in the shoulder is about 180 deg, while the range of torsion in Figure 5.4 is about 15 degrees. If the data in Figure 5.4 suggest any saturation, this saturation must reflect a consequence of neural control, rather than of biomechanics or of musculoskeletal anatomy.

One of the alternative models is the minimum-variance model (Harris and Wolpert 1998). Although we did not explicitly simulate this model, it is easy to explain that the predictions by this model for the pointing movements with the extended arm in this study are identical to the predictions by the minimum work and minimum torque-change models. The minimum-variance model assumes that noise increases with force. Therefore, minimization of end-point variability corresponds to minimization of exerted force during the movement. Minimization of exerted force requires that movements with the extended arm are made by a single-axis rotation along the shortest path, just as predicted by the minimum work and minimum torque-change models. Therefore, the minimum-variance model by Harris and Wolpert (1998) is not compatible with the experimental data presented here. The same holds for the minimum commanded torque change model by Nakano et al. (1999) and the movement strategy proposed in the Knowledge model (Rosenbaum et al. 1995), which corresponds to minimization of angular jerk between given initial and end postures.

Our data demonstrate that neither a posture based model (like Donders' law), nor a trajectory-based model can explain the experimental data. The experimental data fall in between the predictions by these two types of models. This is in agreement with results by Vetter et al. (2002), who concluded that movement strategies reflect a combination of posture-based and trajectory-based constraints. Our results and those by Vetter et al. are, at least qualitatively, in agreement with previous studies on adaptation to kinematic and dynamic transformations (see e.g. Flanagan et al. 1999, Krakauer et al. 2000 and Tong et al. 2002), which have shown that adaptation to changes in kinematic and dynamic transformations is achieved separately. The performance in a task where both transformations are present is better after adaptation to changes in kinematic and dynamic transformations separately, than without previous adaptation. However, the adaptation for each of the two components (kinematic and dynamic) in the task where both transformations are present is less than the adaptation achieved for the separate transformations (see Flanagan et al. 1999). This indicates that kinematic and dynamic transformations are not learned completely independently, suggesting that a strict distinction between posture-based models and trajectory-based models is too much a simplification.

Varying the constraints under which the subjects had to perform the cyclic movements (fast of accurate) had some effect on the performance of the movements (see Figure 5.4). This is compatible with earlier experimental data by Tweed and Vilis (1992), who found that normal movements of the head obey Donders' law, but that instructions to the subject to move as fast as possible between two fixation directions leads to violations of Donders' law, compatible with a minimum energy strategy. These results suggest that normal movements may be the result of various constraints on human movement generation and that variations in instruction to the subject lead to differences in weights in which various constraints affect the movement.

For the REACHING movements to targets within reaching space we found similar results. Torsion for postures to reach a particular position in space did depend on the trajectory towards the target, in a similar manner as reported by Soechting et al. (1995) and Gielen et al. (1997). Obviously, this violates Donders' law. The variations in torsion of the upper arm as a function of initial position before the movement were qualitatively in agreement with the predictions by the minimum-work hypothesis. However, quantitatively they were way off.

In a previous study Okadome and Honda (1999) compared the trajectory of sequential movements with predictions by various models. They reported that experimental movement trajectories were not compatible with the predictions by the minimum-jerk model, the equilibrium-hypothesis, and the minimum-torque-change model. They concluded that the data could be explained by a model that is a weighted combination of the minimum-jerk trajectory and the segmented minimum-angular-jerk model. However, these authors only considered movements in a horizontal plane. For movements in a 2-D horizontal plane the complex issues related to rotations in joints with three degrees of freedom are not relevant, and expanding the workspace to 3-D space may lead to a different weighting and maybe to other constraints and more optimization parameters.

One could wonder whether some of the assumptions that underlie the models evaluated in the present study in 3-D space, might be responsible for the large differences between the experimental data and the predictions by the models. One aspect concerns the neglect of the effect of gravity in the minimum-work model and the minimum-torque-change model. In our view there is good evidence that incorporating gravity will not improve the predictions by the models, since a study by Nishikawa et al. (1999) showed that final postures do not depend on the velocity with which a movement is performed. This speed-invariance of arm postures indicates that final posture only depends on dynamic forces, such as forces related to acceleration of the arm and Coriolis forces, and does not depend on static force components, like anti-gravity force components, which act during the whole movement time. Nishikawa et al. (1999) conclude that gravity does not affect final posture, which suggests that the neglect of gravity in the models has no effect on the disagreement between the predicted and measured data.

Another issue concerns the dependence of arm postures on the previously adopted postures. Several studies (Soechting et al. 1995; Gielen et al. 1997) have shown that arm postures will depend on previous postures, and this raises the question whether postures also depend on the last-but-one posture. Soechting et al. (1995) showed that variability in posture is smallest for targets at the lower left. Therefore, in our study each pair of initial target and end target was preceded by the lower left target (target 4), in order to minimize the variability in the initial posture. A typical sequence would thus look like: target 4 - target 1 - target 3, where only the posture at the end of the movement from target 1 tot target 3 was evaluated. Although Figure 5.5D demonstrates that the variability at target 4 is not completely absent, it is only a few degrees, and it is highly unlikely that this will have a large effect on the following posture (*initial posture*) or on the next posture (*end posture*).

The careful reader will have noticed a difference between the data in Figure 5.7 of the present study and Figure 8 by Soechting et al. (1995). The slope of the data in Figure 5.7, which shows measured torsion against torsion predicted by the minimum work model, is much lower than one (about 0.3), whereas the similar figure in Soechting et al. shows data that lie more or less along the line of unity. As explained in Methods and more extensively in the Appendix, the model described by Soechting et al., had some errors. In order to test whether these errors might explain the difference, we have simulated the model by Soechting and colleagues, using their (incorrect !) equations. This model leads to a better correspondence to the data by Soechting et al. in the sense that the slope of the regression line increased to 0.5. This increase suggests that the apparently good fit between measured and simulated data in Figure 8 of Soechting et al. might be partly due to the omission of terms in the equations used to simulate the minimum-work model in their paper.

Further considerations

Recently, several variations have been presented as an alternative to the minimum torque-change model, such as the minimum variance theory (Harris and Wolpert 1998), the minimum muscle-tension model (Dornay et al. 1996) and the minimum commanded torque-change model (Nakano et al. 1999). In the following paragraph, we will discuss these models shortly.

The minimum variance theory provides a simple, unifying and powerful principle that can be applied to goal-directed movements. It suggests that signal-dependent noise plays a fundamental role in motor planning (Harris and Wolpert 1998). The minimum variance theory predicts, like the minimum work and minimum torque-change model, the shortest path strategy for the pointing movements. As explained before, movements along the shortest path are incompatible with the measured data. Therefore, the minimum variance model cannot predict the results of the pointing experiments.

From a biological point of view, the minimum muscle-tension model (Dornay et al. 1996) might seem more plausible than the others. Because the CNS controls only the muscles in order to orient a joint, a model stating that movements are optimized in muscle space may seem to be more plausible than a model stating that movements are optimized in joint space. However, simulating arm movements with a minimum muscle-tension change model requires many more model parameters, such as optimum muscle length and muscle attachment sites, which introduces many more degrees of freedom and induces many free parameters. Modeling all these degrees of freedom, and dealing with the variability in anatomy between subjects caused too much variability in the simulations to allow an accurate quantitative comparison with experimental data.

The minimum commanded torque-change model presented by Nakano and colleagues (1999) is rather similar to the minimum torque-change model. The only differences are the values of the parameters for inertia and viscosity. Thus, the predictions with the minimum command torque-change model will be compatible with the predictions by the minimization models that were tested in the present study and which appeared to produce predictions that were not in agreement with experimental observations.

In summary, our results demonstrate that there is no single model that can accurately predict the experimental data. The results suggest that motor control is based on a combination of control principles, optimizing a task-dependent combination of constraints, in line with the theory suggested by Todorov and Jordan (2002).

APPENDIX

In this appendix we will give a more extended derivation of the equations, which underlie the minimum work model. Although this derivation is rather straightforward, we provide it in detail because the results differ from the equations in Soechting et al. (1995) where a few terms are missing.

The posture of the arm will be described in terms of the four joint angles η, θ, ς, and ϕ. The angle η refers to rotations about the vertical Z-axis and determines the yaw angle of the arm. A rotation η determines the arm's azimuth. The second angle θ determines the arm's elevation and the third angle ς refers to rotations about the humeral axis of the upper arm. This rotation doesn't change the location of the elbow but does affect the location of the hand in space when the elbow is flexed. We also define ϕ as the angle of elbow flexion; $\phi = 0$ corresponds to full extension.

With these definitions, the location of the elbow $[X_e, Y_e, Z_e]$ is given by:

$$\begin{aligned} X_e &= -L_u \sin\eta \sin\theta \\ Y_e &= L_u \cos\eta \sin\theta \\ Z_e &= -L_u \cos\theta \end{aligned} \tag{5.Ia}$$

where L_u represents the length of the upper arm.

The location of the index finger $[X_f, Y_f, Z_f]$ is given by:

$$\begin{aligned} X_f &= X_e - L_f\left[\sin\varphi \cdot (\cos\varsigma \sin\eta \cos\theta + \sin\varsigma \cos\eta) + \cos\varphi \cdot (\sin\eta \sin\theta)\right] \\ Y_f &= Y_e + L_f\left[\sin\varphi \cdot (\cos\varsigma \cos\eta \cos\theta - \sin\varsigma \sin\eta) + \cos\varphi \cdot (\cos\eta \sin\theta)\right] \\ Z_f &= Z_e + L_f\left[\sin\varphi \cdot (\cos\varsigma \sin\theta) - \cos\varphi \cdot (\cos\theta)\right] \end{aligned} \tag{5.Ib}$$

where L_f refers to the length of the forearm.

The amount of work W that is necessary to move the arm from one point to another is given by Equation 5.2. With the definitions of the coordinate system related to the upper arm, we can derive Equation 5.3 in the main text by using the velocity v_u for the center of mass of the upper arm:

$$v_u = \begin{bmatrix} -\frac{1}{2} L_u \Omega_{Y'} \\ -\frac{1}{2} L_u \Omega_{X'} \\ 0 \end{bmatrix} \tag{5.II}$$

and v_f for the center of mass of the forearm:

$$v_f = \begin{bmatrix} -\Omega_{Y'}\left(L_u + \frac{L_f}{2}\cos\phi\right) & -\Omega_{Z'}\left(\frac{L_f}{2}\sin\phi\right) \\ \Omega_{X'}\left(L_u + \frac{L_f}{2}\cos\phi\right) & + \dot{\phi}\left(\frac{L_f}{2}\cos\phi\right) \\ \Omega_{X'}\left(\frac{L_f}{2}\sin\phi\right) & + \dot{\phi}\left(\frac{L_f}{2}\sin\phi\right) \end{bmatrix} \tag{5.III}$$

With these definitions, the first part of the equation for the total amount of Work corresponds to:

$$
\begin{aligned}
\frac{1}{2} m \vec{v}^{T} \cdot \vec{v} = \frac{m_u}{2} \vec{v}_u{}^{T} \cdot \vec{v}_u \quad + \quad \frac{m_f}{2} \vec{v}_f{}^{T} \cdot \vec{v}_f = \\
= \frac{m_u}{2} \left[\frac{L_u}{4} \Omega_{Y'}{}^2 + \frac{L_u}{4} \Omega_{X'}{}^2 \right] \quad + \\
+ \frac{m_f}{2} \Bigg[\quad \Omega_{Y'}{}^2 \left(L_u + \frac{L_f}{2} \cos\phi \right)^2 + 2\Omega_{Y'} \Omega_{Z'} \left(L_u + \frac{L_f}{2} \cos\phi \right) \left(\frac{L_f}{2} \sin\phi \right) + \\
+ \Omega_{Z'}{}^2 \frac{L_f{}^2}{4} \sin\phi + \Omega_{x'}{}^2 \left(L_u + \frac{L_f}{2} \cos\phi \right)^2 + \\
+ 2\Omega_{X'} \dot{\phi} \left(L_u + \frac{L_f}{2} \cos\phi \right) \left(\frac{L_f}{2} \cos\phi \right) + \dot{\phi}^2 \frac{L_f{}^2}{4} \cos\phi + \\
+ \Omega_{x'}{}^2 \frac{L_f{}^2}{4} \sin^2\phi + 2\Omega_{X'} \dot{\phi} \frac{L_f{}^2}{4} \sin^2\phi + \dot{\phi}^2 \frac{L_f{}^2}{4} \sin^2\phi \quad \Bigg]
\end{aligned}
\tag{5.IV}
$$

The rotational part of the total Work, corresponds to the sum of a part for rotations of the upper arm:

$$
\frac{1}{2} \Omega^T \mathrm{I} \Omega \quad = \quad \frac{1}{2} \begin{pmatrix} \Omega_{X'} \\ \Omega_{Y'} \\ \Omega_{Z'} \end{pmatrix} \cdot \begin{pmatrix} I_{u1} \\ I_{u1} \\ I_{u2} \end{pmatrix} \cdot \begin{pmatrix} \Omega_{X'} \\ \Omega_{Y'} \\ \Omega_{Z'} \end{pmatrix} \tag{5.V}
$$

and a part for rotations of the forearm:

$$
\frac{1}{2} \Omega^T \mathrm{I} \Omega \quad = \quad \frac{1}{2} \begin{pmatrix} \Omega_{X'} + \dot{\phi} \\ \Omega_{Y'} \cos\phi + \Omega_{Z'} \sin\phi \\ \Omega_{Y'} \sin\phi - \Omega_{Z'} \cos\phi \end{pmatrix} \cdot \begin{pmatrix} I_{u1} \\ I_{u1} \\ I_{u2} \end{pmatrix} \cdot \begin{pmatrix} \Omega_{X'} + \dot{\phi} \\ \Omega_{Y'} \cos\phi + \Omega_{Z'} \sin\phi \\ \Omega_{Y'} \sin\phi - \Omega_{Z'} \cos\phi \end{pmatrix} \tag{5.VI}
$$

With the above equations and the abbreviations:

$$
\begin{aligned}
I_1 &= I_{u1} + m_u \frac{L_u{}^2}{4} + m_f L_u{}^2 \\
I_2 &= I_{u2} \\
I_3 &= m_f \frac{L_f{}^2}{4} + I_{f1} \\
I_4 &= I_{f2} \\
A &= m_f L_u \frac{L_f}{2}
\end{aligned}
\tag{5.VII}
$$

the total Work is derived to correspond to:

$$W = \frac{1}{2}\Big[I_1\left(\Omega_{X'}{}^2 + \Omega_{Y'}{}^2\right) + I_2\Omega_{Z'}{}^2 + \\ + I_3\left(\left(\Omega_{x'} + \dot{\phi}\right)^2 + \left(\Omega_{Y'}\cos\phi + \Omega_Z\,'\sin\phi\right)^2\right) + \\ + I_4\left(\Omega_{Y'}\sin\phi - \Omega_{Z'}\cos\phi\right)^2 + \\ + 2A\left(\left(\Omega_{X'}^2 + \Omega_Y^2\right)\cos\phi + \Omega_{Z'}\Omega_{Y'}\sin\phi + \dot{\phi}\Omega_{X'}\cos\phi\right)\Big] \qquad (5.VIII)$$

The last terms in this equation differs from the equation for the total amount of work presented by Soechting et al. (1995). Since we started with the same equations for the angular velocities as Soechting and colleagues, we expect the difference in equations to be due to printing errors in Soechting's equation. The difference includes three extra terms in the total work, which correspond to:

$$extra = \frac{A}{2}\left[\left(\Omega_{X'}^2 + \Omega_{Y'}^2\right)\cos\phi + \Omega_{Z'}\Omega_{Y'}\sin\phi + 2\dot{\phi}\Omega_{X'}\cos\phi\right] \qquad (5.IX)$$

The total work done during the movement from the starting location to the target is zero. The positive work done to accelerate the arm initially is canceled by the negative work required to decelerate the arm at the end of the movement. The work will assume a peak positive value when the torque changes sign from positive to negative, that is, at the peak of the velocity. The posture of the arm at the end of the movement is such that the peak work W is minimized, provided that the arm reaches the target.

BIBLIOGRAPHY

ADAMOVICH SV, BERKINBLIT MB, HENING W, SAGE J, AND POIZNER H, The interaction of visual and proprioceptive inputs in pointing to actual and remembered targets in Parkinson's Disease. *Neuroscience* 104: 1027-1041, 2001.

ADMIRAAL MA, MEDENDORP WP, AND GIELEN CCAM, Three-dimensional head and upper arm orientations during kinematically redundant movements and at rest. *Exp.Brain Res*.142: 181-192, 2002.

ADMIRAAL MA, KEIJSERS NLW, AND GIELEN CCAM, Interaction between gaze and pointing toward remembered visual targets. *J. Neurophysiol.* 90: 2136-2148, 2003.

BARLOW RJ, *Statistics.* Chichester, UK: Wiley, 1989, p. 160-161.

BERKINBLIT MB, FOOKSON OI, SMETATIN B, ADAMOVICH SV, AND POIZNER H, The interaction of visual and proprioceptive inputs in pointing to actual and remembered targets. *Exp. Brain Res.* 107: 326-330, 1995.

BIGUER B, PRABLANC C, AND JEANNEROD M, The contribution of coordinated eye and head movements in hand pointing accuracy. *Exp. Brain Res.* 55: 462-469, 1984.

BLOUIN J, AMADE N, VERCHER JL, TEASDALE N, AND GAUTHIER GM, Visual signals contribute to the coding of gaze direction. *Exp. Brain Res.* 144: 281-292, 2002.

BOCK O, Contribution of retinal versus extraretinal signals towards visual localization in goal-directed movements. *Exp. Brain Res.* 64: 476-482, 1986.

CARPENTER RHS, *Movements of the eyes*. London, UK: Pion Limited, 1988, p. 293-312.

CARROZZO M, STRATTA F, MCINTYRE J, AND LACQUANITI F, Cognitive allocentric representations of visual space shape pointing errors. *Exp. Brain Res.* 147: 426-436, 2002.

CEYLAN MZ, HENRIQUES DYP, TWEED DB, AND CRAWFORD JD, Task-dependent constraints in motor control: Pinhole goggles make the head move like an eye. *J. Neurosci.* 20: 2719-2730, 2000.

COLLEWIJN H, VAN DER MARK F, AND JANSEN TC, Precise recording of human eye movements. *Vision Res.* 15: 447-450, 1975.

CRANE BT, AND DEMER JL, Human gaze stabilization during natural activities: Translation, rotation, magnification and target distance effects. *J. Neurophysiol.* 78: 2129-2144, 1997.

CRAWFORD JD, CEYLAN MZ, KLIER EM, AND GUITTON D, Three-dimensional eye-head coordination during gaze saccades in the primate. *J. Neurophysiol.* 81: 1760-1782, 1999.

DAGHESTANI L, ANDERSON JH, AND FLANDERS M, Coordination of a step with a reach. *J. Vest. Res.* 10: 59-73, 2000.

DESMURGET M, PÉLISSON D, ROSSETTI Y, AND PRABLANC C, From eye to hand: planning goal-directed movements. *Neurosci. Biobehav. Rev.* 22: 761-788, 1998.

DONDERS FC, Beitrag zur lehre von den Bewegungen des menschlichen Auges, *Holland Beitr. Anat. Physiol. Wiss.* 1: 104-145, 1848.

DORNAY M, UNO Y, KAWATO M, AND SUZUKI R, Minimum muscle-tension change trajectories predicted by using a 17-muscle model of the monkey's arm. *J. Motor Behav.* 28: 83-100, 1996.

DUDA RO, AND HART PE, *Pattern Classification and Scene Analysis.* New York, US: Wiley, 1973, p. 22-24.

ELLIOTT D, AND MADALENA J, The influence of premovement visual information on manual aiming. *Q. J. Exp. Psychol.-A* 39: 541-559, 1987.

ENRIGHT JT, The non-visual impact of eye orientation on eye-hand coordination. *Vision Res.* 35: 1611-1618, 1995.

FLANAGAN JR, NAKANO E, IMAMUZI H, OSU R, YOSHIOKA T, AND KAWATO M, Composition and decomposition of internal models in motor learning under altered kinematic and dynamic environments. *J. Neurosci.* 19: RC34, 1999.

FLANDERS M, DAGHESTANI L, AND BERTHOZ A, Reaching beyond reach. *Exp. Brain Res.* 126:19-30, 1999.

FLANDERS M, HELMS-TILLERY SI, AND SOECHTING JF, Early stages in a sensorimotor transformation. *Behav. Brain Sci.* 15: 309-362, 1992.

FLASH T, The control of hand equilibrium trajectories in multi-joint arm movements. *Biol. Cybern.* 57: 257-274, 1987.

FRENS MA, AND ERKELENS CJ, Coordination of hand movements and saccades: evidence for a common and a separate pathway. *Exp. Brain Res.* 85: 682-690, 1991.

GENTILUCCI M, CHIEFFI S, DAPRATI E, SEATTI MC, AND TONI I. Visual illusion and action. *Neuropsychologia* 34: 369-376, 1996.

GEORGOPOULOS AP, KALASKA JF, AND MASSEY JT, Spatial trajectories and reaction times of aimed movements: effects of practice, uncertainty and change in target location. J. *Neurophysiol.* 46: 725-743, 1981.

GEORGOPOULOS AP, KALASKA JF, CRUTCHER MD, CAMINITI R, AND MASSEY JT, The representation of movement direction in the motor cortex: single cell and population studies. In: *Dynamic Aspects of Neocortical Function*, edited by: Edelman GM, Einar Gall W, and Maxwell Cowan W, New York, US: Wiley, 1984, p. 501-524.

GHEZ C, AND GORDON J, Trajectory control in targeted force impulses. *Exp. Brain Res.* 67: 225-240, 1987.

GIELEN CCAM, VAN DEN HEUVEL PJ, AND VAN GISBERGEN JA, Coordination of fast eye and arm movements in a tracking task. *Exp. Brain Res.* 56: 154-161, 1984.

GIELEN CCAM, RAMAEKERS L, AND VAN ZUYLEN EJ, Long-latency stretch reflexes as co-ordinated functional responses in man. *J. Physiol.* 407: 275-292, 1988.

GIELEN SC, Movement dynamics. *Curr. Opin. Neurobiol.* 3: 912-916, 1993.

GIELEN CCAM, VRIJENHOEK EJ, FLASH T, AND NEGGERS SFW, Arm position constraints during pointing and reaching in 3-D space. *J. Neurophysiol.* 78: 660-673, 1997.

GIELEN CCAM, GABEL SF, AND DUYSENS J, Retinal slip during active head motion and stimulus motion. *Exp. Brain Res.*155: 211-219, 2004.

GLENN B, AND VILIS T, Violations of Listing's law after large eye and head gaze shifts. *J. Neurophysiol.* 68: 309-318, 1992.

GORDON J, GHILARDI MF, AND GHEZ C, Accuracy of planar reaching movements. I. Independence of direction and extent variability. *Exp. Brain Res.* 99: 97-111, 1994.

GRÉA H, DESMURGET M, AND PRABLANC C, Postural invariance in three-dimensional reaching and grasping movements. *Exp. Brain Res.* 134: 155-162, 2000.

HARRIS CM, AND WOLPERT DM, Signal-dependent noise determines motor planning. *Nature* 394: 780-784, 1998.

HARRIS LR, JENKIN M, AND ZIKOVITZ DC, Visual and non-visual cues in the perception of linear self-motion. *Exp. Brain Res.* 135:12-21, 2000.

HARUNO M, WOLPERT DM, AND KAWATO M, Multiple paired forward-inverse models for human motor learning and control. *Advances in Neural Information Processing Systems* 11: 31-37, 1999.

HARUNO M, WOLPERT DM, AND KAWATO M, Mosaic model for sensorimotor learning and control. *Neural Comput.* 13: 2201-2220, 2001.

HAUSTEIN W, Considerations on Listing's law and the primary position by means of a matrix description of eye position control. *Biol. Cybern.* 60: 411-420, 1989.

HENRIQUES DYP, KLIER EM, SMITH MA, LOWY D, AND CRAWFORD JD, Gaze-centered remapping of remembered visual space in an open-loop pointing task. *J. Neurosci.* 18: 1583-1594, 1998.

HENRIQUES DYP, AND CRAWFORD JD, Direction-dependent distortions of retinocentric space in the visuomotor transformation for pointing. *Exp. Brain Res.* 132: 179-194, 2000.

HEUER H, AND OWENS DA, Vertical gaze direction and the resting posture of the eyes. *Perception* 18: 363-377, 1989.

HOGAN N, The mechanics of multi-joint posture and movement. *Biol. Cybern.* 52: 315-331, 1985.

HORE J, WATTS S, AND VILIS T, Constraints on arm position when pointing in three dimensions: Donders' law and the Fick gimbal strategy. *J. Neurophysiol.* 68: 374-383, 1992.

HU Y, EAGLESON R, AND GOODALE MA, The effects of delay in the kinematics of grasping. *Exp. Brain Res.* 126: 109-116, 1999.

HU Y, AND GOODALE MA, Grasping after a delay shifts size-scaling from absolute relative metrics. *J. Cogn. Neurosci.* 12: 856-868, 2000.

JUDGE GG, HILL RC, GRIFFITHS WE, LÜTKEPOHL H, AND LEE TC, *Introduction to the Theory and Practice of Econometrics.* New York, US: Wiley, 1988, p. 890-892.

KAWATO M, Internal models for motor control and trajectory planning. *Curr. Opin. Neurobiol.* 9: 718-727, 1999.

KLEIN BRETELER MD, HONDZINSKI JM, AND FLANDERS M, Drawing sequences of segments in 3D: kinetic influences on arm configuration. *J. Neurophysiol.* 89: 3253-3263, 2003.

KRAKAUER JW, PINE ZM, GHILARDI M-F, AND GHEZ C, Learning of visuomotor transformations for vectorial planning of reaching trajectories. *J. Neurosci.* 20: 8916-8924, 2000.

KRAUTH J. Distribution-free statistics: an application-oriented approach. Amsterdam, NL: Elsevier, 1988.

KRÖLLER J, DE GRAAF JB, PRABLANC C, AND PÉLISSON D, Effects of short-term adaptation of saccadic gaze amplitude on hand-pointing movements. *Exp. Brain Res.* 124: 351-362, 1999.

LACQUANITI F, SOECHTING JF, Responses of mono- and bi-articular muscles to load perturbations of the human arm. *Exp. Brain Res.* 65: 135-144, 1986.

MARTENIUK RG, IVENS CJ, AND BERTRAM CP, Evidence of motor equivalence in a pointing task involving locomotion. *Mot. Control* 4: 165-184, 2000.

MCINTYRE J, STRATTA F, AND LACQUANITI F, Viewer-centered frame of reference for pointing to memorized targets in three-dimensional space. *J. Neurophysiol.* 78: 1601-1618, 1997.

MCINTYRE J, STRATTA F, AND LACQUANITI F, Short-term memory for reaching to visual targets: psychophysical evidence for body-centered reference frames. *J. Neurosci.* 18: 8423-8435, 1998.

MEDENDORP WP, MELIS BJM, GIELEN CCAM, AND VAN GISBERGEN JAM, Off-centric rotation axes in natural head movements: implications for vestibular reafference and kinematic redundancy. *J. Neurophysiol.* 79: 2025-2039, 1998.

MEDENDORP WP, VAN ASSELT S, AND GIELEN CCAM, Pointing to remembered visual targets after active one-step self-displacements within reaching space. *Exp. Brain Res.* 125: 50-60, 1999.

MEDENDORP WP, VAN GISBERGEN JAM, HORSTINK MWIM, AND GIELEN CCAM, Donders' law in torticollis. *J. Neurophysiol.* 82: 2833-2838, 1999.

MEDENDORP WP, CRAWFORD JD, HENRIQUES DYP, VAN GISBERGEN JAM, AND GIELEN CCAM, Kinematic strategies for upper-arm forearm coordination in three dimensions. *J. Neurophysiol.* 84: 2302-2316, 2000.

MEDENDORP WP, AND CRAWFORD JD, Visuospatial updating of reaching targets in near and far space. *Neuroreport* 13: 633-636, 2002a.

MEDENDORP WP, VAN GISBERGEN JAM, AND GIELEN CCAM, Human gaze stabilization during active head translations. *J. Neurophysiol.* 87: 295-304, 2002b.

MESSIER J, AND KALASKA JF, Differential effect of task conditions on errors of direction and extent of reaching movements. *Exp. Brain Res.* 115: 469-478, 1997.

MILLER LE, THEEUWEN M, AND GIELEN CCAM, The control of arm pointing movements in three dimensions. *Exp. Brain Res.* 90: 415-426, 1992.

MOONEY CZ, AND DUVAL RD, *Bootstrapping: a Nonparametric Approach to Statistical Inference.* Sage University Paper series on Quantitative Applications in the Social Sciences, 07-095. Newbury Park (CA), US: Sage, 1993, p. 1-29.

MORRISON DF, *Multivariate Statistical Methods.* Tokyo, Japan: McGraw-Hill Kogakusha, 1976, p. 128-136.

NAKANO E, IMAMIZU H, OSU R, UNO Y, GOMI H, YOSHIOKA T, AND KAWATO M, Quantitative examinations of internal representations for arm trajectory planning: minimum commanded torque change model. *J. Neurophysiol.* 81: 2140-2155, 1999.

NEGGERS SF, AND BEKKERING H, Gaze anchoring to a pointing target is present during the entire pointing movement and is driven by a non-visual signal. *J. Neurophysiol.* 86: 961-970, 2001.

NISHIKAWA KC, MURRAY ST, AND FLANDERS M, Do arm postures vary with the speed of reaching? *J. Neurophysiol.* 81: 2582-2586, 1999.

OKADOME T, AND HONDA M, Kinematic construction of the trajectory of sequential arm movements. *Biol. Cybern.* 80: 157-169, 1999.

PAIGE GD, TELFORD L, SEIDMAN SH, AND BARNES GR, Human verstibuloocular reflex and its interactions with vision and fixation distance during linear and angular head movement. *J. Neurophysiol.* 80: 2391-2404, 1998.

PANERAI F, CORNILLEAU-PÉRÈS V, AND DROULEZ J, Contribution of extraretinal signals to the scaling of object distance during self-motion. *Percept. Psychophys.* 60: 717-731, 2002.

PHILBECK JW, Visually directed walking to briefly glimpsed targets is not biased toward fixation location. *Percept.* 29: 259-272, 2000.

PIGEON P, BORTOLAMI SB, DIZIO P, AND LACKNER J, Coordinated turn-and-reach movements. II. Planning in an external frame of reference. *J. Neurophysiol.* 89: 290-303, 2003.

POUGET A, DUCOM JC, TORRI J, AND BAVELIER D, Multisensory spatial representations in eye-centered coordinates for reaching. *Cognition* 83: B1-B11, 2002.

POZZO T, MCINTYRE J, CHERON G, AND PAPAXANTHIS C, Hand trajectory formation during whole body reaching movements in man. *Neurosci. Letters* 240: 159-162, 1998.

PRABLANC C, ECHALLIER JF, KOMILIS E, AND JEANNEROD M, Optimal response of eye and hand motor systems in pointing at a visual target. I. Spatio-temporal characteristics of eye and hand movements and their relationships when varying the amount of visual information. *Biol. Cybern.* 35: 113-124, 1979.

PRABLANC C, PÉLISSON D, AND GOODALE MA, Visual control of reaching movements without vision of the limb. I. Role of retinal feedback of target position in guiding the hand. *Exp. Brain Res.* 62: 293-302, 1986.

RADAU P, TWEED D, VILIS T, Three-dimensional eye, head and chest orientations after large gaze shifts and the underlying neural strategies. *J. Neurophysiol.* 72: 2840-2852, 1994.

ROSENBAUM DA, LOUKOPOULOS LD, MEULENBROEK RGJ, VAUGHAN J, AND ENGELBRECHT SE, Planning reaches by evaluating stored postures. *Psychol. Rev.* .102: 28-67, 1995.

SOECHTING JF, AND LACQUANITI F, Invariant characteristics of a pointing movement in man, *J. Neurosci.* 1: 710-720, 1981.

SOECHTING JF, AND LACQUANITI F, Quantitative evaluation of the electromyographic responses to multidirectional lean perturbations of the human arm. *J. Neurophysiol.* 59: 1296-1313, 1988.

SOECHTING JF, AND FLANDERS M, Sensorimotor representations for pointing to targets in three-dimensional space. *J. Neurophysiol.* 62: 582-594, 1989.

SOECHTING JF, HELMS TILLERY SIH, AND FLANDERS M, Transformation from head- to shoulder-centered representation of target direction in arm movements. *J. Cogn. Neurosci.* 2: 32-43, 1990.

SOECHTING JF, BUNEO CA, HERRMANN U, AND FLANDERS M, Moving effortlessly in three dimensions: Does Donders' law apply to arm movement? *J. Neurosci.* 15: 6271-6280, 1995.

SOECHTING JF, ENGEL KC, AND FLANDERS M, The Duncker illusion and eye-hand coordination. *J. Neurophysiol.* 85: 843-854, 2001.

STOKER JJ, *Pure and applied mathematics, vol. XX: Differential Geometry*, New York, US: Wiley, 1969, p. 191-198.

STRAUMANN D, HASLWANTER TH, HEPP-REYMOND MC, AND HEPP K, Listing's law for eye, head and arm movements and their synergistic control. *Exp. Brain Res.* 86: 209-215, 1991.

THEEUWEN M, MILLER LE, AND GIELEN CCAM, Are the orientations of head and arm related during pointing movements? *J. Mot. Behav.* 25: 242-250, 1993.

TODOROV E, AND JORDAN MI, Optimal feedback control as a theory of motor coordination. *Nature Neurosci.* 5: 1226-1235, 2002.

TONG C, WOLPERT DM, AND FLANAGAN JR, Kinematic and dynamics are represented independently in motor working memory: evidence from an interference study. *J. Neurosci.* 22, 1108-1113, 2002.

TWEED D, AND VILIS T, Implications of rotational kinematics for the oculomotor system in three dimensions. *J. Neurophysiol.* 58: 832-849, 1987.

TWEED D, AND VILIS T, Listing's law for gaze directing head movements. In: *The head-neck sensory-motor system*, edited by: Berthoz A, Vidal PP, Graf W, New York, US: Oxford University Press, 1992, pp. 387-391.

TWEED D, Three-dimensional model of the human eye-head saccadic system. *J. Neurophysiol.* 77: 654-666, 1997.

UNO Y, KAWATO M, AND SUZUKI R, Formation and control of optimal trajectory in human multi-joint arm movement. Minimum torque-change model. *Biol. Cybern.* 61: 89-101, 1989.

VAN BEERS RJ, WOLPERT DM, AND HAGGARD P, When feeling is more important than seeing in sensorimotor adaptation. *Curr. Biol.* 12: 834-837, 2002.

VAN DONKELAAR P, AND STAUB J, Eye-hand coordination to visual versus remembered targets. *Exp. Brain Res.* 133: 414-418, 2000.

VELDPAUS FE, WOLTRING HJ, AND DORTMANS LJMG, A least-squares algorithm for the equiform transformation from spatial marker co-ordinates. *J. Biomech.* 21: 45-54, 1988.

VETTER P, FLASH T, AND WOLPERT DM, Planning movements in a simple redundant task. *Curr. Biol.* 12: 488-491, 2002.

VINDRAS P, DESMURGET M, PRABLANC C, AND VIVIANI P, Pointing errors reflect biases in the perception of the initial hand position. *J. Neurophysiol.* 79, 3290-3294, 1998.

VON HELMHOLTZ H, *Handbuch der Physiologischen Optik*, 3rd edition, Hamburg, Germany: Voss, 1910.

PUBLICATIONS

ARTICLES

ADMIRAAL MA, MEDENDORP WP, AND GIELEN CCAM, Three-dimensional head and upper arm orientations during kinematically redundant movements and at rest. *Exp. Brain Res*., 142, 181-192, 2002.

ADMIRAAL MA, KEIJSERS NLW, AND GIELEN CCAM, Interaction between gaze and pointing toward remembered targets. *J. Neurophysiol.*, 90, 2136-2148, 2003.

ADMIRAAL MA, KUSTERS JMAM, AND GIELEN CCAM, Models on the three-dimensional kinematics of arm movements. In press, *Motor Control*, 2004.

ADMIRAAL MA, KEIJSERS NLW, AND GIELEN CCAM, Gaze affects pointing towards remembered targets after a step. Submitted.

KEIJSERS NLW, ADMIRAAL MA, COOLS AR, BLOEM BR, AND GIELEN CCAM, The accuracy of pointing movements to remembered visual targets in Parkinson's disease. Submitted.

ABSTRACTS

ADMIRAAL M, VAN OPSTAL J, GIELEN S, Strategies for reducing degrees of freedom in human arm movements. *Soc. Neurosci. Abstr.*, 26, 1720, 2000.

ADMIRAAL M, KEIJSERS N, AND GIELEN S, Internal representation of target position after a step. *Neural Control of Movement*, Seville, Spain, 2001.

SUMMARY

This thesis describes studies of perception and storage of the 3-D location of visual targets and the (visual) information that is needed to accurately reach for a target position that was previously viewed. We addressed the question in what frame of reference the target position is stored, and what are the contributions of visual and proprioceptive information on the perception and execution of the reaching movements. We also investigated the criteria used by the CNS to select the appropriate arm posture to reach the remembered target position. Several kinematic and dynamical models that propose ways for the CNS to overcome the difficulties of a kinematically redundant system such as the arm or head were evaluated and we compared various strategies hypothesized in the literature on arm movement control.

In Chapter 2 we examined the role of gaze in a task where subjects had to reproduce the position of a remembered visual target with the tip of the index finger. Subjects were tested in three visual feedback conditions: complete darkness (DARK), complete darkness with visual feedback of the finger position (FINGER), and with vision of a well-defined environment and feedback of the finger position (FRAME). We found that pointing accuracy increases with feedback about the finger or visual environment. In the FINGER and FRAME conditions, the 95% confidence regions of the variable errors have an ellipsoidal distribution with the main axis oriented towards the subjects' head. During this task, we also measured the fixation position of the two eyes (*binocular gaze*), and during the one-second period when the target is visible, gaze was almost on target. However, gaze drifted away from the target relative to the subject in the delay period after target disappearance. In the FINGER and FRAME conditions, gaze returned towards the remembered target during pointing. In all three feedback conditions, the correlations between the variable errors of gaze and pointing position increased during the delay period, reaching highly significant values at the time of pointing.

Our results demonstrated that gaze affects the accuracy of pointing. We conclude that the covariance between gaze and pointing position reflects a common drive for gaze and arm movements and an effect of gaze on pointing accuracy at the time of pointing. Previous studies interpreted the orientation of variable errors as indicative for a frame of reference used for pointing. Our results suggest that the orientation of the error ellipses towards the head is -at least partly- the result of gaze drift in the delay period.

Chapter 3 describes pointing movements towards remembered targets after an intervening self-generated body movement. We tested to what extent visual information about the environment or finger position is used in updating target

position relative to the body after a step, and whether gaze plays a similar role in the accuracy of the pointing movement as it does in the static situation described in Chapter 2. Again, subjects were tested in the three visual conditions DARK, FINGER and FRAME.

For pointing after a step the accuracy was rather poor in the FINGER and DARK conditions, which did not provide vision of the environment. Constant pointing errors were mainly in the direction of the step and ranged from 10 to 20 cm. Differences between binocular fixation and target position were often related to the step size and direction. At the beginning of the trial, when the target was visible, fixation was on target. After target extinction, fixation drifted away from the target relative to the subject, similar to the static condition described in Chapter 2. The variability in the pointing positions appeared to be related to the variable errors in fixation, and the covariance increased during the delay period after the step, reaching a highly significant value at the time of pointing. The significant covariance between fixation position and pointing was not the result of a mutual dependence on the step, since we corrected for any direct contributions of the step in both signals.

We conclude that the covariance between fixation and pointing position reflects (1) an effect of fixation on pointing accuracy at the time of pointing and (2) a common command signal that describes the target position for gaze and for the hand.

In order to accurately reach the target position, the command signal to the arm must be transformed into an adequate motor command, which brings the hand to the right location in space. In the tasks described in Chapters 2 and 3, there were no further requirements on the orientation of the arm while pointing, which left one degree of freedom of the arm undefined. Although this could lead to a large variability in arm orientations for the same target position for the hand, several previous studies have shown that the orientation of the arm is very consistent within and across subjects. Thus, the central nervous system (CNS) might use a systematic strategy to overcome the problem of kinematic redundancy. The CNS may use this strategy every time it encounters more degrees of freedom than needed for a task, which can concern the orientation of the arm, but also the orientation of the head. Both for the arm and for the head, the number of degrees of freedom often exceeds the number required, which relates both to kinematics (multiple postures correspond to the same position of the hand in space) as well as to dynamics (the same posture can be reached by various movement trajectories in space).

Therefore, in Chapter 4 we studied whether 3-D orientations of the head and arm are the same at rest and during movement for corresponding pointing or facing directions, respectively. Two separate experiments were performed: one focused on head orientations, the other focused on upper arm orientations. We instructed subjects to direct the nose or to point the extended arm in the direction of targets, which appeared in a quasi-random order at 2-second intervals. In a notation in terms

of rotation vectors, the head and upper arm orientations at rest were described by a 2-D surface with a scatter less than 3 or 4 degrees, respectively. This is in agreement with Donders' law, which states that the orientation of the task-specific degrees of freedom (like azimuth and elevation in pointing) define the orientation of the remaining (e.g. torsional) degree of freedom. Both for arm and head movements, orientations started and ended near this 2-D surface, but for a number of the target pairs the orientations deviated from those predicted by the 2-D surface during movement, in a way that was consistent and reproducible for movements between each target pair. For upper arm movements we often found that deviations of arm orientations from the 2-D surface increased with increasing movement velocity. Such a positive correlation between deviation and movement velocity was not found for head movements. These results clearly indicate violations of Donders' law during movement and argue against several models on movement control in the literature.

In order to study whether other models on the control of arm movements than Donders' law give a better description of the postures of the arm, in Chapter 5 we compared the predictions by various models on human motor control with experimental data. We studied goal-directed pointing and reaching movements of the arm in 3-D space towards targets either out of the arm's reach (POINTING experiment) or towards targets at a distance that could be reached with elbow flexion (REACHING experiment).

We found that the orientation of the arm, when pointing to a target or while reaching for a target, depended on initial position of the movement, which is in contradiction to kinematic models such as Donders' law. Other models, such as the minimum work model, the minimum torque-change model, and the minimum variance model, predict that the posture at the end of a movement depends on previous postures. The experimental data demonstrated that postures of the arm for a particular target position were not uniquely defined by target position, but depended on previous postures of the arm. This contradicts Donders' law. However, the minimum work and minimum torque-change models predicted a much larger effect of initial posture than observed in the experimental data. Thus, neither Donders' law, nor the models based on dynamical constraints were able to predict the kinematics of arm postures.

SAMENVATTING

Dit proefschrift gaat over de visuele waarneming van de driedimensionale ruimte om ons heen, en over het onthouden van de 3-D positie van voorwerpen om er later naar te kunnen grijpen of wijzen. Dat is iets wat we dagelijks doen, en waar we nauwelijks bij stil staan, maar de vertaalslag van visuele informatie naar het activeren van de spieren van een arm is nog een hele klus voor het brein.

In het onderzoek beschreven in dit proefschrift, hebben we het referentie kader bestudeerd dat het brein gebruikt om 3-D posities in de buitenwereld te onthouden, en in hoeverre de visuele informatie die beschikbaar is invloed heeft op de uiteindelijke reikbeweging: In een lege vierkante kamer ligt het misschien voor de hand om een positie te onthouden ten opzichte van de wanden en het plafond. Maar uiteindelijk moet de beweging worden gemaakt met een arm die aangestuurd wordt met spieren rond een aantal gewrichten. Vanuit dat oogpunt is het misschien juist handiger om de positie uit te drukken in de benodigde hoeken van die gewrichten of de gewenste lengtes van de spieren. Omdat de positie van een voorwerp veelal visueel wordt waargenomen, zou je die positie ook in richting en afstand ten opzichte van het oog kunnen onthouden. Een extra moeilijkheid voor het brein is dat de arm beschikt over meer gewrichtshoeken dan strikt noodzakelijk om met de hand alle posities binnen reikafstand te bereiken. Dat betekent dat er verschillende combinaties van gewrichtshoeken mogelijk zijn die tot dezelfde positie van de hand in de ruimte leiden. Maar het blijkt dat het brein steeds bij eenzelfde taak dezelfde combinatie van hoeken kiest. In de literatuur hebben velen zich al gebogen over de reden van die specifieke keuze. Zo zijn er modellen voorgesteld die er van uitgaan dat het brein een of andere kinematische parameter optimaliseert, bij andere modellen wordt een optimum in dynamische parameters verondersteld. Deze verschillende modellen hebben we in dit proefschrift vergeleken, en we hebben gekeken welke van die modellen het beste de gemeten keuze van het brein voorspelt.

In Hoofdstuk 2 hebben we bestudeerd wat de invloed is van waar je kijkt op waar je heen beweegt wanneer je het topje van je wijsvinger moet bewegen naar een doelpositie die je eerder gezien hebt. Deze doelpositie werd aangeboden als een klein lichtgevend puntje in 3D. Proefpersonen werden in drie verschillende visuele condities gemeten: 1) in een volledig duistere omgeving, 2) in volledig duister met een lichtje op het topje van de wijsvinger, en 3) in het donker, maar met zicht op een goedgedefinieerde omgeving van lichtgevende lijnen en met een lichtje op het topje van de wijsvinger. De nauwkeurigheid waarmee proefpersonen de taak uitvoerden, bleek af te hangen van de hoeveelheid zicht op de vinger en de omgeving. In alle behalve in de volledig duistere conditie bleek de variabiliteit in de wijsbewegingen het grootst in de richting van het hoofd van de proefpersoon.

Tijdens deze taak hebben we ook de kijkrichting van beide ogen gemeten. Daaruit kunnen we de 3-D kijkpositie bepalen. Terwijl het doel gedurende 1 seconde werd aangeboden kwam deze 3-D kijkpositie goed overeen met de doelpositie. Na de doelpresentatie volgde een wachtperiode van 2 seconden voordat de wijsbeweging gemaakt mocht worden. In die wachtperiode verschoof de 3-D kijkpositie weg van de doel positie, naar een positie verder weg van de proefpersoon. Wanneer bij het reiken naar de doelpositie een LED op de vingertop was aangebracht -en proefpersonen dus konden zien waar ze hun vingertop plaatsen- kwam de kijkpositie weer terug richting de doelpositie. Dit was niet het geval wanneer proefpersonen hun vingertop niet terugzagen tijdens het reiken. Maar, in alle drie condities nam de correlatie tussen de 3-D kijkfouten en de fouten in reiken toe tijdens de wachtperiode, en de correlatie was zeer significant op het moment van reiken.We kunnen concluderen dat de covariantie tussen kijken en reiken aangeeft dat de sturing van de ogen en die van de arm op een zelfde stuursignaal gebaseerd zijn, en dat de fouten die je maakt tijdens reiken, afhangen van waar je kijkt op het moment van reiken. In voorgaande studies werd de oriëntatie van de variabiliteit van fouten bij reiken naar steeds dezelfde doelpositie gezien als indicatie voor het referentiekader dat werd gebruikt voor het reiken. Immers, wanneer de doelpositie in drie onafhankelijke parameters wordt onthouden (bijvoorbeeld in X,Y, en Z), en de nauwkeurigheid in die drie parameters niet gelijk is, dan zullen ook de fouten in de ene richting groter zijn dan in een de andere. De 3-D verdeling van de variabiliteit zal dan een oriëntatie hebben in de richting van de minst nauwkeurige parameter. Onze data laten echter zien dat de grotere variabiliteit gericht naar het hoofd -tenminste ten dele- veroorzaakt wordt door het verschuiven van de 3-D kijkpositie tijdens de wachtperiode.

In Hoofdstuk 3 beschrijven we een vervolgstudie op Hoofdstuk 2, waarin we kijken naar reikbewegingen naar herinnerde doelposities nadat eerst een stap gemaakt is. Hier hebben we gekeken in hoeverre het zicht op de omgeving en op het topje van de wijsvinger gebruikt wordt voor het aanpassen van de herinnerde doelpositie aan de nieuwe uitgangspositie na de stap. Bovendien hebben we gekeken wat de invloed is van de 3-D kijkpositie voor, tijdens en na de stap op de uiteindelijke reikfouten. We hebben opnieuw gebruik gemaakt van de drie visuele condities uit Hoofdstuk 2.

Tijdens de presentatie van het doel correspondeerde de 3-D kijkpositie goed met de doelpositie. Wanneer het doel uit was en de stap werd ingezet, verschoof de kijkpositie van het doel weg ten opzicht van de proefpersoon, net als in de stilstaande situatie uit Hoofdstuk 2. In die condities waar de stap in het volledig duister werd gemaakt (condities 1 en 2), waren de reikbewegingen niet erg nauwkeurig. De gemiddelde reikfout was voornamelijk in de richting van de stap, en proefpersonen reikten gemiddeld tussen de 10 en 20 cm van het doel. Verschillen tussen de 3-D kijkpositie en de doelpositie waren veelal gerelateerd aan de stapgrootte en staprichting. De variabiliteit in de reikposities bleken gerelateerd aan de variabiliteit in kijkpositie, en de covariantie tussen beide nam toe tijdens de

wachtperiode na de stap tot een zeer significantie waarde op het moment dat de vinger de herinnerde doelpositie had bereikt. Deze significante relatie was niet het gevolg van een gemeenschappelijke afhankelijkheid van de stap, omdat we voor de bijdrage van de stap hebben gecorrigeerd. Desondanks bleef er een significantie relatie tussen kijken en reiken. We kunnen daarom concluderen dat de covariantie tussen kijken en reiken aangeeft (1) dat de 3-D kijkpositie op het moment van reiken van invloed is op de reiknauwkeurigheid en (2) dat de ogen en de hand een gemeenschappelijke doelsignaal aangeboden kregen.

Om het doel nauwkeurig te bereiken, moet dit doelsignaal worden aangepast tot een adequaat bewegingssignaal voor de arm, zodat de hand op de juiste positie in de ruimte terechtkomt. In de studies in Hoofdstuk 2 en 3 is verder niet voorgeschreven welke oriëntatie de arm moet aannemen tijdens het reiken met de wijsvinger. Dat betekent dat het brein nog een keuze (één *vrijheidsgraad*) overhad om de arm te positioneren. Hoewel dit aanleiding kan geven tot een veelheid aan armoriëntaties voor dezelfde vingerpositie, blijkt uit veel voorgaande studies dat de armoriëntatie in een dergelijke taak zeer consistent is, zowel binnen één proefpersoon, als tussen proefpersonen. Kennelijk gebruikt het brein een bepaalde strategie om dit probleem van teveel vrijheidsgraden op te lossen. Het zou zo kunnen zijn dat het brein deze strategie steeds toepast wanneer een taak niet alle beschikbare vrijheidsgraden voorschrijft, wat kan voorkomen voor bewegingen van de arm, maar ook voor het oriënteren van het hoofd. Voor beide geldt, dat het aantal beschikbare vrijheidsgraden het benodigde aantal veelal overstijgt, wat zowel de kinematica alsook de dynamica kan betreffen. Er zijn immers meer oriëntaties van de arm die tot dezelfde positie van de vinger in de ruimte leiden (kinematica) en eenzelfde oriëntatie van de arm in de ruimte kan worden bereikt met verschillende bewegingspaden in de 3-D ruimte (dynamica).

In Hoofdstuk 4 beschrijven we een studie naar de 3-D oriëntatie van het hoofd en van de gestrekte arm tijdens en aan het eind van een beweging, wanneer alleen de uiteindelijke kijk- of wijsrichting is voorgeschreven. We hebben dit in twee afzonderlijke experimenten uitgevoerd, één voor het hoofd en één voor de arm. Proefpersonen werden geïnstrueerd om met hun neus of met hun gestrekte arm naar veraf gelegen doelposities te wijzen, die op een semi-willekeurige volgorde verschenen met een interval van 2 seconden. Wanneer de oriëntatie van het hoofd of de bovenarm werd beschreven in rotatievector notatie, dan konden de 3-D oriëntaties van beide -tijdens stilstand- goed worden beschreven met een 2-D oppervlak. Dit betekent dat de oriëntatie van de taakafhankelijke vrijheidsgraden (in dit geval de *azimuth*• en *elevatie*) bepalend zijn voor de oriëntatie van de overgebleven vrijheidsgraad, in dit geval *torsie*. Zowel voor de arm- als voor de

• Azimuth is de draaiing naar links of rechts, elevatie de rotatie naar boven of onder. Torsie is gedefinieerd als de draaiing van de arm om diens lengte as, ofwel de draaiing van het hoofd om de as langs de richting waarin de neus wijst.

hoofdbewegingen, begonnen en eindigden de bewegingen met oriëntaties op dit 2-D oppervlak. Echter, voor een aantal combinaties van begin- en eind- wijsrichtingen weken de oriëntaties tijdens de beweging op een systematisch en reproduceerbare wijze af van dit 2-D vlak. Bovendien vonden we dat de mate van afwijking van dit vlak voor armbewegingen veelal afhing van de snelheid waarmee werd bewogen. Dit effect van bewegingssnelheid op de mate van afwijking vonden we niet voor de hoofdbewegingen. De resultaten van deze studie laten duidelijk schendingen zien van het 2-D oppervlak en zijn strijdig met een aantal modellen voor bewegingssturing dat eerder in de literatuur is gepresenteerd.

Om te zien of een van de andere modellen uit de literatuur een betere beschrijving geeft van de oriëntatie van de arm, hebben we in Hoofdstuk 5 de voorspellingen van verschillende van deze modellen vergeleken met experimentele data. We hebben daarbij doelgerichte wijsbewegingen bestudeerd, en ook reikbewegingen van de arm in de 3-D ruimte. Doelen bevonden zich ofwel buiten het bereik van de gestrekte arm (wijsbewegingen) ofwel op een afstand minder dan een armlengte (reikbewegingen). In deze studie vonden we dat de oriëntatie van de arm voor zowel wijs- als reikbewegingen afhing van de positie van de wijsvinger en de oriëntatie van de arm voorafgaand aan de beweging. Dit is in strijd met kinematische modellen, zoals de reductie van oriëntaties naar een 2-D oppervlak. Andere modellen, zoals het model van *minimalisatie van arbeid* of het model van *minimalisatie van moment-verandering* voorspellen wel dat de armoriëntatie aan het einde afhangt van de oriëntatie aan het begin van de beweging. Maar deze modellen voorspellen een veel groter effect dan in werkelijkheid wordt gevonden. Dus noch de Wet van Donders, noch de modellen gebaseerd op een dynamische optimalisatie bleken in staat de kinematica van arm oriëntaties aan het einde van de wijs- en reikbewegingen te voorspellen.

DANKWOORD

Promotieonderzoek doen is leuk, lastig, spannend en bij tijd en wijle enorm frustrerend. De eindstreep zou ik niet gehaald hebben, als ik de mensen om mij heen niet had gehad die mij uit allerlei wetenschappelijke en technische problemen op weg hebben geholpen.

Allereerst natuurlijk Stan. Ongeacht hoe vast ik soms ook zat, en hoe druk jij het soms had, als het nodig was wist je altijd een gaatje in je agenda te vinden om me aan nieuwe motivatie en ideeën te helpen. Na een bezoekje op jouw kamer kwam ik opgewekt en met nieuwe ideeën weer beneden. Eenmaal terug beneden wist ik natuurlijk al gauw weer een hoop *maar*'s en *tenzij*'s te bedenken, maar jouw enthousiasme had mij wel geïnspireerd om verder te gaan. Ook Pieter wil ik hier bedanken voor het wegwijs maken in het lab en in het aio-schap. Veel goeie suggesties voor de interpretatie van de data en ideeën voor nieuwe experimenten heb ik aan jou te danken. Maar met nieuwe ideeën, moet je vaak ook nieuwe opstellingen bouwen. Gelukkig waren Ton en Hans er dan om mee te denken over het bouwen en aansturen van de benodigde opstelling, en Ger, Vic en Günter voor het aanpassen van allerlei versies van de bestaande programmatuur. En als alles eenmaal draait, dan moet er natuurlijk nog gemeten worden. Daarbij kon ik rekenen op de hulp van verschillende stagiaires: Ingrid, Wietske, Bastiaan, Jeroen en Martijn bij de metingen, en op een hoop collega's en studenten als proefpersoon. Sommigen van hen waren zelfs bereid om daarbij (twee!) oogspoeltjes te dragen!

Maar ik zou dit boekje nooit hebben afgekregen zonder de steun van een heleboel mensen die samen met mij blij waren bij goede resultaten, en voor gezelligheid zorgden wanneer het allemaal even niet zo liep. Dit is natuurlijk de uitgelezen plek om hen te bedanken.

Allereerst mijn collega en kamergenoot Noël. Het grootste deel van mijn tijd aan de KUN zat ik met jou op kamer -1.16 (bij brand 0.11). Jouw imitatie van Kit uit *The night rider* is erg treffend: ten alle tijden kon ik op je rekenen! Of het nou ging om het proefdraaien van een setup, het bespreken van belangrijke persoonlijke en wetenschappelijke zaken of het lenen van je auto voor belangrijke uitstapjes met Ieke en Joyce. Ik had me geen betere kamergenoot kunnen wensen! Zeker in het begin van mijn promotietijd kon ik voor een praatje ook terecht bij Sonja met wie ik de eerste tijd de kamer deelde, en bij de buurtjes Ieke, Henk, Rico en Chris, waar altijd wel iemand in was voor een praatje, een kleurplaat of een kopje koffie. De laatste tijd werkten deze buren vooral veel buiten het lab, maar als Henk er was dan zorgde hij wel voor een flinke pot koffie! En gelukkig spraken Ieke en ik ook buiten werktijd regelmatig af om te gaan hardlopen (en soms deden we dat dan ook nog echt!). Tijdens het rekken en het kopje thee na afloop bespraken we dan alles wat er in de week gebeurd was, en de dingen die ons dwars zaten (niet in het minste de

eindeloosheid van een promotietijd). Maar je ziet het, die hobbel is te nemen, net als alle zeven heuvelen! Ook met Joyce heb ik heel wat uren zitten praten over het klussen in en om het huis, het begeleiden van een student of het organiseren van allerlei uitjes. Jouw enthousiasme werkt erg aanstekelijk en ik waardeer het enorm dat ik altijd op je hulp kan rekenen. Bovendien laat ik de vakgroep met een gerust hart achter, omdat ik weet dat jij af en toe wel zorgt voor koekjes bij de koffie. Zonder de gezelligheid op de vakgroep zou ik het een stuk moeilijker hebben gehad om de eindstreep te halen. Daarvoor wil ik alle collega's van de afgelopen jaren heel erg bedanken! Dat de vakgroep een hechte groep is, blijkt niet alleen uit de dagelijkse gezamenlijke koffiepauze, maar ook uit het karten, squashen, schaatsen, lasergamen, bowlen en de vele uitstapjes naar terrasjes die we buiten werktijd met collega's ondernamen. Maar ook onder werktijd was er af en toe tijd een praatje met Ger, Judith, Annet en Margriet, en tijdens de spannende *Inter Kamer Competitie* met Ronald, Rens en Noël heb ik een hoop frustraties van me af kunnen gooien! En het vrijdagse biertje is ondertussen uitgegroeid tot een vaste traditie, met -in wisselende samenstelling- John, Anton, Marcel, Jeroen, Joyce, Ronald, Thamar, Rens, Tom, Martijn, Marc, Noël, Sigrid, Bernke, Kees, Frouke, Martijn, Onno, Jan Joost, en Carla. Iedereen: heel erg bedankt voor een hartstikke leuke tijd bij de vakgroep!

Naast alle collega's en vrienden van de vakgroep wil ik ook Yvette bedanken voor de gezellige (lange) telefoongesprekken als ik m'n verhaal weer eens kwijt moest, en voor je nuchtere kijk op de wereld.

Niet alleen tijdens mijn promotietijd, maar ook alle jaren daarvoor heb ik altijd veel steun gekregen van mijn familie. Mijn keuze om aan een promotie te beginnen heeft mijn ouders misschien - net als mijzelf - verbaasd, maar op jullie liefde en steun heb ik altijd kunnen rekenen op momenten dat ik het even niet zo zag zitten. Het is heerlijk te weten dat jullie trots zijn op dingen die ik doe! Trudy, jij hebt me ooit de advertentie van de KUN gestuurd omdat je dacht dat dit promotieonderzoek wel wat voor mij was. Dat had je goed gezien, want ik heb een hele leuke tijd achter me! We wonen sindsdien niet meer zo dicht bij elkaar, maar ik ben heel erg blij met een vriendin en zus als jij! En Andor, ik hoop dat we elkaar in de toekomst weer vaker zullen zien, nu we dichter bij elkaar werken. Dank jullie wel!

Lieve Joost, we schreven tegelijkertijd aan een proefschrift en dat betekende dat we elkaar soms niet zo vaak zagen als we wel zouden willen. Maar we wisten allebei welke druk een promotie bij tijd en wijle met zich mee kan brengen, en ik ben je heel dankbaar voor je geduld en de rust die je me hebt weten te geven wanneer die druk weer eens een beetje te hoog opliep. Maar ook mijn proefschrift is nu af, en ik heb net zoveel zin in onze toekomst als jij!

CURRICULUM VITAE

Op 11 juni 1974 werd ik geboren in Tegelen, en ik woonde tot mijn zesde jaar in het naburige Belfeld. Daarna verhuisde ik met mijn ouders naar Hoorn, waar ik de basisschool en middelbare school doorlopen heb. In september 1992 begon ik aan de studie Experimentele Natuurkunde aan de Universiteit van Amsterdam, met een afstudeerstage op de afdeling Radiotherapie van het Academisch Medisch Centrum. Interesse voor de medische toepassingen van de natuurkunde bracht mij ertoe om een extra stage te lopen op het Max Planck Institüt für Neuropsychology in Leipzig (Duitsland), alvorens af te studeren. In Leipzig heb ik gewerkt aan het inzichtelijk maken van (veeldimensionale) data uit ERP studies. Na deze stage begon ik in 1998 als assistent in opleiding aan promotieonderzoek bij de vakgroep Medische Fysica & Biofysica aan de Katholieke Universiteit in Nijmegen. Het proefschrift dat nu voor u ligt, beschrijft de resultaten van dit onderzoek. Sinds 2004 werk ik bij het Nederlands Forensisch Instituut bij de afdeling Wetenschap en Onderwijs.